

---

## Atmospheric Chemistry: Response to Human Influence

Jennifer A. Logan, M. J. Prather, S. C. Wofsy and M. B. McElroy

*Phil. Trans. R. Soc. Lond. A* 1978 **290**, 187-234

doi: 10.1098/rsta.1978.0082

---

### Email alerting service

Receive free email alerts when new articles cite this article - sign up in the box at the top right-hand corner of the article or click [here](#)

---

To subscribe to *Phil. Trans. R. Soc. Lond. A* go to: <http://rsta.royalsocietypublishing.org/subscriptions>

---

# ATMOSPHERIC CHEMISTRY: RESPONSE TO HUMAN INFLUENCE

BY JENNIFER A. LOGAN, M. J. PRATHER, S. C. WOFSY  
AND M. B. McELROY

*Center for Earth and Planetary Physics, Harvard University,  
Cambridge, Massachusetts 02138, U.S.A.*

*(Communicated by D. R. Bates, F.R.S. – Received 25 November 1977)*

## CONTENTS

	PAGE
1. INTRODUCTION	188
2. CHEMISTRY	189
3. THE PRESENT ATMOSPHERE	197
4. PERTURBATIONS	212
5. RESULTS	217
6. CONCLUDING REMARKS	226
REFERENCES	227

Present understanding of global atmospheric chemistry is reviewed. Models are presented and compared with a wide range of atmospheric observations, with emphasis on the stratosphere. In general, excellent agreement is found between the calculated and observed distributions of long lived trace gases. The abundances of many shorter lived species are also satisfactorily reproduced, including  $\text{NO}_2$ ,  $\text{HNO}_3$ ,  $\text{O}$ ,  $\text{O}_3$ ,  $\text{OH}$  and  $\text{ClO}$ . Discrepancies between theory and observation are examined and their significance assessed.

The influence of human perturbations due to combustion, agriculture and chloro-carbon releases is discussed with emphasis on  $\text{O}_3$ . Uncertainties associated with present models are highlighted. Combustion related releases of  $\text{CO}$  cause a decrease in the abundance of tropospheric  $\text{OH}$  with consequent increase in the concentrations of  $\text{CH}_4$ ,  $\text{H}_2$ ,  $\text{CH}_3\text{Cl}$  and other halocarbons.  $\text{CO}$  emissions may become sufficiently large during the next century to induce substantial increases in tropospheric ozone on a global scale. Recombination of nitrogen fixed by agriculture and combustion may lead to an enhanced source of atmospheric  $\text{N}_2\text{O}$  with a related impact on stratospheric  $\text{NO}_x$ . Chlorocarbon industry provides an important source of stratospheric chlorine, and enhanced levels of stratospheric  $\text{Cl}_x$  and  $\text{NO}_x$  may cause a significant reduction in the abundance of atmospheric  $\text{O}_3$ , by as much as 10% during the next century. Perturbations due to various anthropogenic activities interact in a nonlinear fashion and the influence on atmospheric chemistry is correspondingly complex.

## 1. INTRODUCTION

Atmospheric chemistry has enjoyed a period of remarkable growth over the past decade. Interest has been stimulated mainly by concern that a variety of human influences might lead to detectable change in the abundance of stratospheric ozone.

Advances have occurred in all important areas of the subject. New techniques have been developed for detection of reactive species at exceedingly low concentration. They have been applied in the laboratory to study a wide range of important reactions. Corresponding developments have provided a wealth of new data on the concentration of important atmospheric species including  $\text{CH}_4$  (Ehhalt 1974),  $\text{CO}$  (Seiler 1974; Volz, Ehhalt, Heidt & Pollock 1976),  $\text{NO}$  (Ridley, Bruin, Schiff & McConnell 1976),  $\text{NO}_2$  (Noxon 1975; Noxon, Whipple & Hyde 1977),  $\text{HNO}_3$  (Murcray *et al.* 1975),  $\text{N}_2\text{O}$ , (Ehhalt, Heidt, Lueb & Pollock 1975*b*; Schmeltekopf *et al.* 1977),  $\text{OH}$  (Anderson 1976; Burnett 1976),  $\text{Cl}$  and  $\text{ClO}$  (Anderson, Margitan & Stedman 1977),  $\text{HCl}$  (Farmer, Raper & Norton 1976; Williams, Kusters, Goldman & Murcray 1976; Eyre & Roscoe 1977), and various halomethanes (Lovelock 1974, 1975, 1977; Grimsrud & Rasmussen 1975*a, b*; Heidt, Pollock & Lueb 1976).

On the conceptual level it has become clear that the stratosphere cannot be regarded as an isolated compartment. Ozone in the natural environment is removed, at least in part, by catalytic reactions involving  $\text{NO}$  (Crutzen 1970; Johnston 1971). Nitric oxide is formed in the stratosphere by photochemical decomposition of  $\text{N}_2\text{O}$  (Nicolet & Vergison 1971; McElroy & McConnell 1971; Crutzen 1971) generated by microbial processes at and below the Earth's surface (Bates & Witherspoon 1952; Goody & Walshaw 1953; Bates & Hays 1967). Stratospheric chemistry is coupled, not only to the mesosphere and troposphere, but also, in an important manner to the biosphere.

This paper is concerned primarily with an attempt to assess Man's impact on atmospheric chemistry. The anthropogenic influence is diverse and complex. Combustion of fossil fuels provides important sources of atmospheric  $\text{CO}$ ,  $\text{CO}_2$  and  $\text{H}_2$  (Keeling 1973; Jaffe 1973; Schmidt 1974). Emissions of  $\text{CO}$  may produce a significant enhancement of tropospheric ozone with possibly important consequences for air quality on a global scale. An increased burden of tropospheric  $\text{CO}$  should also lead to reduction in the concentration of tropospheric  $\text{OH}$ , with an associated increase in the lifetimes and abundances of gases such as  $\text{CH}_4$ ,  $\text{CH}_3\text{Cl}$  and  $\text{H}_2$  (Sze 1977; Penner, McElroy & Wofsy 1977). These gases play a significant rôle in stratospheric chemistry. Reaction of chlorine atoms with  $\text{CH}_4$  represents the chain terminating step for catalytic chlorine chemistry. In this sense combustion might be expected to lead to an increase in  $\text{O}_3$ . On the other hand enhanced concentrations of  $\text{CH}_3\text{Cl}$  and other halogenated hydrocarbons have the opposite effect, increasing the supply of reactive chlorine to the stratosphere. Combustion results in both direct (Pierotti & Rasmussen 1976; Weiss & Craig 1976) and indirect (McElroy, Wofsy & Yung 1977) sources of  $\text{N}_2\text{O}$  with corresponding perturbations to the nitrogen catalytic cycle. The nitrogen and chlorine cycles are coupled, resulting in further complications.

Previous attempts to assess human influences on atmospheric chemistry have emphasized effects to be expected from a single perturbation. It was estimated that a fleet of supersonic aircraft as contemplated by the United States in 1970, 500 aircraft flying 8 h per day at 16 km, would result in a global scale reduction to the level of atmospheric  $\text{O}_3$  by about 4% (C.I.A.P. 1974). Release of  $\text{CCl}_2\text{F}_2$  and  $\text{CFCl}_3$  from aerosol spray cans and refrigeration systems at rates

applicable in 1974,  $5 \times 10^5$  t (Cl) per year, was predicted to cause a 7% reduction in  $O_3$  at steady state (National Academy of Sciences 1976). Nitrous oxide formed by denitrification of agriculturally related nitrogen could lead to reductions in  $O_3$  as large as 20% by the end of the next century (McElroy 1976; McElroy *et al.* 1977).

The calculations on which these estimates were based employed a number of simplifying assumptions. With two exceptions, a single calculation described by the National Academy of Sciences (1976) and a recent study by Kurzeja (1977), mathematical models used diurnally averaged values to describe solar radiation. They omitted complexities associated with non-linear interactions of perturbations.

It is important that the model used to assess perturbations should provide results consistent with present laboratory and atmospheric constraints. This matter is pursued in §§ 2 and 3. Section 2 discusses present understanding of relevant chemical reactions, attempting to identify reactions of potential importance in the atmosphere for which data are either lacking or ambiguous. Models are compared with atmospheric measurements in § 3 in an effort to develop a consistent chemical scheme. The rationale for selection of specific emission models is described in § 4, while atmospheric implications are investigated in § 5.

## 2. CHEMISTRY

The chemical processes of importance for the atmosphere have been reviewed extensively in the recent literature. An excellent summary of information available up to mid 1975 is given by Nicolet (1975). We shall concentrate here on subsequent developments, focusing attention on more significant uncertainties. An overview of the important chemistry is presented schematically in figures 1–4.

Reactions important for the mesosphere include



and



The temperature dependence of the rate constant for (1) has been measured recently by Clyne & Monkhouse (1977). They found that the reaction has an activation energy of 4.2 kJ mol<sup>-1</sup> which results in a relatively slow rate for (1) at altitudes near 70 km. Reactions (2) and (3) have been investigated by Burrows, Harris & Thrush (1977). The rate constant for (3) is smaller than the value reported by Hochanadel, Ghormley & Ogren (1972) by almost a factor of 5. The measurement for (2),  $3 \times 10^{-11}$  cm<sup>3</sup> s<sup>-1</sup> at 300 K, represents the first experimental determination of a rate constant for this reaction. We adopted a value  $9 \times 10^{-11} \exp(-300/T)$  for reaction (4) consistent with measurements by Campbell & Hardy (1977) and Westenberg, deHaas & Roscoe (1970). Rate constants adopted for present purposes are summarized in table 1. We assumed small temperature dependences for reactions (2)–(4). As we shall see, the model described here affords a satisfactory representation of the available mesospheric data.

A new development in stratospheric chemistry concerns the potential importance of ClNO<sub>3</sub> (Rowland, Spencer & Molina 1976*a*). Chlorine nitrate is formed by



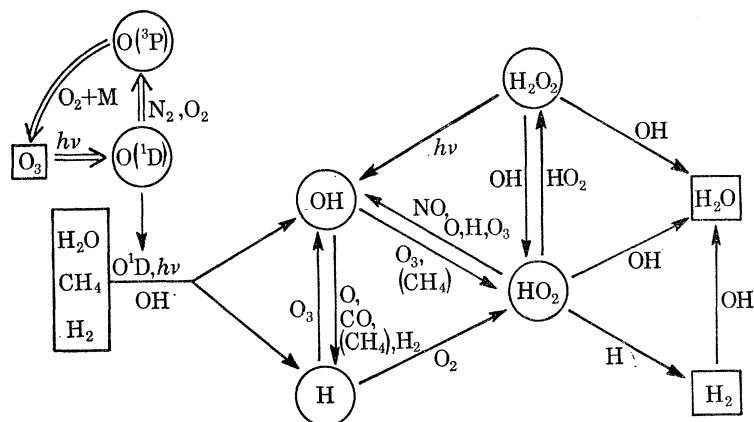


FIGURE 1. The major chemical reactions affecting  $\text{HO}_x$  ( $\text{OH}$ ,  $\text{H}$ ,  $\text{HO}_2$  and  $\text{H}_2\text{O}_2$ ) are illustrated schematically.

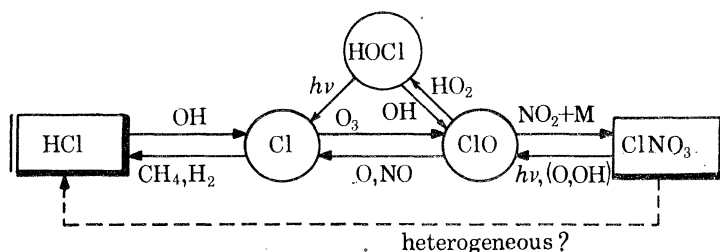


FIGURE 2. The major chemical reactions affecting  $\text{Cl}_x$  ( $\text{HCl}$ ,  $\text{Cl}$ ,  $\text{ClO}$ ,  $\text{HOCl}$  and  $\text{ClONO}_2$ ) are illustrated schematically. The dashed lines represent possible paths which are not included in the standard chemical model.

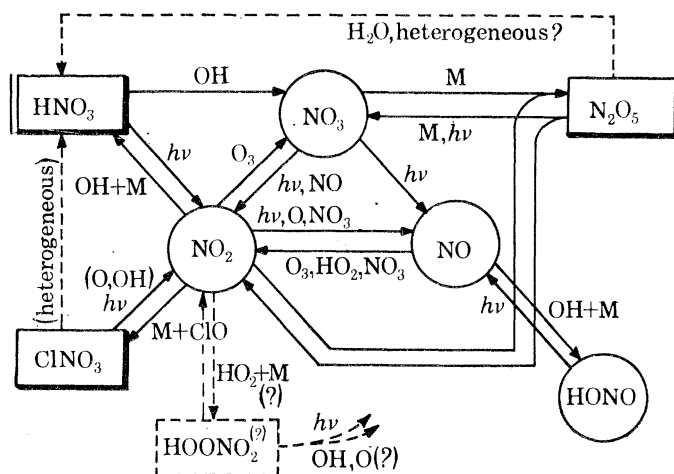


FIGURE 3. The major chemical reactions affecting  $\text{NO}_x$  ( $\text{HNO}_3$ ,  $\text{NO}_3$ ,  $\text{NO}_2$ ,  $\text{NO}$ ,  $\text{N}_2\text{O}_5$ ,  $\text{HO}_2\text{NO}_2$ ,  $\text{HONO}$ ,  $\text{ClONO}_2$ ) are illustrated schematically.

and removed both by photolysis and by reaction with  $\text{OH}$ . Products of these reactions are unknown. Smith, Chou & Rowland (1977) believe that the photolytic path may involve initial production of  $\text{ClONO}$ , by



which should be followed rapidly in the stratosphere (Molina & Molina 1977) either by



or by



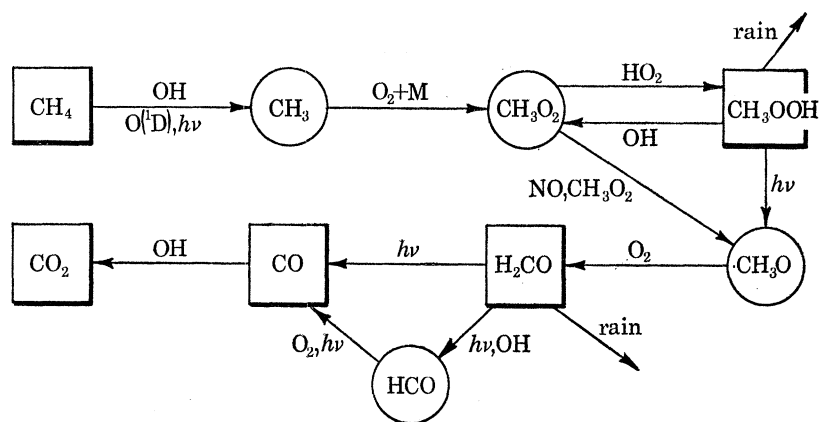


FIGURE 4. The reaction pathway from  $\text{CH}_4$  to  $\text{CO}_2$  is illustrated schematically.

This scheme involves no net change in the concentration of stratospheric odd oxygen. A similar conclusion holds for photolysis through



the path adopted by the National Academy of Sciences (1976). Photolysis of  $\text{ClNO}_3$  through



followed by

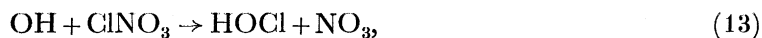


provides a possible catalytic mechanism for removal of odd oxygen. The rate for (11) is approximately 30% of the net rate for removal of  $\text{NO}_3$ , which proceeds mainly by

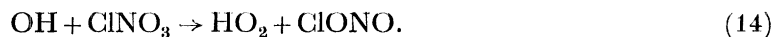


We shall adopt the reaction path favoured by the National Academy of Sciences (1976). The scheme favored by Smith *et al.* (1977) would give essentially identical results. We shall investigate the possible rôle of (10) and (11), which could have a significant impact at high concentrations of  $\text{Cl}_x$  (see figure 28).

Reaction with OH represents a minor path for removal of  $\text{ClNO}_3$ . We assume that the reaction proceeds through



though an alternate path might involve



Reaction (13) could provide a detectable source of HOCl, which may be formed in addition by



Reaction (15) followed by



and



represents a potentially important sink for  $\text{O}_3$  below about 25 km. Cross sections for photolysis of HOCl have been measured by DeMore (1977). The rate constant for (15) is unknown. A value in excess of  $10^{-11} \text{ cm}^3 \text{ s}^{-1}$  would imply a major rôle for HOCl in stratospheric chemistry.



TABLE 1a

number	reaction	rate expression†	references and notes
1	$O(^1D) + N_2 \rightarrow O(^3P) + N_2$	2.0–11 exp (+107/T)	Streit <i>et al.</i> (1976)
2	$O(^1D) + O_2 \rightarrow O(^3P) + O_2$	2.9–11 exp (+67/T)	Streit <i>et al.</i> (1976)
3a	$O(^1D) + N_2O \rightarrow NO + NO$	5.5–11	Davidson <i>et al.</i> (1977)
3b	$\rightarrow N_2 + O_2$	5.5–11	Davidson <i>et al.</i> (1977)
4a	$O(^1D) + CH_4 \rightarrow OH + CH_3$	1.3–10	Davidson <i>et al.</i> (1977)
	$\rightarrow H_2 + H_2CO$	1.3–11	Hampson & Garvin (1975)
5	$OH + CH_4 \rightarrow CH_3 + H_2O$	2.36–12 exp (–1710/T)	Davis <i>et al.</i> (1974a)
6	$OH + CO \rightarrow CO_2 + H$	2.10–13 $f(M)$ exp (–115/T) $f(M) = 1.0 (M < 7.9 + 17)$ $f(M) = 2.24 (M > 1.27 + 19)$ $f(M) = 0.92 + 1.02 - 19 M$ (7.97 + 17 < M < 1.27 + 19)	Greiner (1969); Davis <i>et al.</i> (1974a); Cox <i>et al.</i> (1976); Sic <i>et al.</i> (1976); Chan <i>et al.</i> (1977); Overend & Paraskevopoulos (1977); Perry <i>et al.</i> (1977)
7	$CO + O + M \rightarrow CO_2 + M$	2.2–36	Stuhl & Niki (1971), Slinger <i>et al.</i> (1972)
8	$O(^1D) + H_2O \rightarrow OH + OH$	2.3–10	Streit <i>et al.</i> (1976)
9	$O(^1D) + H_2 \rightarrow OH + H$	1.0–10	Davidson <i>et al.</i> (1977)
10	$O + OH \rightarrow O_2 + H$	9.0–11 exp (–300/T)	Westenberg <i>et al.</i> (1970), Campbell & Hardy (1977) est. $E_a$ .
11	$H + O_3 \rightarrow OH + O_2$	9.89–11 exp (–516/T)	Clyne & Monkhouse (1977)
12	$OH + O_3 \rightarrow HO_2 + O_2$	1.3–12 exp (–956/T)	Anderson & Kaufman (1973)
13	$HO_2 + O_3 \rightarrow OH + 2O_2$	8.3–14 exp (–1250/T)	$(k_{13}/k_{24})^{1/2}$ from Simonaitis & Hecklen (1973)
14a	$O + H_2O_2 \rightarrow O_2 + H_2O$	1.38–12 exp (–2175/T)	Davis <i>et al.</i> (1974b)
14b	$\rightarrow OH + HO_2$	1.38–12 exp (–2175/T)	Est. branching ratio
15a	$H + H_2O_2 \rightarrow H_2 + HO_2$	2.8–12 exp (–1900/T)	Baulch <i>et al.</i> (1972)
15b	$\rightarrow OH + H_2O$	5.2–12 exp (–1400/T)	Klemm <i>et al.</i> (1975)
16a	$H + HO_2 \rightarrow H_2 + O_2$	4.2–11 exp (–350/T)	Baulch <i>et al.</i> (1972)
16b	$\rightarrow OH + OH$	4.2–10 exp (–950/T)	Baulch <i>et al.</i> (1972)
17	$H + O_2 + M \rightarrow HO_2 + M$	1.90–32 exp (+350/T)	Wong & Davis (1974)
18	$OH + OH \rightarrow H_2O + O$	1.7–12	Clyne & Down (1974)
19	$O + HO_2 \rightarrow OH + O_2$	6.8–11 exp (–200/T)	Burrows <i>et al.</i> (1977) est. $E_a$
20	$OH + H_2 \rightarrow H_2O + H$	1.8–11 exp (–2350/T)	Smith & Zellner (1974)
21	$O + H_2 \rightarrow OH + H$	5.3–11 exp (–5100/T)	Westenberg & deHaas (1969)
22	$OH + H_2O_2 \rightarrow HO_2 + H_2O$	8.0–12 exp (–670/T)	Hack <i>et al.</i> (1975)
23	$OH + HO_2 \rightarrow H_2O + O_2$	1.0–10 exp (–200/T)	Burrows <i>et al.</i> (1977) est. $E_a$
24	$HO_2 + HO_2 \rightarrow H_2O_2 + O_2$	1.9–11 exp (–500/T)	Paukert & Johnston (1972) Hamilton (1975), est. $E_a$
25	$N + O_2 \rightarrow NO + O$	1.1–14 $T$ exp (–3150/T)	Baulch <i>et al.</i> (1973)
26	$OH + HCl \rightarrow H_2O + Cl$	2.0–12 exp (–313/T)	Zahniser <i>et al.</i> (1974)
27	$Cl + H_2 \rightarrow HCl + H$	4.7–11 exp (–2340/T)	Watson (1977)
28	$H + HCl \rightarrow Cl + H_2$	2.3–11 exp (–1816/T)	estimated from the reverse reaction
29	$O + HCl \rightarrow OH + Cl$	2.5–12 exp (–2980/T)	Brown & Smith (1975)
30	$Cl + O_3 \rightarrow ClO + O_2$	2.7–11 exp (–257/T)	Watson (1977)
31	$Cl + Cl + M \rightarrow Cl_2 + M$	1.6–33 exp (+800/T)	Widman & DeGraff (1973)
32	$ClO + NO \rightarrow Cl + NO_2$	1.7–11	Clyne & Watson (1974)
33	$ClO + O \rightarrow Cl + O_2$	1.1–10 exp (–220/T)	Clyne & Nip (1976)
34	$ClO + NO_2 + M \rightarrow ClONO_2 + M$	$3.33 - 23T^{-3.34}M$ $1 + 8.7 - 9T^{-0.6}M^{0.5}$	Zahniser <i>et al.</i> (1977)
35	$O + ClONO_2 \rightarrow$ products	3.4–12 exp (–840/T)	Molina <i>et al.</i> (1977) products taken to be ClO + NO <sub>2</sub>
36	$OH + ClONO_2 \rightarrow$ products	1.2–12 exp (–333/T)	Zahniser <i>et al.</i> (1977) products taken to be HOCl + NO <sub>2</sub>
37	$H + Cl_2 \rightarrow HCl + Cl$	1.40–10 exp (–589/T)	Bemand & Clyne (1977)
38	$O + Cl_2 \rightarrow ClO + Cl$	4.15–12 exp (–1368/T)	Watson (1977)
39	$H + ClO \rightarrow OH + Cl$	1.0–11	estimated
40	$Cl + H_2O_2 \rightarrow HCl + HO_2$	2.0–11 exp (–1050/T)	Watson (1977), est. $E_a$
41	$Cl + HO_2 \rightarrow HCl + O_2$	8.1–11 exp (–300/T)	Leu & DeMore (1976) est. $E_a$
42	$ClO + HO_2 \rightarrow HOCl + O_2$	2.0–12	estimated
43	$OH + HOCl \rightarrow H_2O + ClO$	8.0–12 exp (–670/T)	estimated
44	$Cl + CH_4 \rightarrow CH_3 + HCl$	8.2–12 exp (–1320/T)	Zahniser <i>et al.</i> (1978)
45	$OH + CH_3Cl \rightarrow$ products	2.18–12 exp (–1142/T)	Watson (1977)

TABLE 1a. (cont.)

number	reaction	rate expression†	references and notes
46	$\text{OH} + \text{CH}_3\text{CCl}_3 \rightarrow \text{products}$	3.72–12 exp (–1627/T)	Watson <i>et al.</i> (1977)
47	$\text{OH} + \text{CH}_2\text{O} \rightarrow \text{HCO} + \text{H}_2\text{O}$	1.4–11	Morris & Niki (1971)
48	$\text{N} + \text{NO} \rightarrow \text{N}_2 + \text{O}$	8.2–11 exp (–410/T)	Clyne & McDermid (1975)
49	$\text{O} + \text{NO}_2 \rightarrow \text{NO} + \text{O}_2$	9.12–12	Davis <i>et al.</i> (1973a)
50	$\text{O}_3 + \text{NO} \rightarrow \text{NO}_2 + \text{O}_2$	1.5–12 exp (–1330/T)	Baulch <i>et al.</i> (1973)
51	$\text{H} + \text{NO}_2 \rightarrow \text{OH} + \text{NO}$	4.81–10 exp (–405/T)	Clyne & Monkhouse (1977)
52	$\text{O}_3 + \text{NO}_2 \rightarrow \text{O}_2 + \text{NO}_3$	1.34–13 exp (–2466/T)	Graham & Johnston (1974)
53	$\text{O} + \text{NO} + \text{M} \rightarrow \text{NO}_2 + \text{M}$	4.0–33 exp (+940/T)	Baulch <i>et al.</i> (1973)
54	$\text{O} + \text{NO}_2 + \text{M} \rightarrow \text{NO}_3 + \text{M}$	1.0–31	Hampson (1973)
55	$\text{NO} + \text{NO}_3 \rightarrow \text{NO}_2 + \text{NO}_2$	8.7–12	Harker & Johnston (1973)
56	$\text{NO}_2 + \text{NO}_3 \rightarrow \text{NO} + \text{NO}_2 + \text{O}_2$	2.3–13 exp (–1600/T)	Baulch <i>et al.</i> (1973)
57	$\text{NO}_3 + \text{NO}_3 \rightarrow 2\text{NO}_2 + \text{O}_2$	5.0–12 exp (–3000/T)	Schott & Davidson (1958)
58	$\text{N} + \text{NO}_2 \rightarrow \text{N}_2\text{O} + \text{O}$	1.4–12	Clyne & McDermid (1975)
59	$\text{OH} + \text{HNO}_3 \rightarrow \text{H}_2\text{O} + \text{NO}_3$	8.9–14	Margitan <i>et al.</i> (1975)
60	$\text{HO}_2 + \text{NO} \rightarrow \text{OH} + \text{NO}_2$	8.25–11 exp (–700/T)	Howard & Evenson (1977)
61	$\text{N} + \text{O}_3 \rightarrow \text{NO} + \text{O}_2$	5.7–13	Phillips & Schiff (1962)
62	$\text{OH} + \text{NO} + \text{M} \rightarrow \text{HNO}_2 + \text{M}$	$k_2 = 2.74\text{--}12 \exp (+850/T)$ $k_2/k_3 = 1.12 + 20$ $\left(\frac{1}{k_1}\right)^{\frac{1}{2}} = \left(\frac{1}{k_2}\right)^{\frac{1}{2}} + \left(\frac{1}{k_3 M}\right)^{\frac{1}{2}}$ $k(M = \text{N}_2) = 1.5 k_1(M = \text{Ar})$	fit to data of Atkinson <i>et al.</i> (1975)
63	$\text{O} + \text{HNO}_3 \rightarrow \text{OH} + \text{NO}_3$	3.0–17	Chapman & Wayne (1974)
64	$\text{H} + \text{HNO}_3 \rightarrow \text{H}_2 + \text{NO}_3$	2.0–15	Chapman & Wayne (1974)
65	$\text{O} + \text{O}_2 + \text{M} \rightarrow \text{O}_3 + \text{M}$	1.05–34 exp (+510/T)	Huie <i>et al.</i> (1972)
66	$\text{O} + \text{O}_3 \rightarrow \text{O}_2 + \text{O}_2$	2.0–11 exp (–2280/T)	Davis <i>et al.</i> (1973c)
67	$\text{O} + \text{O} + \text{M} \rightarrow \text{O}_2 + \text{M}$	9.59–34 exp (+480/T)	fit to data of Campbell & Gray (1973)
68	$\text{NO} + \text{NO} + \text{O}_2 \rightarrow \text{NO}_2 + \text{NO}_2$	3.30–39 exp (+530/T)	Baulch <i>et al.</i> (1973)
69	$\text{NO}_2 + \text{NO}_3 + \text{M} \rightarrow \text{N}_2\text{O}_5 + \text{M}$ $\text{N}_2\text{O}_5 + \text{M} \rightarrow \text{NO}_2 + \text{NO}_3$		see expression adopted by McConnell & McElroy (1973)
70	$\text{N} + \text{OH} \rightarrow \text{NO} + \text{H}$	6.8–11	Campbell & Thrush (1968)
71	$\text{N} + \text{O} \rightarrow \text{NO} + h\nu$	1.0–17	Nicolet (1965)
72	$\text{H} + \text{H} + \text{M} \rightarrow \text{H}_2 + \text{M}$	8.3–33	Baulch <i>et al.</i> (1972)
73	$\text{NO} + \text{O} \rightarrow \text{NO}_2 + h\nu$	4.2–18	Becker <i>et al.</i> (1973)
74	$\text{OH} + \text{HNO}_2 \rightarrow \text{H}_2\text{O} + \text{NO}_2$	6.6–12	Cox <i>et al.</i> (1976)
75	$\text{HO}_2 + \text{NO}_2 \rightarrow \text{HNO}_2 + \text{O}_2$	3.0–15	Howard (1977)
76a	$\text{HO}_2 + \text{NO}_2 \xrightarrow{\text{M}} \text{HO}_2\text{NO}_2$	$k_2 = 1.0\text{--}13$ $k_2/k_3 = 5.0 + 17$ $\frac{1}{k} = \frac{1}{k_2} + \frac{1}{k_3 M}$	$k_3$ from Howard (1977) $k_2$ estimated
76b	$\text{HO}_2\text{NO}_2 \xrightarrow{\text{M}} \text{HO}_2 + \text{NO}_2$	1.4 + 14 exp (–10400/T)	Graham <i>et al.</i> (1977)
77	$\text{OH} + \text{HO}_2\text{NO}_2 \rightarrow \text{H}_2\text{O} + \text{O}_2 + \text{NO}_2$	5.0–13	estimated
78	$\text{OH} + \text{CH}_3\text{OOH} \rightarrow \text{CH}_3\text{O}_2 + \text{H}_2\text{O}$	5.2–12 exp (–670/T)	estimated
79	$\text{CH}_3\text{OO} + \text{NO} \rightarrow \text{CH}_3\text{O} + \text{NO}_2$	5.3–12 exp (–500/T)	estimated
80	$\text{CH}_3\text{OO} + \text{HO}_2 \rightarrow \text{CH}_3\text{OOH} + \text{O}_2$	5.3–12 exp (–500/T)	estimated
81	$\text{CH}_3\text{OO} + \text{CH}_3\text{OO} \rightarrow 2\text{CH}_3\text{O} + \text{O}_2$	2.00–12 exp (–500/T)	Hochandel <i>et al.</i> (1977) est. $E_a$
82	$\text{OH} + \text{NO}_2 + \text{M} \rightarrow \text{HNO}_3 + \text{M}$	$k_2 = 2.77\text{--}11$ $k_3 = 7.14\text{--}32 \exp (1080/T)$ $\left(\frac{1}{k_1}\right)^{\frac{1}{2}} = \left(\frac{1}{k_2}\right)^{\frac{1}{2}} + \left(\frac{1}{k_3 M}\right)^{\frac{1}{2}}$ $k(M = \text{air}) = 0.95 k_1(M = \text{N}_2)$	fit to the data of Anastasi & Smith (1976)
83	soluble gas $\rightarrow$ precipitation scavenging (units: $\text{s}^{-1}$ ) (HCl, HNO <sub>3</sub> , HNO <sub>2</sub> , HO <sub>2</sub> NO <sub>2</sub> , H <sub>2</sub> O <sub>2</sub> , H <sub>2</sub> CO, CH <sub>3</sub> OOH)	2.31–6 0 < z ≤ 4 km 1.16–6 4 < z ≤ 6 km 5.79–6 6 < z ≤ 8 km 2.31–7 8 < z ≤ 10 km 7.72–8 10 < z ≤ 14 km 0 14 km < z	see Wofsy (1976)



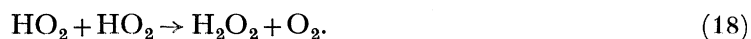
TABLE 1*a*. (*cont.*)

number	photolytic process	references and notes
84	$\text{NO} + h\nu \rightarrow \text{N} + \text{O}$	see table 1 <i>b</i>
85	$\text{N}_2\text{O}_5 + h\nu \rightarrow \text{NO}_2 + \text{NO}_3$	Graham & Johnston (1978)
86	$\text{NO}_2 + h\nu \rightarrow \text{NO} + \text{O}$	Hall & Blacet (1952)
87	$\text{HNO}_2 + h\nu \rightarrow \text{OH} + \text{NO}$	Cox & Derwent (1976)
88	$\text{HNO}_3 + h\nu \rightarrow \text{OH} + \text{NO}_2$	Johnston & Graham (1974)
89	$\text{N}_2\text{O} + h\nu \rightarrow \text{N}_2 + \text{O}(^1\text{D})$	$\lambda > 1730 \text{ \AA}$ Selwyn <i>et al.</i> (1977) values at 243 K $\lambda < 1730 \text{ \AA}$ Zelikoff <i>et al.</i> (1953), Romand & Mayence (1949)
90 <i>a</i>	$\text{NO}_3 + h\nu \xrightarrow{1} \text{NO} + \text{O}_2$	Graham & Johnston (1978)
90 <i>b</i>	$\xrightarrow{2} \text{NO}_2 + \text{O}$	
91	$\text{O}_3 + h\nu \rightarrow \text{O}_2 + \text{O}$	Griggs (1968), Philen <i>et al.</i> (1977)
92	$\text{O}_2 + h\nu \rightarrow \text{O} + \text{O}$	$\lambda < 2000 \text{ \AA}$ † See table 1 <i>b</i> $\lambda > 2000 \text{ \AA}$ Ditchburn & Young (1962)
93	$\text{H}_2\text{O} + h\nu \rightarrow \text{H} + \text{OH}$	$\lambda > 1800 \text{ \AA}$ Thompson <i>et al.</i> (1963) $\lambda < 1800 \text{ \AA}$ Watanabe & Zelikoff (1953)
94	$\text{CH}_4 + h\nu \rightarrow \text{CH}_2 + \text{H}_2$	Sun & Weissler (1954), Watanabe <i>et al.</i> (1953)
95	$\text{CO}_2 + h\nu \rightarrow \text{CO} + \text{O}$	Shemansky (1972)
96	$\text{H}_2\text{O}_2 + h\nu \rightarrow \text{OH} + \text{OH}$	Schumb <i>et al.</i> (1955)
97	$\text{CH}_3\text{OOH} + h\nu \rightarrow \text{CH}_3\text{O} + \text{OH}$	$0.65 \times J_{\text{H}_2\text{O}_2}$ estimated
98	$\text{HO}_2 + h\nu \rightarrow \text{OH} + \text{H}$	Paukert & Johnston (1972)
99	$\text{H}_2\text{CO} + h\nu \rightarrow \text{HCO} + \text{H}$ $\rightarrow \text{H}_2 + \text{CO}$	Calvert <i>et al.</i> (1972)
100	$\text{Cl}_2 + h\nu \rightarrow \text{Cl} + \text{Cl}$	Seery & Britton (1964), Gibson & Bayliss (1933)
101	$\text{HCl} + h\nu \rightarrow \text{H} + \text{Cl}$	Inn (1975)
102	$\text{ClO} + h\nu \rightarrow \text{Cl} + \text{O}$	Johnston <i>et al.</i> (1969), Clyne & Coxon (1968)
103	$\text{ClNO}_3 + h\nu \rightarrow \text{ClO} + \text{NO}_2$	Rowland <i>et al.</i> (1976 <i>b</i> )
104	$\text{CF}_2\text{Cl}_2 + h\nu \rightarrow \text{CF}_2\text{Cl} + \text{Cl}$	Chou <i>et al.</i> (1977) (230 K)
105	$\text{CFCl}_3 + h\nu \rightarrow \text{CFCl}_2 + \text{Cl}$	Chou <i>et al.</i> (1977) (230 K)
106	$\text{CCl}_4 + h\nu \rightarrow \text{CCl}_3 + \text{Cl}$	Rowland & Molina (1975)
107	$\text{CH}_2\text{Cl} + h\nu \rightarrow \text{CH}_2 + \text{Cl}$	Robbins (1976)
108	$\text{CH}_3\text{CCl}_3 + h\nu \rightarrow \text{CH}_3\text{CCl}_2 + \text{Cl}$	Chou, Ruiz, Moe & Rowland, private communication in Watson (1977)
109	$\text{HOCl} + h\nu \rightarrow \text{OH} + \text{Cl}$	DeMore <i>et al.</i> (1977)
110	$\text{HO}_2\text{NO}_2 + h\nu \rightarrow \text{OH} + \text{NO}_3$	$1.5 \times J_{\text{H}_2\text{O}_2}$ estimate

† Units:  $\text{cm}^3 \text{ s}^{-1}$  for bimolecular reactions;  $\text{cm}^6 \text{ s}^{-1}$  for termolecular reactions. The notation 1.0–1.1 is intended to be read as  $1.0 \times 10^{-11}$ .

‡  $1 \text{ \AA} = 0.1 \text{ nm} = 10^{-10} \text{ m}$ .

We adopted a somewhat smaller value, basing our choice on laboratory studies of the iso-electronic process



Assessment of the possible rôles of  $\text{ClNO}_3$  and  $\text{HOCl}$  requires an accurate treatment for the diurnal cycle of solar radiation. The important species  $\text{OH}$ ,  $\text{HO}_2$ ,  $\text{O}$ ,  $\text{NO}_2$ ,  $\text{ClO}$  and  $\text{ClNO}_3$  exhibit significant and complex diurnal variations, as shown in figure 5. Models based on the assumption of a diurnal mean insolation lead to an underestimate of the net rate for the key reaction



The discrepancy arises in part due to inadequacies of the simple models, which tend to overestimate the daytime concentration of  $\text{ClNO}_3$ . It may be attributed also to difficulties which arise due to covariance of the concentrations for  $\text{ClO}$  and  $\text{O}$ . Our model allows for backscatter of solar radiation from the lower atmosphere, as described by Yung (1976). Scattered radiation

is important at longer wavelengths where it leads to a significant increase in the rates for photolysis of  $\text{ClNO}_3$ ,  $\text{HOCl}$  and  $\text{NO}_2$  and to an enhanced source for  $\text{O}(^1\text{D})$ .

Another development of note concerns the rate for reaction of  $\text{NO}$  with  $\text{HO}_2$ ,



Howard & Evenson (1977), using laser magnetic resonance to monitor  $\text{HO}_2$ , find a rate for this reaction at room temperature of  $8 \times 10^{-12} \text{ cm}^3 \text{ s}^{-1}$ , significantly larger than indirect measurements reported earlier by Davis, Payne & Stief (1973*b*), Cox & Derwent (1975), Hack, Hoyerman & Wagner (1975) and Simonaitis & Hecklen (1976). The reaction is of considerable

TABLE 1*b*. SCHUMANN-RUNGE BAND PARAMETERS

wavelength interval Å	temp. K	cross sections/cm <sup>2</sup>					
1775-1783	190	4.33 (-21)	4.89 (-21)	6.63 (-21)	1.60 (-20)	7.20 (-20)	1.59 (-18)
1783-1793	190	2.10 (-21)	2.32 (-21)	3.02 (-21)	6.30 (-21)	3.46 (-20)	7.52 (-19)
1793-1804	190	5.95 (-22)	9.75 (-22)	2.53 (-21)	7.57 (-21)	7.38 (-20)	7.44 (-19)
1804-1816	190	3.33 (-22)	1.02 (-21)	4.09 (-21)	1.63 (-20)	8.79 (-20)	3.81 (-19)
1816-1825	190	1.09 (-21)	1.16 (-21)	1.45 (-21)	3.32 (-21)	2.00 (-20)	4.04 (-19)
1825-1831	270	1.15 (-21)	1.30 (-21)	1.90 (-21)	4.89 (-21)	2.62 (-20)	4.08 (-19)
1831-1846	270	3.90 (-22)	4.90 (-22)	9.49 (-22)	3.33 (-21)	2.14 (-20)	2.39 (-19)
1846-1863	270	1.29 (-22)	2.18 (-22)	8.28 (-22)	3.46 (-21)	1.94 (-20)	1.06 (-19)
1863-1882	270	6.26 (-23)	7.80 (-23)	2.62 (-22)	1.83 (-21)	1.25 (-20)	6.95 (-20)
1882-1902	270	2.74 (-23)	3.58 (-23)	8.64 (-23)	4.03 (-22)	2.13 (-21)	1.95 (-20)
1902-1925	270	1.95 (-23)	2.44 (-23)	4.89 (-23)	2.87 (-22)	1.95 (-21)	1.36 (-20)
1925-1947	230	1.84 (-23)	1.96 (-23)	2.71 (-23)	8.52 (-23)	6.48 (-22)	3.89 (-21)
1947-1972	230	1.80 (-23)	1.81 (-23)	1.87 (-23)	2.69 (-23)	1.34 (-22)	1.52 (-21)
1972-1985	230	1.80 (-23)	1.80 (-23)	1.82 (-23)	2.40 (-23)	5.71 (-23)	5.70 (-22)
1985-2000	230	1.76 (-23)	1.76 (-23)	1.76 (-23)	1.76 (-23)	1.76 (-23)	3.50 (-23)
2000-2025	230	1.71 (-23)	1.71 (-23)	1.71 (-23)	1.71 (-23)	1.71 (-23)	2.68 (-23)
weight( $w_i$ )		0.05	0.20	0.25	0.25	0.20	0.05

The transmission  $T$  in any wavelength interval is given by

$$T(\lambda_1, \lambda_2) = \sum_{i=1}^6 w_i \exp [-(\sigma_i C + Q)/\cos \chi],$$

where  $\chi$  is the solar zenith angle,  $C$  is the  $\text{O}_2$  vertical column and  $Q$  is any additional opacity source. The photodissociation rate  $J_{\text{O}_2}$  is given by

$$J_{\text{O}_2}(\lambda_1, \lambda_2) = F(\lambda_1, \lambda_2) \sum_{i=1}^6 w_i \sigma_i \exp [-(\sigma_i C + Q)/\cos \chi],$$

where  $F$  is the solar flux incident on the top of the atmosphere. Photolysis of  $\text{NO}$  in the  $\delta(0, 0)$  band is associated with transmission in the wavelength interval 1902-1925 Å and with a mean cross section of  $3.67 \times 10^{-18} \text{ cm}^2$ . The  $\delta(1, 0)$  band lies in the interval 1816-1825 Å and has a mean cross section of  $1.96 \times 10^{-17} \text{ cm}^2$ . This formulation provides a representation of the opacity distribution functions of Fang *et al.* (1974), and adequately reproduces the observed transmission of  $\text{O}_2$  reported by Hudson & Mahle (1972).

importance for the stratosphere. It provides a source for  $\text{OH}$  and, coupled with photolysis of  $\text{NO}_2$ , a source also for odd oxygen. The large discrepancy between new and old measurements for (20) raises questions with regard to the validity of rate expressions reported earlier for other reactions involving  $\text{HO}_2$ , for example,



and reaction (18). We shall return to this matter later, in § 5.

Several investigators (Simonaitis & Hecklen 1976; Niki, Maker, Savage & Breitenbach 1977; Howard 1977) have raised the possibility that reaction of  $\text{NO}_2$  with  $\text{HO}_2$  might lead to

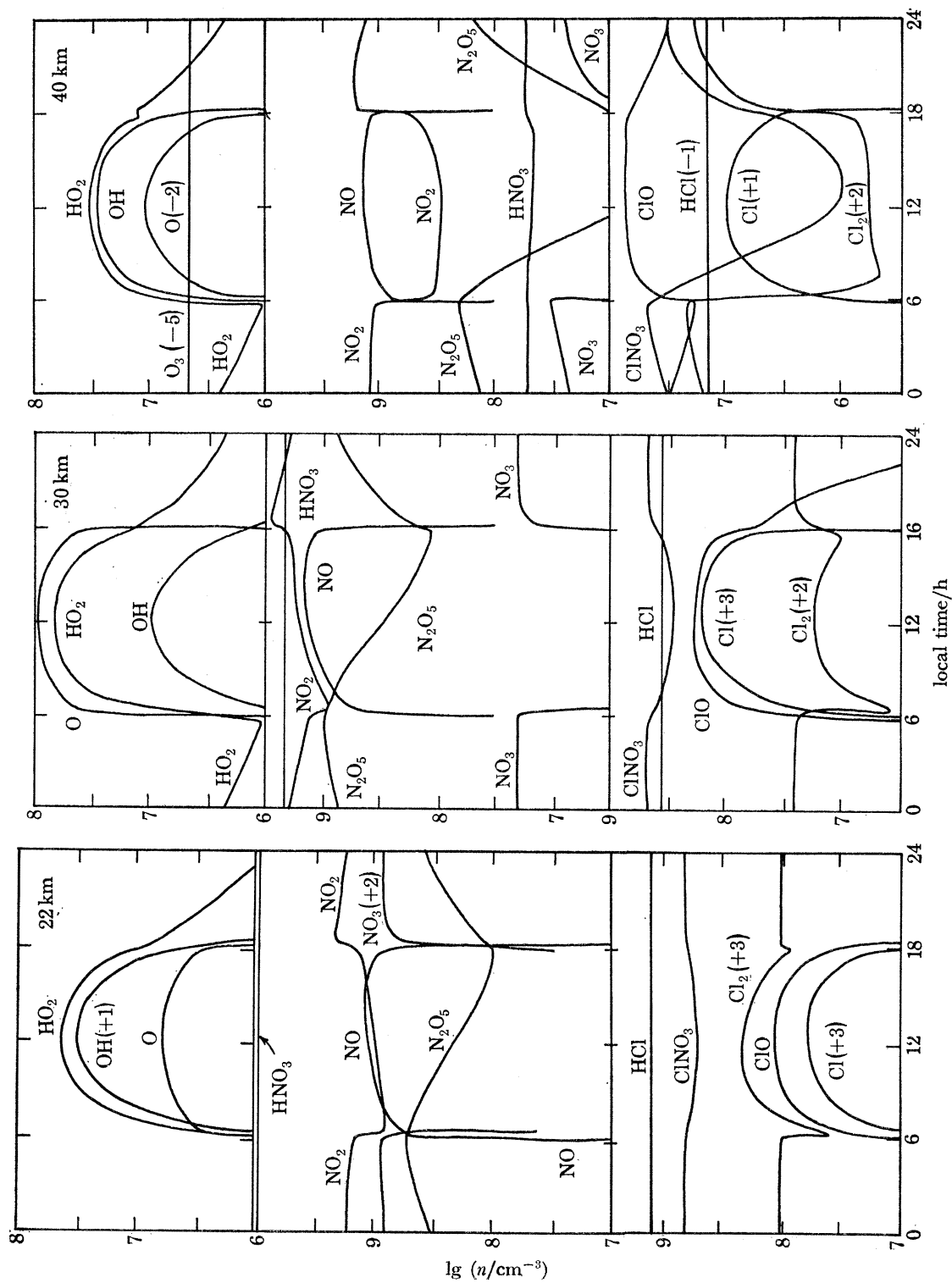


FIGURE 5. The diurnal variations of several species at 22, 30 and 40 km are shown for 30° N latitude and 0° solar declination. The notation (-2) indicates that the number density for that species has been multiplied by  $10^{-2}$ .

formation of pernitric acid,  $\text{HO}_2\text{NO}_2$ . The subsequent chemistry of this compound is unknown. It will be treated here according to the scheme



followed by



by thermal decomposition (Graham, Winer & Pitts 1977), or by rain out. The rate for (22) has been measured by Howard (1977). Table 1 includes estimates of rates for (23) and (24). Pernitric acid could represent a sink for odd nitrogen in the lower stratosphere and troposphere. It could provide also a source of tropospheric odd oxygen, through (23) followed by (12), and it might be detectable in the atmosphere with current spectroscopic techniques. With our estimated reaction rates,  $\text{HO}_2\text{NO}_2$  plays only a minor rôle in atmospheric chemistry.

Recent studies of the reaction



indicate that the rate for this process may be a function of ambient pressure (Cox, Derwent & Holt 1976; Sie, Simonaitis & Heicklen 1976; Chan, Uselman, Calvert & Shaw 1977; Overend & Paraskevopoulos 1977; Perry, Atkinson & Pitts 1977). The effective rate constant at a pressure of one atmosphere appears to exceed the low pressure value by about a factor of 2, with consequent implications for the budgets of tropospheric CO and OH. The mechanism for reaction of CO with OH at high pressures is not well understood. The laboratory data indicate that the effective reaction rate is a sensitive function of the particular choice of background gas and data to define the behaviour in air are incomplete. Further work is clearly required in order to resolve this issue. The pressure dependent rate expression used here is given in table 1.

### 3. THE PRESENT ATMOSPHERE

This section addresses the question of whether models based on our understanding of chemistry as discussed above provide results consistent with available atmospheric constraints. Of special relevance in this context are measurements of mesospheric and stratospheric OH by Anderson (1971, 1975, 1976) and Burnett (1976, 1977), measurements of stratospheric Cl and ClO by Anderson *et al.* (1977), measurements of stratospheric HCl by Lazrus, Gandrud & Woodard (1976), Ackerman *et al.* (1976), Raper, Farmer, Toth & Robbins (1977) and Eyre & Roscoe (1977), data on  $\text{O}_3$  from a variety of sources (Miller & Stewart 1965; Evans, Hunten, Llewellyn & Jones 1968; Hilsenrath, Serdon & Goodman 1969; Krueger, Heath & Mateer 1973; Hering & Borden 1967; Hering 1975; Watanabe & Tohmatsu 1976), measurements of total column  $\text{NO}_2$  densities (Noxon 1975; Noxon *et al.* 1977), and measurements of total column  $\text{HNO}_3$  densities by Murcray *et al.* (1975).

Mesospheric OH and  $\text{O}_3$  data give indirect information on the concentration of mesospheric  $\text{H}_2\text{O}$ , together with some check on the validity of rate expressions adopted for reactions (1)–(4). The concentration of stratospheric OH reflects assumptions regarding the concentration of stratospheric  $\text{H}_2\text{O}$ , and rates for the  $\text{HO}_2$  reactions, (2), (3), (20) and (21). Measurements of stratospheric Cl, ClO and HCl have implications with regard to the total concentration of stratospheric chlorine, and for the validity of the scheme used to treat the chlorine catalytic

cycle. Column densities of  $\text{NO}_2$  and  $\text{HNO}_3$  provide global perspective on the distribution of nitrogen oxides.

Concentrations of the long lived gases  $\text{N}_2\text{O}$ ,  $\text{NO}_x$ ,  $\text{CH}_4$ ,  $\text{H}_2$ ,  $\text{Cl}_x$  and chlorocarbons were calculated using the concept of quasi-horizontal mixing surfaces (McElroy, Elkins, Wofsy &

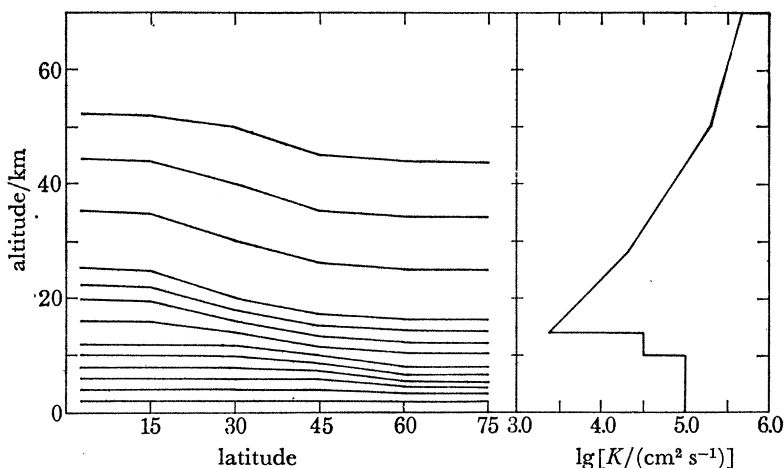


FIGURE 6a. The left panel shows preferred surfaces for horizontal mixing. The vertical diffusion coefficient at  $30^\circ\text{N}$  latitude is shown on the right.

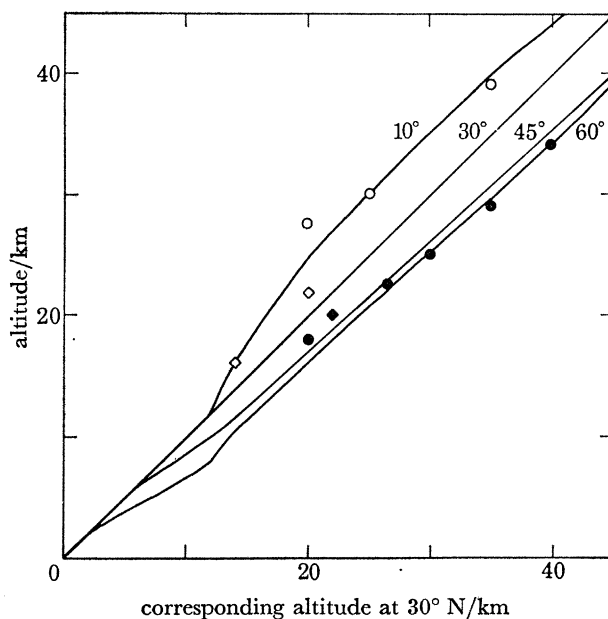


FIGURE 6b. An alternative representation of the mixing surfaces in figure 6a is given. For each latitude, a given altitude at  $30^\circ\text{N}$  (abscissa) is projected onto the corresponding altitude on the ordinate. The symbols show the data used to construct the mixing surfaces; ● ( $40^\circ$ – $50^\circ\text{N}$ ) and ○ ( $10^\circ\text{N}$ ) are from the  $\text{N}_2\text{O}$  measurements of Schmeltekopf *et al.* (1977) and Goldan (1977); ◆ ( $40^\circ$ – $50^\circ\text{N}$ ) and ◇ ( $10^\circ\text{N}$ ) are from  $\text{C}^{14}$  and  $\text{Sr}^{90}$  measurements of List & Telegadas (1969).

Yung 1976) to define latitudinal distributions, in combination with a one-dimensional model to specify average vertical structure. Preferred surfaces for horizontal mixing were identified by using observations of  $\text{Sr}^{90}$  and  $\text{C}^{14}$  (List & Telegadas 1969), supplemented in the equatorial region with recent data for  $\text{N}_2\text{O}$  (Schmeltekopf *et al.* 1977; Goldan 1977). The mixing surfaces



are shown in figure 6. The one-dimensional model is applied at 30° N latitude where data exist for several important trace species including CH<sub>4</sub>. Observations of CH<sub>4</sub> were used to select a set of effective vertical diffusion coefficients as described by Wofsy & McElroy (1973). These coefficients are included in figure 6. They are similar to values used in a variety of recent atmospheric studies (McElroy, Wofsy, Penner & McConnell 1974; Wofsy, McElroy & Sze 1975*a*; Wofsy, McElroy & Yung 1975*b*; Johnston 1976; Hunten 1975; McElroy *et al.* 1977) and agree with results for N<sub>2</sub>O reported by Schmeltekopf *et al.* (1977).

TABLE 2. BOUNDARY CONDITIONS (1975)

species	volume mixing ratio (0 km)	species	volume mixing ratio (0 km)
N <sub>2</sub> O	3.0–7	CFCl <sub>3</sub>	1.2–10
NO <sub>x</sub> †	5.0–10	CF <sub>2</sub> Cl <sub>2</sub>	2.0–10
CH <sub>4</sub>	1.44–6	CCl <sub>4</sub>	1.1–10
CO	1.19–7	CH <sub>3</sub> Cl	1.0–9
H <sub>2</sub>	5.0–7	CH <sub>3</sub> CCl <sub>3</sub>	5.0–11
O <sub>3</sub>	2.6–8	Cl <sub>x</sub> ‡	1.0–9

Upper boundary conditions: zero flux at 80 km

† NO<sub>x</sub> = NO + NO<sub>2</sub> + NO<sub>3</sub> + 2 × N<sub>2</sub>O<sub>5</sub> + ClNO<sub>3</sub> + HNO<sub>3</sub> + HONO + HO<sub>2</sub>NO<sub>2</sub>.

‡ Cl<sub>x</sub> = HCl + Cl + ClO + ClNO<sub>3</sub> + HOCl + Cl<sub>2</sub>.

The atmosphere contains gases with a wide range of chemical lifetimes. Our selection of long lived gases includes only those species for which the chemical lifetime is very much longer than a day. The concentration,  $n_i$ , of these species at 30° N latitude is assumed to satisfy a continuity relation of the form

$$\frac{\partial n_i}{\partial t} + \frac{\partial \phi_i}{\partial z} = \bar{P}_i - \bar{L}_i, \quad (26)$$

where  $\phi_i$  denotes the vertical flux (molecules cm<sup>-2</sup> s<sup>-1</sup>) of species  $i$  and the symbols  $\bar{P}_i$  and  $\bar{L}_i$  indicate diurnally averaged values for the production and loss rates of  $i$  at altitude  $z$ . Equation (26) is solved subject to boundary conditions as summarized in table 2. The chemical terms  $\bar{P}_i$  and  $\bar{L}_i$  are influenced in general by the complex diurnal variation of other species. The concentrations of short lived species,  $j$ , defined to include gases with chemical lifetimes shorter than relevant times for transport, are found by solving local continuity equations

$$dn_j/dt = P_j(\{n_k\}, t) - L_j(\{n_k\}, t). \quad (27)$$

Short lived species include O(<sup>3</sup>P), O(<sup>1</sup>D), NO, NO<sub>2</sub>, NO<sub>3</sub>, N<sub>2</sub>O<sub>5</sub>, HNO<sub>2</sub>, HNO<sub>3</sub>, HO<sub>2</sub>NO<sub>2</sub>, ClNO<sub>3</sub>, HCl, Cl, Cl<sub>2</sub>, ClO, HOCl, H, OH, HO<sub>2</sub> and H<sub>2</sub>O<sub>2</sub>. Averaged production and loss rates for species  $i$  were obtained by numerical integration of the instantaneous rates  $P_i(t)$  and  $L_i(t)$ .

The coupled set of equations defined by (27) was treated numerically with an implicit finite difference representation adapted from Richtmeyer (1957),

$$n_j(\Delta t)/\Delta t - [P(\{n_k(\Delta t)\}, \Delta t) - L(\{n_k(\Delta t)\}, \Delta t)] - n_j(0)/\Delta t = 0. \quad (28)$$

This equation must be solved with a precision adequate to ensure conservation of mass to high accuracy over a diurnal cycle. The method adopted here conserves mass to better than 1 part in 10<sup>6</sup>. Periodic boundary conditions are imposed by a simple variational technique (see, for example, Wofsy 1978).

Height profiles at various latitudes as calculated for several of the longer lived species are

shown in figures 7 ( $\text{N}_2\text{O}$ ), 8 ( $\text{CH}_4$ ,  $\text{CO}$ ) and 9 ( $\text{CFCl}_3$ ,  $\text{CF}_2\text{Cl}_2$ ,  $\text{CCl}_4$ ,  $\text{CH}_3\text{Cl}$ ). Figure 7 includes a comparison of model results with vertical profiles for  $\text{N}_2\text{O}$  as measured at mid-latitudes by Heidt *et al.* (1976), Schmeltekopf *et al.* (1977), and Goldan (1977). A similar comparison with data for  $\text{CH}_4$  (Ehhalt 1974; Ehhalt *et al.* 1975*b*; Volz *et al.* 1976) and  $\text{CO}$  (Volz *et al.* 1976) is given in figure 8. Model results are in satisfactory accord with observational data for all gases with the exception of  $\text{CF}_2\text{Cl}_2$  and  $\text{CO}$ . The discrepancy which appears for  $\text{CF}_2\text{Cl}_2$  at higher altitudes may be attributed to its short lifetime relative to  $\text{N}_2\text{O}$  or  $\text{CH}_4$ , and is unimportant for present purposes. The agreement lends confidence to the procedures adopted to simulate both vertical and lateral transport, at least for the lower stratosphere. Extension of the data base to higher altitudes is obviously desirable. Results in figures 5 and 7–9 were obtained by using the standard chemical model as defined in table 1.

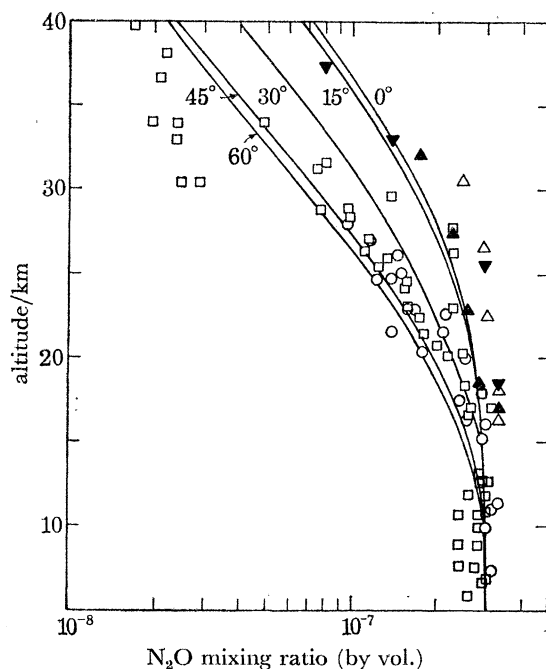


FIGURE 7. Altitude profiles at various latitudes for  $\text{N}_2\text{O}$ . The curves were calculated as discussed in the text for  $0^\circ$  solar declination. The experimental data were taken at  $32^\circ$  N,  $\square$  (Heidt *et al.* 1976);  $41^\circ$  N,  $\circ$ , and  $9^\circ$  N,  $\blacktriangle$  (Schmeltekopf *et al.* 1977),  $\triangle$ ,  $\blacktriangledown$  (Goldan 1977).

The discrepancy between calculated and observed  $\text{CO}$  is more difficult to explain. The  $\text{CO}$  chemical lifetime is fairly short ( $2\text{--}8 \times 10^6$  s) above 20 km and its abundance in the model is controlled largely by chemical production from  $\text{CH}_4$ ,



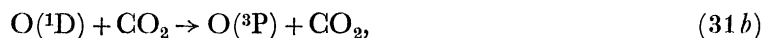
and loss by reaction (25) (see figure 4). Since (29) and (25) both involve reaction with  $\text{OH}$ , the  $\text{CO}$  abundance should be approximately given by

$$[\text{CO}] \approx [\text{CH}_4]k_{29}/k_{25}. \quad (30)$$

This scheme yields  $\text{CO}$  abundances too small by at least a factor of 5, as shown in figure 8. An additional source of  $\text{CO}$  is evidently required. Photolysis of  $\text{CO}_2$  would have to be 100 times faster than current estimates in order to be significant and we consider this to be unlikely. A possible source of  $\text{CO}$  might be reaction of  $\text{O}(^1\text{D})$  with  $\text{CO}_2$ ,



Preston & Cvetanovic (1966) estimated a rate for (31a) of approximately 5% of the rate for quenching process,



although Shortridge & Lin (1975) estimated a much lower value,  $k_{31a} < 10^{-14} \text{ cm}^3 \text{ s}^{-1}$ . The dashed line in figure 8 demonstrates that a model which includes (31a) ( $k_{31a} = 1 \times 10^{-11} \text{ cm}^3 \text{ s}^{-1}$ ) is in agreement with observed CO in the stratosphere. This process would have negligible influence on other species, and would not affect CO in the lower atmosphere. Evidently measurements of the rate for (31a) are needed to resolve this question.

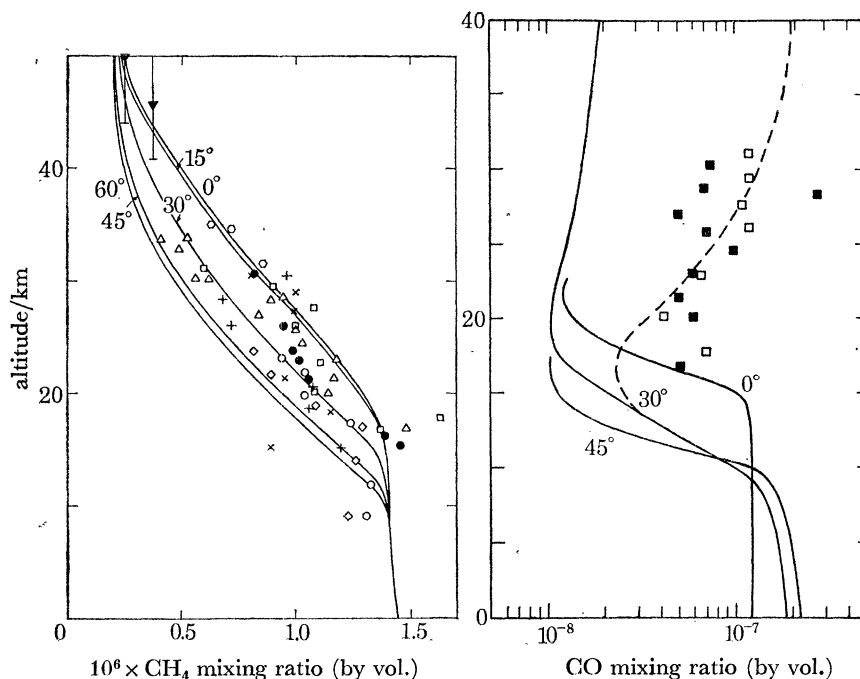


FIGURE 8. Altitude profiles at various latitudes for  $\text{CH}_4$  and CO. The  $\text{CH}_4$  curves were calculated as discussed in the text. The methane data were taken at  $32^\circ \text{ N}$ , with the exception of one profile from  $32^\circ \text{ S}$  ( $\bullet$ ). The points  $\blacktriangledown$  are from rocket flights. The different symbols indicate individual profiles, and are from Ehhalt (1974), Ehhalt *et al.* (1975), and Volz *et al.* (1976). The CO profiles in the troposphere were taken from the data of Seiler & Schmidt (1974). In the stratosphere the solid curve results from the standard chemical model, while the dashed curve results from inclusion of the process  $\text{O}(^1\text{D}) + \text{CO}_2$  ( $k = 1 \times 10^{-11} \text{ cm}^3 \text{ s}^{-1}$ ) as a source of CO. The CO data were taken at  $32^\circ \text{ N}$ ,  $\square$ ,  $\blacksquare$  (Volz *et al.* 1976).

Figures 10 and 11 show profiles as calculated for the concentrations of mesospheric OH and  $\text{O}_3$ . The lifetime for odd oxygen in the mesosphere is relatively short and  $\text{O}_3$  must be treated as a short lived species in this region; see equation (28). The diurnal variations of several species of importance in mesospheric chemistry ( $\text{H}$ , OH,  $\text{HO}_2$ ,  $\text{O}_3$ ) are shown in figure 12. Concentrations of mesospheric OH and  $\text{O}_3$  depend in a direct manner on the abundance of mesospheric  $\text{H}_2\text{O}$ . Our model assumes  $\text{H}_2\text{O}$  abundances as shown in figure 13. The rise in the mixing ratio of  $\text{H}_2\text{O}$  above 20 km reflects conversion of  $\text{CH}_4$  to  $\text{H}_2\text{O}$  and  $\text{CO}_2$ .

The results shown in figures 10 and 11 are in excellent agreement with the available observational data set. Figure 11 includes a model in which the room temperature measurements for reactions (2)–(4) were taken to apply throughout the atmosphere. Both models are in satisfactory accord with Anderson's (1975) observations of OH, and with available measurements of

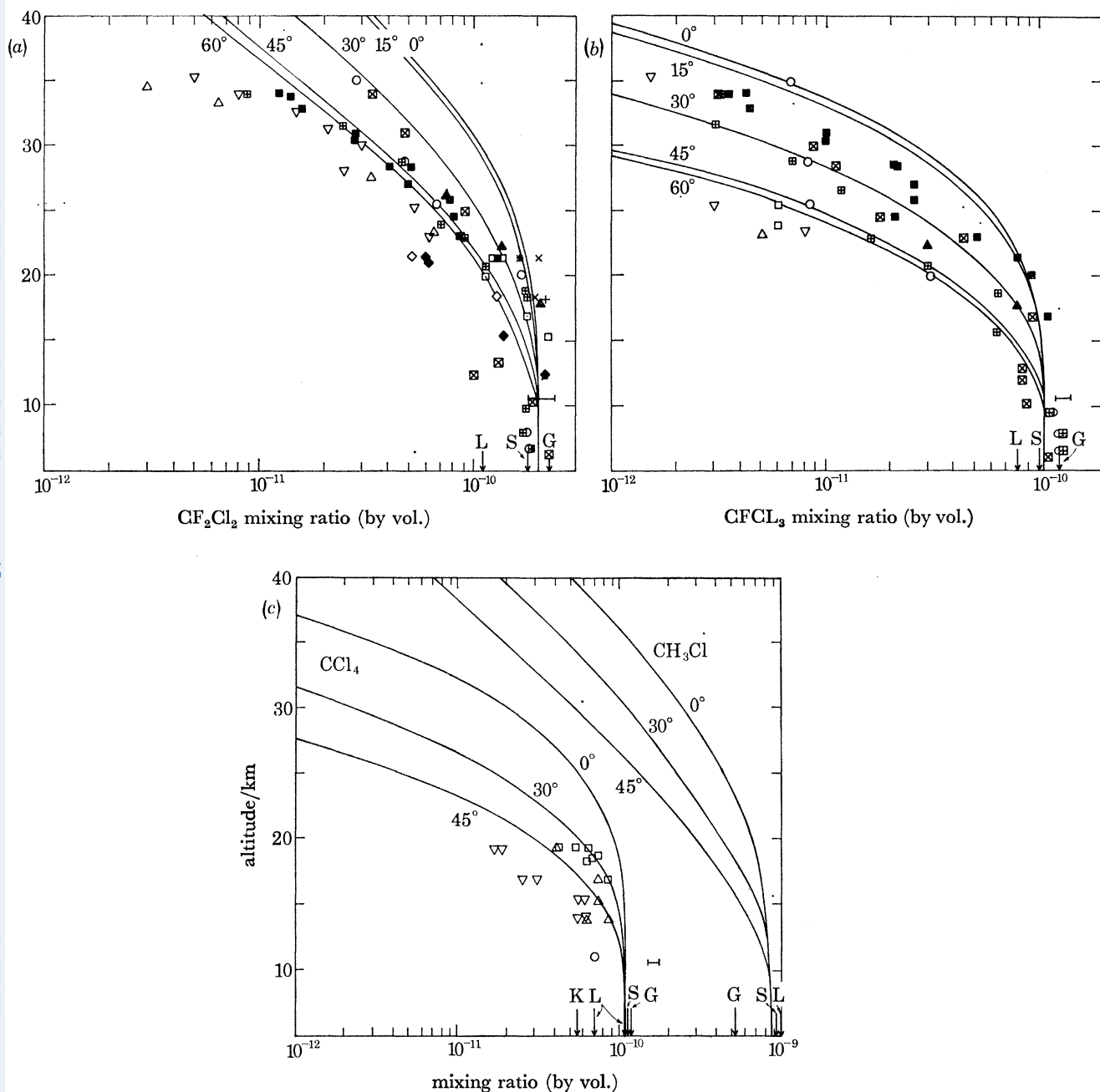


FIGURE 9. Altitude profiles at various latitudes for (a) CF<sub>2</sub>Cl<sub>2</sub>, (b) CFCl<sub>3</sub>, (c) CCl<sub>4</sub> and CH<sub>3</sub>Cl. The curves were calculated as discussed in the text for 0° solar declination. The experimental data for CFCl<sub>3</sub> and CF<sub>2</sub>Cl<sub>2</sub> are as follows: ■, □, ▢ (32° N), ○ (51° N), Heidt *et al.* (1975, 1976); ▲ (41° N), Schmeltekopf *et al.* (1975); ▽, △ (44° N), Fabian *et al.* (1977); × (9° N), + (16° N), □ (30° N), ◇ (60° N), ◆ (75° N), Inn *et al.* (1977a); † Inn *et al.* (1977b). The arrows on both panels indicate ground level measurements and are from Lovelock *et al.* (1973, 1974) (L), Grimsrud & Rasmussen (1975a, b) (G), and Singh *et al.* (1977a) (S). The data for CCl<sub>4</sub> are from Krey *et al.* (1977): □ (10°–30° N), △ (30°–45° N), ▽ (45°–60° N), ○ (mean 10–12 km value), K (mean 0–10 km value); and Inn *et al.* (1977b) †.

mesospheric  $O_3$ . Day to night differences are adequately reproduced. Watanabe & Tohmatsu (1976) suggest that  $O_3$  may exhibit significant seasonal variations, with winter concentrations at 65 km larger than summer values by a factor of 2.8. It is difficult to account for variations of this magnitude unless we invoke correspondingly large changes in the concentration of mesospheric  $H_2O$ . A model with seasonally invariant  $H_2O$  would predict a modest winter to summer variation in  $O_3$ , about 10%, in the opposite sense to that reported by Watanabe & Tohmatsu (1976).

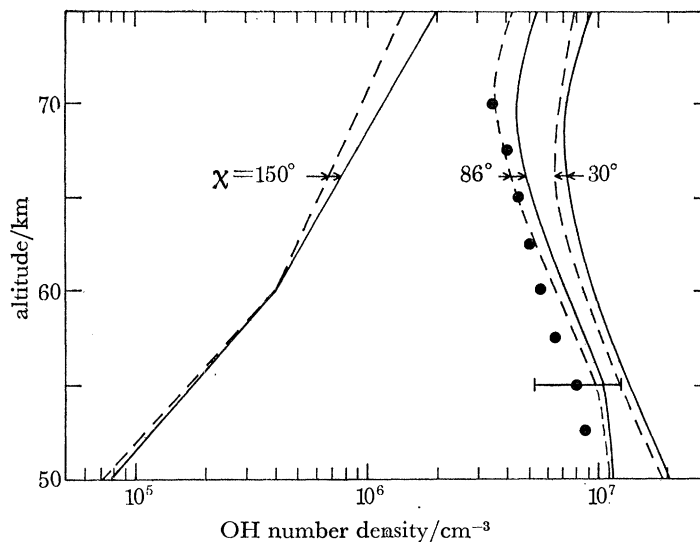


FIGURE 10. Altitude profiles for OH above 50 km. The solid lines were calculated with the standard model, at  $30^\circ$  N latitude and  $0^\circ$  solar declination for solar zenith angles ( $\chi$ ) corresponding to noon, late afternoon and midnight. The dashed lines were calculated with temperature independent rate constants for reactions (2)–(4). The data are from Anderson (1975), taken at  $32^\circ$  N, with  $\chi = 86^\circ$ . Representative error bars are shown.

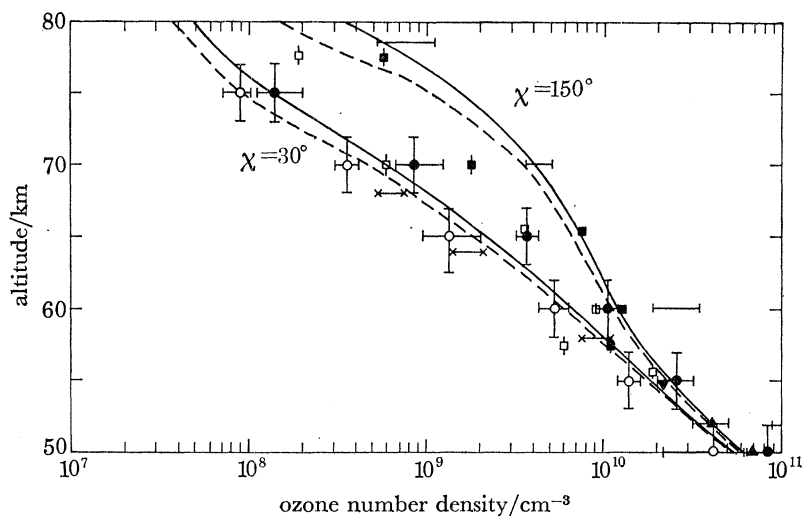


FIGURE 11. Altitude profiles for ozone above 50 km. The solid and dashed lines are for conditions as described in figure 10. The data are as follows:  $\blacktriangledown$  (sunset, June,  $32^\circ$  N), Johnson, Purcell & Tousey's 1949 distribution, as corrected by Krueger (1969);  $\blacktriangle$  (day, September,  $38^\circ$  N), Hilsenrath *et al.* (1969);  $\square$  (day),  $\blacksquare$  (night, March,  $38^\circ$  N), Hilsenrath (1971);  $\times$ — $\times$  (sunset, June,  $28^\circ$  S), Miller & Ryder (1973);  $\square$  (day),  $\blacksquare$  (night, February,  $31^\circ$  N), Penfield *et al.* (1976);  $\circ$  (summer mean),  $\bullet$  (winter mean,  $31^\circ$  N), Watanabe & Tohmatsu 1976;  $\text{H}$  (night, June–July,  $6^\circ$ – $12^\circ$  S), Riegler *et al.* (1977).



Water vapour is known to exhibit significant, factor of 3, variations in the lower stratosphere (Mastenbrook 1971). The measurements of OH (Anderson 1976), Cl and ClO (Anderson *et al.* 1977) between 25 and 40 km may reflect an upward extension of this variability. Model results are compared with stratospheric OH, O, Cl, and ClO measurements in figures 14 and 15, illustrating the dependence of results on the choice of profile for H<sub>2</sub>O.

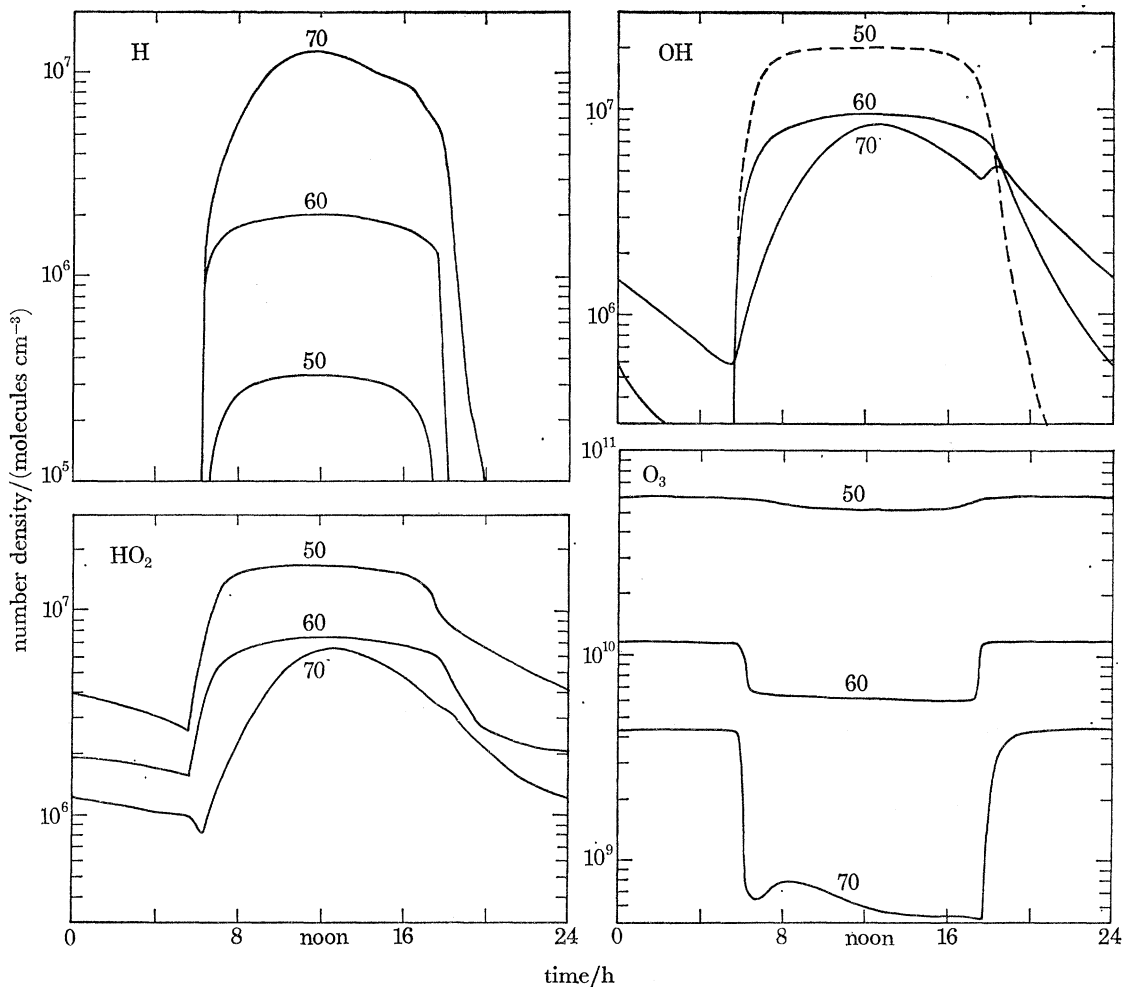


FIGURE 12. The diurnal variations of H, OH, HO<sub>2</sub> and O<sub>3</sub> at 50, 60 and 70 km are shown for 30° N latitude and 0° solar declination. The standard water profile given in figure 13 was used in these calculations.

It would appear that the high values for the concentrations of Cl and ClO cannot be attributed solely to variations in the water vapour mixing ratio, unless the mixing ratios for H<sub>2</sub>O are much larger than 10<sup>-5</sup>. On the other hand the low values for Cl and ClO are consistent with H<sub>2</sub>O mixing ratios in the range reported by Mastenbrook (1971). Part of the ClO variability might be attributed to temporal changes in the concentration of total chlorine. We may note in this context that several precursors for stratospheric chlorine, in particular CFCI<sub>3</sub>, CF<sub>2</sub>Cl<sub>2</sub>, CCl<sub>4</sub> and CH<sub>3</sub>CCl<sub>3</sub>, are distributed quite inhomogeneously in the lower atmosphere with abundances in the northern hemisphere typically twice those for the southern hemisphere (Lovelock, Maggs & Wade 1973; Lovelock 1977; Rasmussen, Pierotti, Krasnec & Halter 1976; Inn, Tyson & Arvesen 1977*b*). Changes in the ClO abundance may also result from variations

in the concentration of upper atmospheric  $\text{CH}_4$ , which could arise due to fluctuations in  $\text{H}_2\text{O}$ . A high concentration of  $\text{H}_2\text{O}$  favours a large source for  $\text{OH}$ , with a consequent reduction in  $\text{CH}_4$ . Both influences act to enhance the abundance of  $\text{Cl}$  and  $\text{ClO}$  relative to  $\text{HCl}$ , as illustrated in figures 15 and 17. A more comprehensive test of the chemical model would require simultaneous measurements of  $\text{OH}$ ,  $\text{Cl}$ ,  $\text{ClO}$ ,  $\text{HO}_2$ ,  $\text{H}_2\text{O}$ ,  $\text{O}_3$ ,  $\text{HCl}$ ,  $\text{ClNO}_3$ , and  $\text{CH}_4$ .

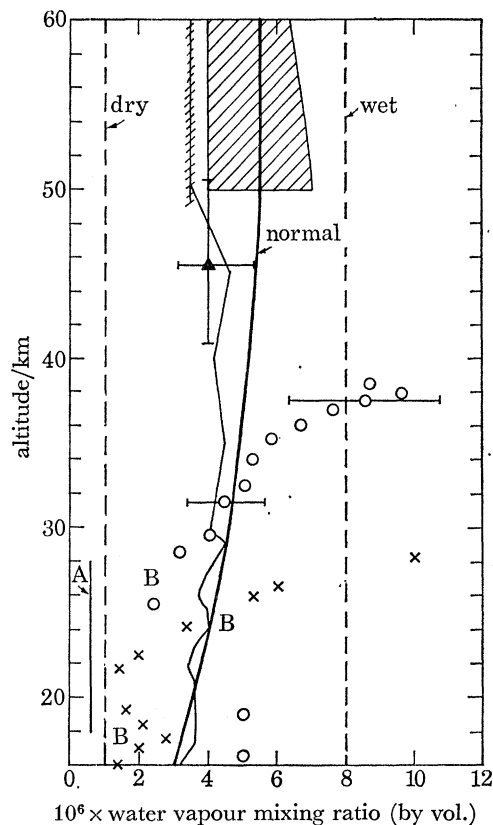


FIGURE 13. Altitude profiles for water. The heavy line shows the profile adopted in the standard model; the wet and dry models (dashed lines) used a water mixing ratio of 8 and 1 parts in  $10^6$  (by vol.) respectively, as indicated. The profiles were assumed to be constant above 60 km. Also shown is the mean mid-latitude northern hemispheric profile from the recent review by Harries (1976) (light line) and the data of Chaloner *et al.* (1975) ( $\circ$ ); Burkert *et al.* (1974) ( $\times$ ); Ehhalt *et al.* (1975a) ( $\blacktriangle$ ); Murcray *et al.* (1974) (A, from Fairbanks, Alaska; B from Holloman, N. M.); Waters *et al.* (1977) (shaded region); and Rogers *et al.* (1977) (//////).

Measurements of  $\text{HCl}$  provide important information with regard to the rôle of  $\text{ClNO}_3$  in stratospheric chemistry and may be used to place constraints on the total abundance of stratospheric chlorine. Figure 16 shows a comparison of computed concentrations for acidic chlorine, taken as  $\text{HCl} + \text{ClNO}_3 + \text{HOCl}$ , with measurements by Lazrus *et al.* (1976). Figure 17 shows model results for the seasonal dependence of  $\text{HCl}$  concentrations, illustrating the sensitivity of the model to choice of  $\text{H}_2\text{O}$  profile. The model results show little seasonal variation for  $\text{ClNO}_3$ , shown in figure 18. The structure in the  $\text{HCl}$  profile below 30 km reflects the importance of  $\text{ClNO}_3$ , with largest concentrations of this gas predicted to occur near 20 km. A direct comparison with observation is difficult, given the apparent scatter of the data, and given the possibility of significant temporal variations in  $\text{H}_2\text{O}$  as discussed above. The observations are consistent with the postulate the  $\text{ClNO}_3$  should play a significant rôle in stratospheric chemistry

(Rowland *et al.* 1976*a*). Major uncertainties remain however and clearly point to the need for a careful observational search for  $\text{ClNO}_3$ . Results presented here are in accord with a recent observational upper limit to the concentration of  $\text{ClNO}_3$  set by Murcay *et al.* (1977).

Figures 19 and 20 show a comparison as a function of latitude of predicted and observed column densities for stratospheric  $\text{NO}_2$  and  $\text{HNO}_3$ . The height integrated concentrations of these compounds are relatively insensitive to the more uncertain aspects of the model. The

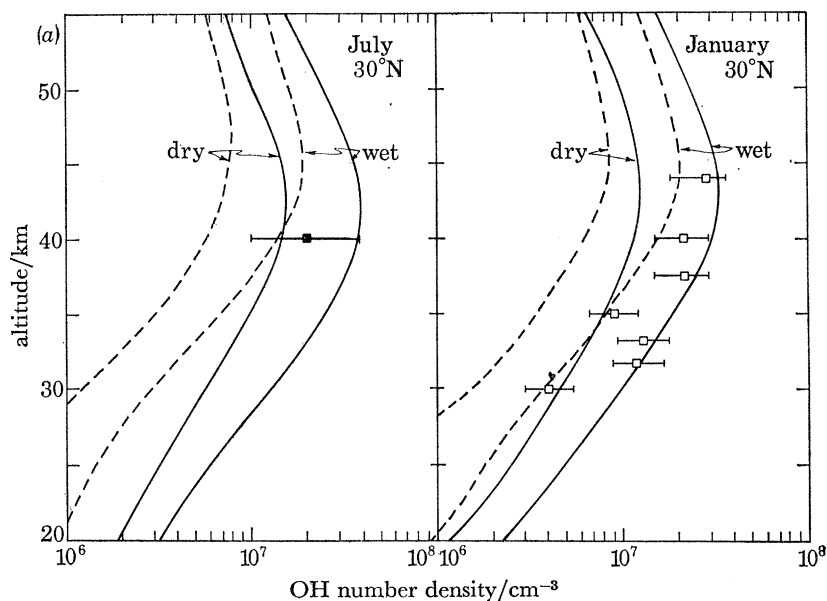


FIGURE 14*a*. Altitude profiles are shown for OH at 30° N in summer and winter, for wet ( $\text{H}_2\text{O} = 1$  part in  $10^6$ ) and dry ( $\text{H}_2\text{O} = 8$  parts in  $10^6$ ) conditions. The solid curves show values at noon, and the dashed curves are for late afternoon ( $\chi = 80^\circ$ ). The data points are from Anderson (1976) for  $\chi = 80^\circ$ .

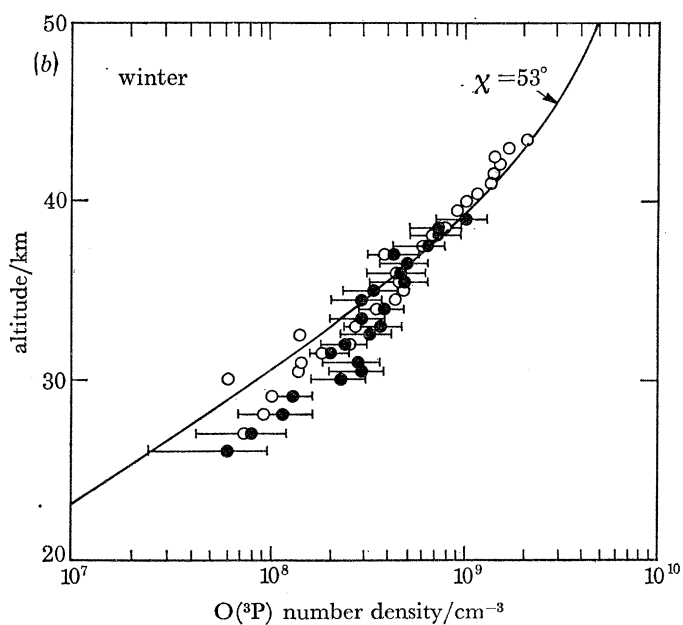


FIGURE 14*b*. The altitude profile of O is shown for 30° N latitude in winter with a solar zenith angle of  $53^\circ$ . The standard water profile from figure 13 is used. The data are from Anderson (1975): ●, November,  $\chi = 56^\circ$ ; ○, February,  $\chi = 51^\circ$ .

good agreement of theory with observation exhibited by the figures indicates that the total abundance of odd nitrogen is well predicted by the model, and that the model satisfactorily accounts for the apportionment of  $\text{NO}_x$  among its more abundant constituents. It lends confidence to the validity of procedures adopted to treat lateral transport (see also Wofsy 1978).

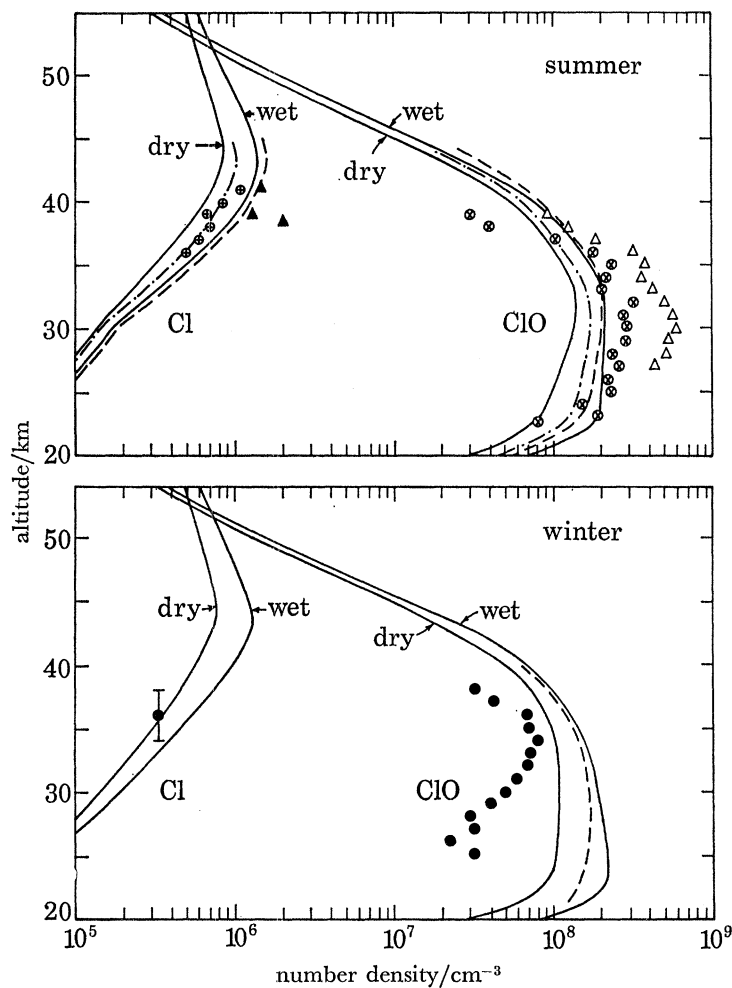


FIGURE 15. Altitude profiles are shown for Cl and ClO at  $30^\circ$  N in summer and winter for wet and dry conditions (solid lines) at noon. The broken lines were calculated by using the standard water profile but employed high (— · —) and low (---) values for methane consistent with the range of the data shown in figure 8. The data points are from Anderson *et al.* (1977) and were taken at  $32^\circ$  N in December ( $\bullet$ ,  $\chi = 50^\circ$ ), July ( $\otimes$ ,  $\oplus$ ,  $\chi = 16^\circ$ ), and October ( $\Delta$ ,  $\blacktriangle$ ,  $\chi = 35^\circ$ ).

Noxon *et al.* (1977) report very low column abundances for stratospheric  $\text{NO}_2$  poleward of  $50^\circ$  N, during winter. The calculations exhibit a significantly smaller decrease of  $\text{NO}_2$  in this region. This discrepancy could be resolved in large part by a slight temperature dependence in the photolysis rate of  $\text{HNO}_3$ , which is the dominant  $\text{NO}_x$  species at these latitudes.

Figure 21 shows a comparison of observed and calculated profiles for  $\text{O}_3$  below 50 km. The gas is treated in this height range as a long lived chemical species by using the one-dimensional diffusion model, equation (26). We did not use mixing surfaces to simulate horizontal transport since chemical lifetimes are too short to permit use of this model above 22 km.

Ozone is formed in the troposphere by



followed by



and



equivalent to

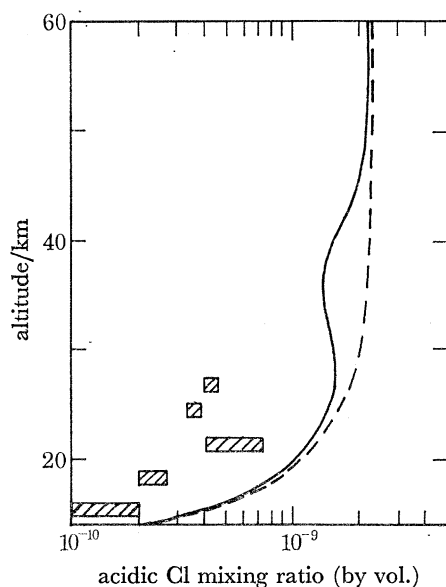
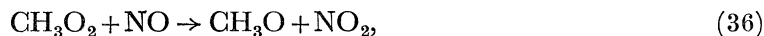


FIGURE 16. Altitude profiles are shown for acidic chlorine taken as  $\text{HCl} + \text{HOCl} + \text{ClNO}_3$  (—) and total chlorine (---) for  $30^\circ \text{N}$  latitude and  $0^\circ$  solar declination, at noon, and compared with the data of Lazrus *et al.* (1976).

Anthropogenic CO leads therefore to some net increase in the abundance of tropospheric  $\text{O}_3$ . Ozone may be formed also as a by-product of  $\text{CH}_4$  oxidation (Levy 1971; Chameides & Walker 1973), by

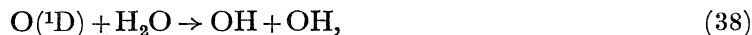


followed by (33) and (34). The rate for (36) is unknown, however, and we are unable therefore to offer any quantitative assessment of its importance.

The recent measurement of a fast rate for (20) establishes a central rôle for nitrogen oxides in the chemistry of tropospheric  $\text{O}_3$ . Indeed the ozone source strength for the lower troposphere is large enough to cause difficulties in our attempt to define a balanced chemical system. The time constant for  $\text{O}_3$  below 5 km is about 10 days. The production due to (35) and (36) could be balanced by heterogeneous processes either in the atmosphere or at the surface. A quantitative discussion of this possibility is difficult however. Photolysis,



followed by



and reaction with  $\text{HO}_2$ , equation (21), represent the most important gas phase sinks for  $\text{O}_3$  in the troposphere.



Figure 21 shows profiles in which we omit the possibility of heterogeneous loss processes for  $O_3$  in the atmosphere, using Simonaitis & Heicklen's (1973) value for the rate constant of reaction (21). The agreement of model with observation is satisfactory at heights above the

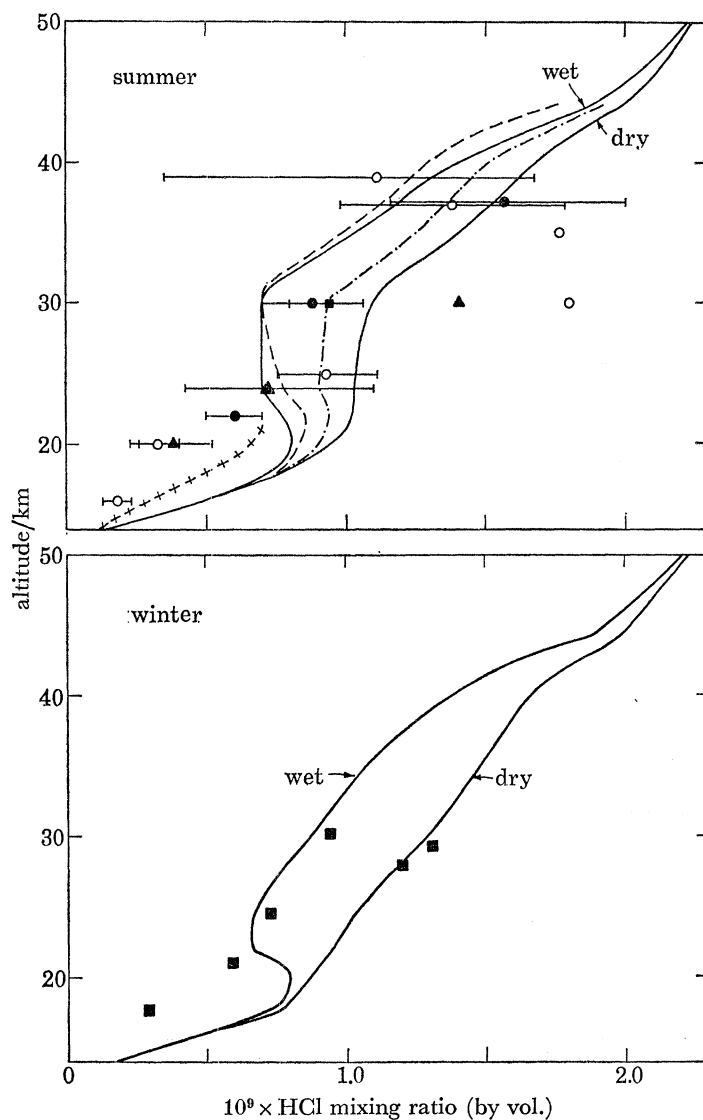


FIGURE 17. Altitude profiles are shown for HCl at  $30^\circ N$ , at noon, in summer and winter for wet and dry conditions (solid lines). The broken lines were calculated with the standard water profile and high (— · —) and low (---) values for methane, consistent with the range of the data shown in figure 8. The data are from Ackerman *et al.* (1976) ( $\blacktriangle$ , October); Farmer *et al.* (1976) (+ + +, average profile); Williams *et al.* (1976) ( $\blacksquare$ , December); Eyre & Roscoe (1977) ( $\circ$ , March); and Raper *et al.* (1977) ( $\bullet$ , May and September). Representative error bars are included.

$O_3$  maximum. A comparison with observational data at  $30^\circ N$  (Hering 1975; Watanabe & Tohmatsu 1976) suggests that important discrepancies arise below 26 km.

The model is characterized by a peak broader in altitude than that exhibited by the data. The vertical column density of  $O_3$  in the model has a value  $10.2 \times 10^{18} \text{ cm}^{-2}$ , which may be compared with the observed value of  $7.5 \times 10^{18} \text{ cm}^{-2}$ . The discrepancy might reflect

inadequacies of the chemical model. On the other hand, it should be noted that the difficulty arises in a region of the atmosphere where transport should play an important rôle for  $O_3$ .

As noted earlier, use of one-dimensional vertical diffusion models is somewhat suspect for  $O_3$ . Most of the global abundance of atmospheric  $O_3$  is supplied by transport from a source region confined to a relatively narrow altitude region at low latitudes. A major fraction of the vertical column of  $O_3$  at higher latitudes must lie in the dynamical régime, as may be inferred

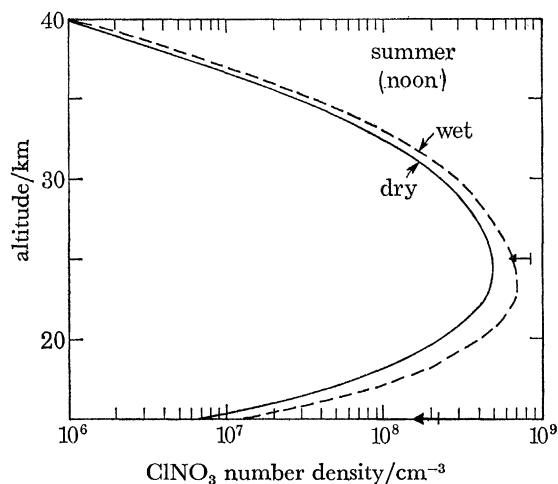


FIGURE 18. Altitude profiles are shown for  $ClONO_2$  at  $30^\circ N$  at noon in summer for wet and dry conditions. The arrow symbols show the upper limit of Murcray *et al.* (1977).

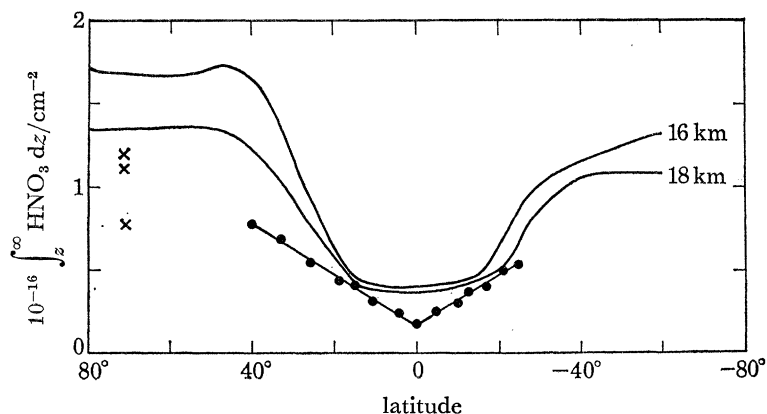


FIGURE 19. The column abundance of  $HNO_3$  is shown as a function of latitude at  $20^\circ$  solar declination. The column integral is started at altitudes of 16 and 18 km. The data are from Murcray *et al.* (1975) and were taken from an aircraft flying at 18 km in January ( $\bullet$ ), and from balloon flights in September ( $\times$ ).

from the latitudinal distributions of total  $O_3$  shown in figure 22. The calculated distribution results from a model which allows only for vertical transport of ozone. Evidently, the observed latitudinal variations require transport of ozone from the tropics into the higher latitudes.

In light of this discussion, it is perhaps not surprising that one-dimensional models should fail to reproduce the global mean abundance of  $O_3$ . The disagreement however emphasizes the difficulty associated with use of one-dimensional models for the assessment of human influence on  $O_3$ . One might hope that one-dimensional models should give a reasonable estimate for the magnitude of any particular perturbation to  $O_3$ , even though the model might fail to reproduce

details of the vertical distribution. As an alternate approach one might follow the procedures described by McElroy *et al.* (1974) and seek to define a suitable scaling factor with which to model the influence of perturbations in the dynamical zone. Neither procedure is totally satisfactory. A definitive assessment requires a fully integrated chemical-dynamical model for the lower atmosphere.

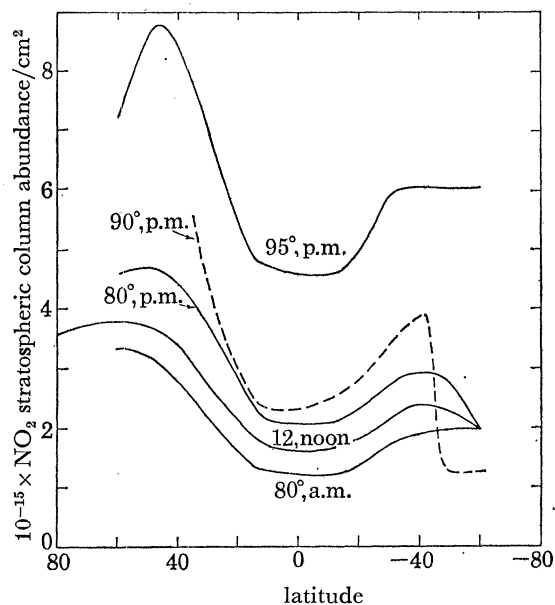


FIGURE 20. The column abundance of  $\text{NO}_2$  is shown as a function of latitude at  $20^\circ$  solar declination for several solar zenith angles. The dashed line shows the twilight data of Noxon *et al.* (1977).

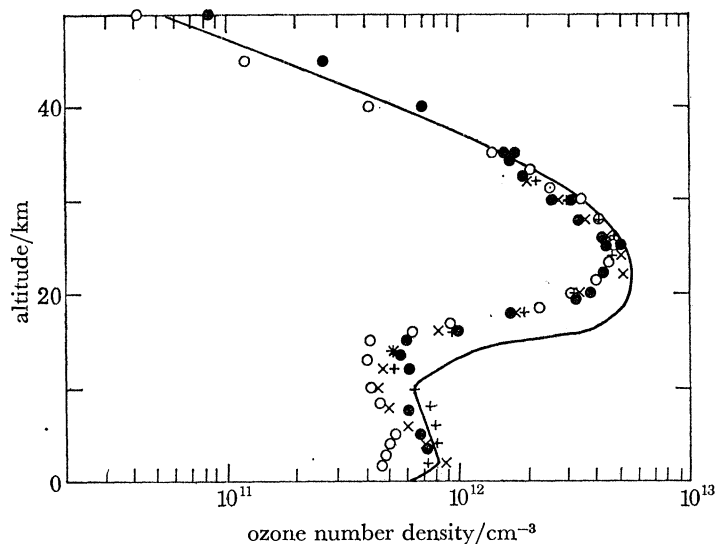


FIGURE 21. The altitude profile for ozone calculated with the standard one-dimensional diffusion model described in the text is shown. The data at  $30^\circ \text{N}$  are from Watanabe & Tohmatsu (1976) (O, summer mean, ● winter mean); and Hering (1975) (x summer mean, + winter mean).

## 4. PERTURBATIONS

Our interest here is directed towards human activities which might be expected to lead to significant changes in the global atmospheric environment. We shall emphasize perturbations which might affect the global distribution of atmospheric  $O_3$ .

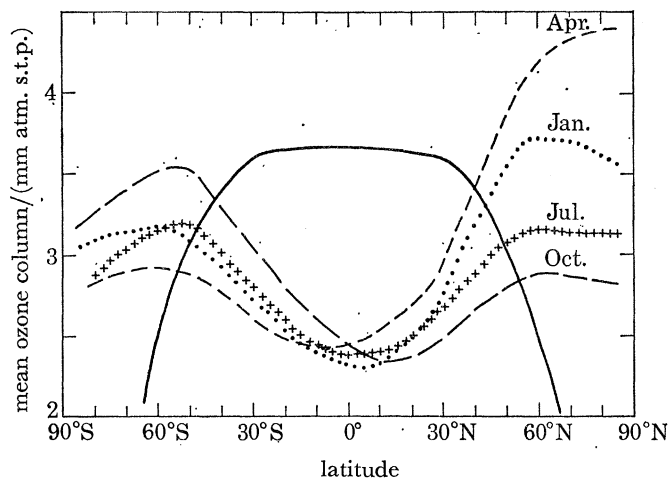


FIGURE 22. The column density of ozone is shown as a function of latitude. The solid line is the calculated ozone column abundance. The computation employs latitudinal transport of long lived species and vertical diffusion of ozone but ignores the effects of latitudinal transport of ozone. The broken lines show the observed mean ozone column as a function of season (Gebhart *et al.* 1970).

These perturbations fall into two general classes: those which are considered essential to modern society, and those which may be regarded as largely discretionary. Among the essential perturbations, we shall focus mainly on combustion and agriculture. More discretionary human influences include the use of certain halocarbons as working fluids in refrigeration systems, as propellants in aerosol cans, and as solvents and cleaning fluids.

Combustion of fossil fuels provides important direct sources of atmospheric  $CO_2$ ,  $CO$ ,  $H_2$ ,  $NO_x$  and  $N_2O$ . Biological activity plays a major rôle in regulating the concentrations of these gases in the natural atmospheric environment.

Respiration and decay release  $CO_2$  at rates which can replace the present concentrations of the gas in the atmosphere on a time scale of less than 20 years (see, for example, McElroy 1976; Bolin 1977). Combustion provides a source strength for  $CO_2$  equal to approximately 10% of that from respiration and decay (Keeling 1973; Delwiche & Likens 1977).

Methane, formed as a by-product of microbial fermentation, is the primary natural precursor for atmospheric  $CO$  and  $H_2$ . Carbon monoxide is produced (see figure 4) by



and by



Reaction (39) is the primary natural source for  $H_2$ , giving a global source strength of magnitude  $3.5 \times 10^7$  t per year. The source strength for  $CO$  has magnitude  $1.7 \times 10^{11}$  molecules  $cm^{-2} s^{-1}$ ,  $5.5 \times 10^8$  t C per year. These inputs may be compared to current estimates for combustion related sources of  $H_2$  and  $CO$  of magnitude  $2 \times 10^7$  t per year and  $3 \times 10^8$  t C per year respectively (Jaffe 1973; Schmidt 1974; Seiler 1974; Seiler & Schmidt 1974; Penner *et al.* 1977). The

methane-related source strengths for CO and H<sub>2</sub> were estimated by using the pressure dependent rate expression for reaction (25). They are lower therefore than earlier estimates based on a pressure independent value for this coefficient. The revised estimate for the source of CO from CH<sub>4</sub> oxidation, and associated implications for tropospheric OH, introduce some difficulty in attempts to balance the budget for northern hemisphere CO. Either the rate constant for (25) must be less than values assumed here, or there must be sources for CO in the northern hemisphere larger than values usually associated with combustion, by about a factor of 3. Oxidation of terpenes or other hydrocarbon emissions from the terrestrial biosphere could provide an important natural source of CO (cf. Wofsy, McConnell & McElroy 1972). For example, the hemiterpene, isoprene, is a major component of volatile emissions from many species of land plants (Sanadze 1963; Rasmussen 1970). Isoprene is likely to react rapidly with OH radicals (cf. Atkinson, Perry & Pitts 1977), and the ultimate yield of CO could be between 40% and 60%, based on olefin oxidation pathways which we might expect to apply in the atmosphere (Demerjian, Kerr & Calvert 1974; Niki, Maker, Savage & Breitenbach 1978). If global emission rates for isoprene were comparable to those found by Sanadze (1963) and Rasmussen & Jones (1973) under laboratory conditions, photooxidation of isoprene could provide a source for CO comparable to or larger than anthropogenic emissions.

Combustion provides a direct source of fixed nitrogen, NO<sub>x</sub>, of magnitude  $2.3 \times 10^7$  t N per year at the present time. Fixation of nitrogen for fertilizer contributes an additional source of magnitude  $4.2 \times 10^7$  t N per year. These anthropogenic inputs may be compared to estimates for biological fixation which range from about  $1-2 \times 10^8$  t N per year (Burns & Hardy 1975; Soderlund & Svensson 1976; McElroy 1976; Sweeney, Lui & Kaplan 1977; Delwiche & Likens 1977). Both the combustion and fertilizer sources of fixed nitrogen are growing at a steady rate, as illustrated in figure 23, and it is difficult to avoid the conclusion that anthropogenic effects must play a dominant rôle in global nitrogen fixation in the near future.

Our estimates for the combustion source of fixed nitrogen before 1970 use data for the United States published by the U.S. Environmental Protection Agency (Cavender, Kircher & Hoffman 1973). These data were scaled by a factor of approximately 2.7 in order to obtain an estimate of global emissions. The scale factor reflects consumption patterns for various fossil fuels as given by Hamilton (1977). We assumed a growth rate for combustion of fossil fuels equal to 3.6% per year between 1970 and 2000, consistent with projections by the Organization for Economic Co-operation and Development (1976) (see also The National Energy Plan (1977)). The growth rate was taken equal to 2.4% per year between 2000 and 2050, and was lowered to 1% per year for the period 2050 to 2100 (see model C in figure 23). A second model for combustion nitrogen, model D in figure 23, anticipates stringent regulation of NO<sub>x</sub> and CO emissions.

We shall explore two models for future use of nitrogenous fertilizers. The models are similar to those used by McElroy *et al.* (1977). Both models assume a relatively stable world population after the turn of the century. Model A allows for grain production equivalent to  $4 \times 10^2$  kg per person per year for a population assumed to grow to  $6.5 \times 10^9$  by the year 2000. Model B assumes grain production per person close to current values,  $2.5 \times 10^2$  kg per person per year, with a similar demographic projection.

Combustion is known to provide a direct source for N<sub>2</sub>O as well as NO<sub>x</sub> (Pierotti & Rasmussen 1976; Weiss & Craig 1976). Weiss & Craig (1976) report measurements of N<sub>2</sub>O and CO<sub>2</sub> emanating from the power plants in California. They find ratios N<sub>2</sub>O to CO<sub>2</sub> of  $2.05 \times 10^{-4}$



for coal and fuel oil plants respectively. Their data, combined with Keeling's (1973) discussion of  $\text{CO}_2$  emissions, were used to construct the direct release model for  $\text{N}_2\text{O}$  given in figure 23 (model E). Figure 24 shows the release patterns for  $\text{CO}$ ,  $\text{CO}_2$  and  $\text{H}_2$ . We used Seiler's (1974) estimate for  $\text{CO}$  release and  $\text{CO}$  to  $\text{H}_2$  emission ratios given by Schmidt (1974).

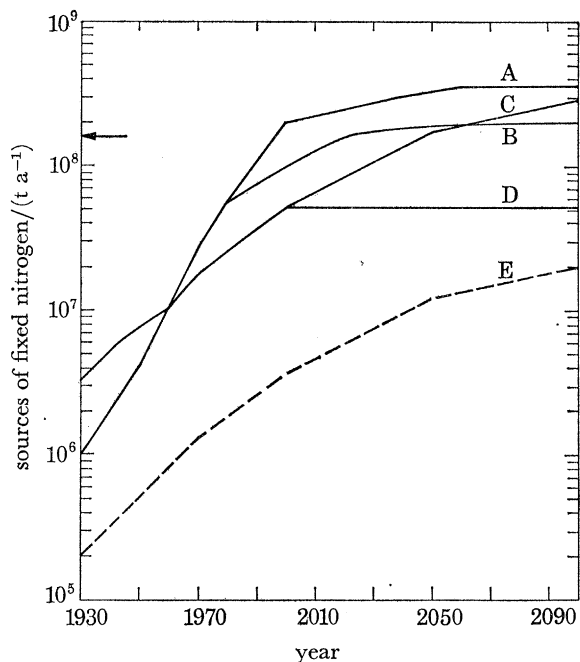


FIGURE 23.

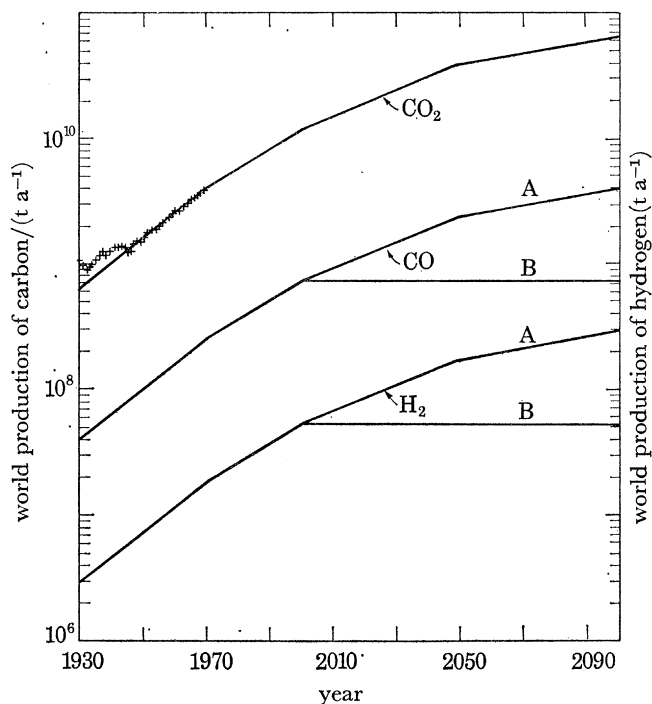


FIGURE 24.

FIGURE 23. Projections for anthropogenic nitrogen fixation. A and B show the nitrogen fixed in the manufacture of fertilizer, C and D show  $\text{NO}_x$  from combustion of fossil fuels, and E shows the direct production of  $\text{N}_2\text{O}$  in combustion. The arrow indicates the biological fixation rate. The models are discussed further in the text.

FIGURE 24. Projections for  $\text{CO}_2$ ,  $\text{CO}$  and  $\text{H}_2$  emissions from fossil fuel use. Model A assumes a growth rate of 3.6% per year, 1970–2000, reduced to 2.4% per year, 2000–2050, and 1% per year, 2050–2100. Model B assumes constant release of  $\text{CO}$  and  $\text{H}_2$  after 2000, anticipating regulation of emissions. The historical data for  $\text{CO}_2$  are from Keeling (1973).

Catalytic converters on automobiles (Pierotti & Rasmussen 1976; Weiss & Craig 1976) are known to provide additional direct sources of  $\text{N}_2\text{O}$ . The automotive source is currently small, much less than  $1 \times 10^6$  t N per year. We chose to omit this source in light of uncertainties in future development and use of catalytic converters.

The anthropogenic sources of fixed nitrogen shown in figure 23 undergo a complex series of transformations resulting ultimately in recombination of fixed N, with release of both  $\text{N}_2\text{O}$  and  $\text{N}_2$ . On sufficiently long time scales release of nitrogen as  $\text{N}_2\text{O}$  and  $\text{N}_2$  should balance the net global source of fixed N.

An estimate for the anthropogenically related source of  $\text{N}_2\text{O}$  in any given year requires a relatively complete understanding of the global nitrogen cycle. Discussions of this cycle emphasizing Man's impact are given by McElroy (1976) and McElroy *et al.* (1977). The  $\text{N}_2\text{O}$  source strength may be calculated by using the concept of a well defined delay pattern for recombination of fixed N, along with an estimate for the fraction of recombination events resulting in emission of  $\text{N}_2\text{O}$  rather than  $\text{N}_2$ . The release patterns adopted here are illustrated in figure 25.

The fraction of recombination events leading to release of  $N_2O$  in the present system may be estimated if we assume a balance between natural fixation and recombination, and use estimates for the lifetime of atmospheric  $N_2O$  to evaluate the current source strength of the gas. We shall adopt for this purpose a natural fixation rate of  $1.6 \times 10^8$  t N per year, consistent with the range of values quoted above, and we shall assume the same yield of  $N_2O$  from recombination of anthropogenic and natural nitrogen.

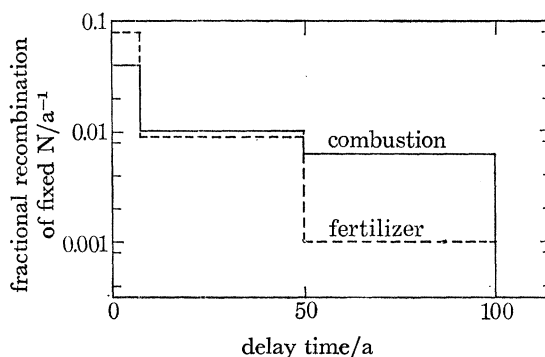


FIGURE 25. The fraction of anthropogenic nitrogen recombined annually is shown as a function of the time elapsed since release of the nitrogen to the environment. The average delay time for recombination is assumed to be considerably larger for combustion nitrogen than for fertilizer.

The uncertainty in the lifetime of atmospheric  $N_2O$  is more serious than the ambiguity associated with the fixation rate, with values in the literature ranging from 1.8 a (Hahn & Junge 1977) to an upper limit of about 140 a imposed by stratospheric photolysis. Lifetimes less than about 10 a would appear to require sources for  $N_2O$  in addition to denitrification. A source due to nitrification would not obviate the difficulty since the sum of the sources from nitrification and denitrification must be balanced by fixation. Lightning discharges offer a further possibility (Griffing 1977; Zipf & Dubin 1976), though quantitative estimates (Griffing 1977) for the associated source strength suggest that it should be small, less than  $2 \times 10^6$  t N per year. We shall investigate models with two values for the  $N_2O$  lifetime, a low value of 20 a, only slightly larger than the range 4–12 a recommended by Hahn & Junge (1977), and a high value of 140 a, which would apply if stratospheric photolysis were the major sink. Corresponding release rates for  $N_2O$  are given in figure 26.

With our choice of fixation rate, the yield of  $N_2O$  relative to  $N_2$  in recombination of fixed N is either 6% or 40% for the long and short lifetimes respectively. A yield of 6% agrees with soil data quoted by the Council for Agricultural Science and Technology (1976). Moreover, the long lifetime and low yield would be consistent with the lack of variability for atmospheric  $N_2O$  as reported by Weiss, Dowd & Craig (1976) from measurements over the Pacific Ocean, and Goldan *et al.* (1978) from continental measurements. It disagrees however with relatively large variations of the total  $N_2O$  column density as measured spectroscopically by Goody (1969). It should be noted that other investigators (Hahn & Junge 1977; Singh, Salas, Shiegeshi & Crawford 1977*b*) using chromatographic techniques find greater variability than that seen by Weiss *et al.* (1976) and Goldan *et al.* (1978). The apparent discrepancies might be attributed to a predominant rôle for continental influences on the budget of atmospheric  $N_2O$ . Data from this laboratory (Kaplan *et al.* 1978) indicate that fresh water systems can provide both sources and sinks for  $N_2O$ . It would seem possible that aqueous systems could play an important rôle

and that biological uptake might represent a major sink (see, for example, Brice, Eggleton & Penkett 1977), though heterogeneous chemistry could also contribute (Ausloos, Rebbert & Glasgow 1977). The issue is clearly unresolved. The weight of the evidence, in our view, appears to point towards a relatively long lifetime for  $N_2O$ , in that it is difficult to account for source strengths or sinks much larger than about  $5 \times 10^7$  t N per year (McElroy *et al.* 1976).

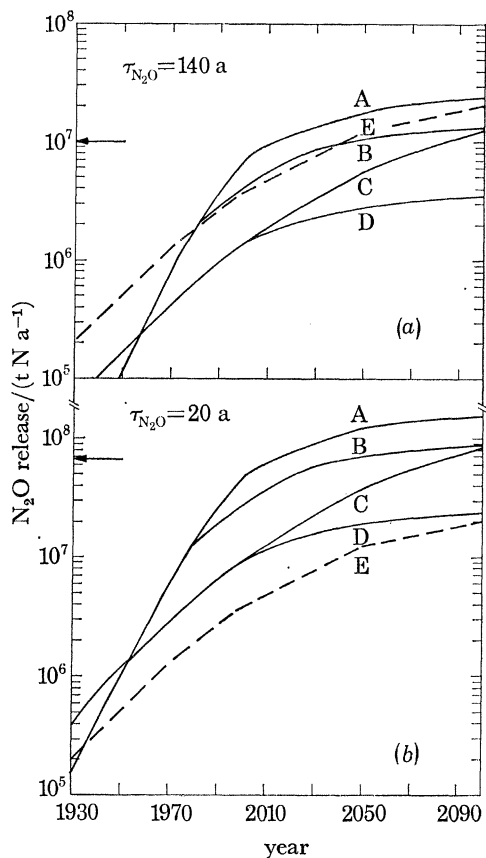


FIGURE 26. Projections for release rates of  $N_2O$ , assuming the sources of fixed nitrogen given in figure 23, the delay times for denitrification given in figure 25, a natural fixation rate of  $1.6 \times 10^8$  t N/a and  $N_2O$  lifetimes as shown. The labels are described in figure 23, and the arrows indicate the source of  $N_2O$  from natural processes.

Figure 27 shows historical data for industrial sources of several halocarbons which are ultimately released to the atmosphere. We focus here on chlorinated species. The possible impact of brominated compounds is discussed elsewhere (Wofsy *et al.* 1975*b*). The compounds  $CFCl_3$  and  $CF_2Cl_2$  are released to the atmosphere on an average of less than a year following manufacture (McCarthy, Bower & Jesson 1977). The data in figure 27 are from McCarthy *et al.* (1977) for  $CFCl_3$  and  $CF_2Cl_2$ , from Galbali (1976) for  $CCl_4$ , and from Neely & Plonka (1978) for  $CH_3CCl_3$ . The figure also summarizes models devised to explore possible future release patterns for  $CFCl_3$ ,  $CF_2Cl_2$ ,  $CCl_4$  and  $CH_3CCl_3$ . We consider two models for  $CFCl_3$ ,  $CF_2Cl_2$  and  $CH_3CCl_3$ . In model A, release rates are assumed to remain constant at values applicable in 1974. Model B envisages regulation of these compounds and the source is abbreviated accordingly in the period subsequent to 1980 (see figure 27). Trichloroethane is used as an intermediate in the manufacture of vinylidene chloride and as a cleaning solvent, with the latter

accounting for most of the release to the atmosphere. Release rates have grown rapidly in recent years as this compound is used to replace the chloroethylenes  $C_2Cl_4$  and  $C_2HCl_3$ . The models in figure 27 envisage continued growth in the release of  $CH_3CCl_3$  until 1980, followed by slow growth thereafter.

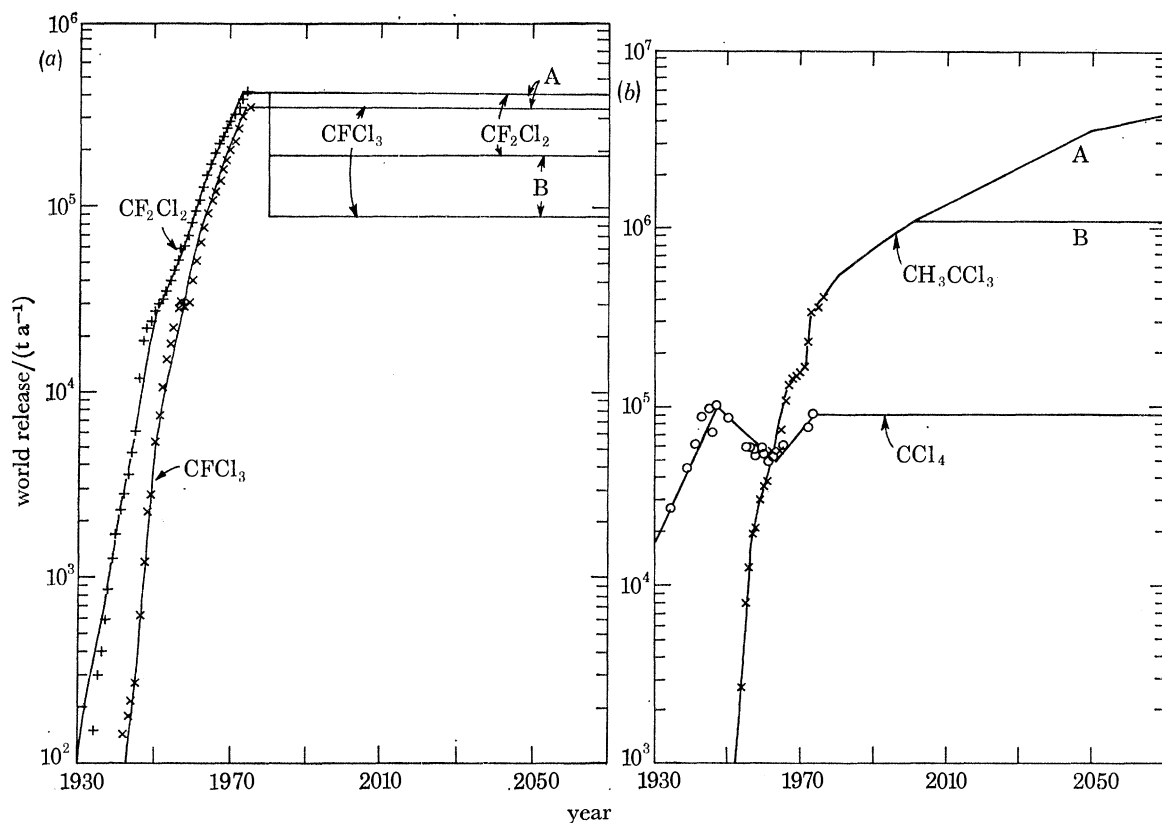


FIGURE 27. (a) Historical data and projections for release of  $CFC_{13}$  ( $\times$ ) and  $CFC_{12}$  ( $+$ ). The data are from McCarthy *et al.* (1977). Model A assumes continued release at 1974 rates, while model B assumes that the use of these compounds as aerosol propellants is discontinued in 1980. (b) Historical data and projections for release of  $CH_3CCl_3$  ( $\times$ ) and  $CCl_4$  ( $\circ$ ). The data are from Neely & Plonka (1978) and Galbali (1975) respectively. For  $CH_3CCl_3$ , the growth patterns given for fossil fuel emissions in figure 24 are adopted; a constant release rate after 1974 is assumed for  $CCl_4$ .

## 5. RESULTS

We shall describe results from a number of models exploring consequences of combustion, anthropogenic changes to the nitrogen cycle and the chlorocarbon release patterns described above. The anthropogenic perturbations will be treated by using the standard chemical model summarized in table 1, with diurnal variations incorporated as described in § 3. We begin with a brief discussion of results obtained for steady state conditions, assuming a range of values for tropospheric  $N_2O$  and stratospheric  $Cl_x$ .

Figure 28 presents global average column densities of  $O_3$  as functions of the  $N_2O$  mixing ratio, for several concentrations of stratospheric  $Cl_x$ , calculated by using the one-dimensional diffusion model. It shows the dependence of results on procedures used to treat insolation. The mixing ratios for  $N_2O$  and  $Cl_x$  in the present atmosphere are taken as  $3 \times 10^{-7}$  and  $2.3 \times 10^{-9}$ ,

respectively. The value for  $N_2O$  reflects the mean surface concentration of the gas. The value for  $Cl_x$  reflects conditions at an altitude of 40 km.

The model with diurnally averaged insolation (figure 28*b*) has somewhat less  $O_3$  than the more complete model (figure 28*a*). Differences arise largely at altitudes below 30 km. They may be attributed in part to the larger source of odd oxygen in the standard model due to (20), in part to a reduction in the removal rates for odd oxygen due to



and

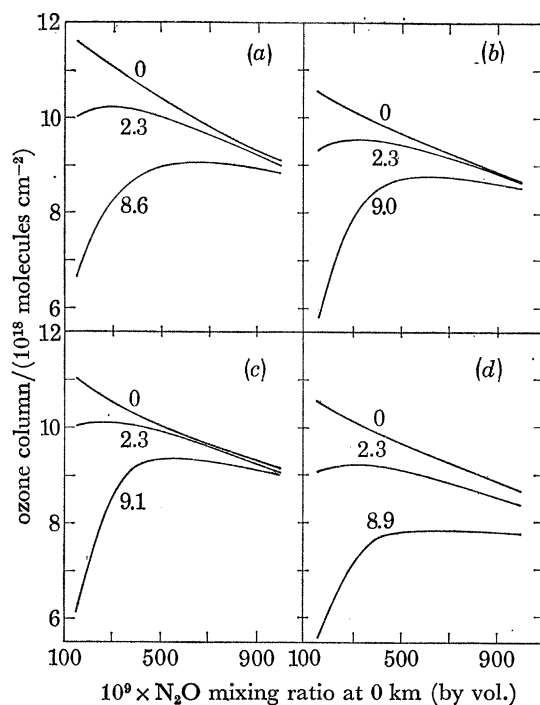


FIGURE 28. Global average column densities of ozone as a function of the tropospheric  $N_2O$  mixing ratio. The labels on the curves indicate the  $Cl_x$  mixing ratios (unit: parts/ $10^9$  by vol.) at 40 km. The steady state calculations with a  $Cl_x$  mixing ratio of *ca.*  $8.6/10^9$  at 40 km result from  $CFCl_3$  and  $CF_2Cl_2$  fluxes of 341 000 t/a and 410 000 t/a respectively, with the boundary conditions for other constituents taken from table 2. A  $Cl_x$  mixing ratio of *ca.*  $2.3/10^9$  corresponds to  $CFCl_3$  and  $CF_2Cl_2$  fluxes which are smaller by a factor of 10, and approximate present-day conditions. The results shown in (a) are obtained with the full diurnal model described in the text, which includes backscatter of solar radiation from the lower atmosphere. The results in (b), (c) and (d) are calculated with diurnally averaged insolation. (a), (b) and (d) allow for Rayleigh scattering and planetary albedo, while (c) does not. (a), (b) and (c) use the standard chemical model given in table 1, while (d) assumes that photolysis of  $ClNO_3$  follows reaction 10 rather than 9 (see text).

Concentrations of OH,  $HO_2$ , O and NO all tend to peak near noon, whereas the concentration of  $NO_2$  attains its highest value soon after sunset. The diurnally averaged model underestimates therefore the sink for odd hydrogen, reaction (3), resulting in a small excess in the average concentrations computed for OH and  $HO_2$ . In a similar fashion the diurnally averaged model overestimates the product of O and  $NO_2$  concentrations and underestimates the product of [NO] and [ $HO_2$ ].

The differences in the variation of  $O_3$  column densities with  $N_2O$  exhibited in figure 28*a-c*



reflect the manner in which the computational schemes treat  $\text{ClNO}_3$ , in addition to the reactions noted above. Reaction (42) plays a dominant rôle at high concentrations of  $\text{N}_2\text{O}$ , where chlorine chemistry is effectively suppressed owing to formation of  $\text{ClNO}_3$ . At lower concentrations of  $\text{N}_2\text{O}$ , errors in the treatment of  $\text{ClNO}_3$  and (42) by the average model are compensatory.

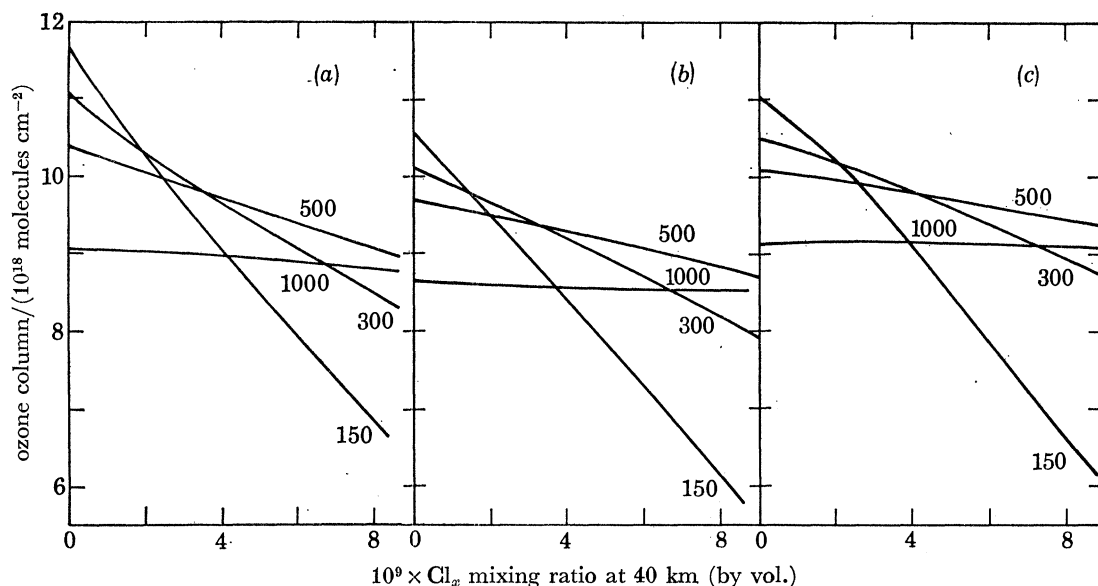
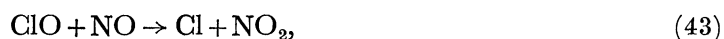


FIGURE 29. Global average column densities of ozone as a function of the  $\text{Cl}_x$  mixing ratio at 40 km. The labels on the curves refer to the  $\text{N}_2\text{O}$  mixing ratios (unit: parts/ $10^9$  by vol.) at 0 km. The panels (a), (b), and (c) are described in figure 28.

Figure 29 shows calculated values for the integrated column density of  $\text{O}_3$ , with the standard chemical model, as a function of chlorine concentration at 40 km, for several values of the  $\text{N}_2\text{O}$  mixing ratio in the troposphere. As before, these results were obtained by using the one-dimensional diffusion model. The average insolation model tends to underestimate  $\text{O}_3$  depletion for any given perturbation. The incremental effect of chlorine is small in both models for high concentrations of  $\text{N}_2\text{O}$ . This behaviour reflects the importance of  $\text{ClNO}_3$  and the rôle of the reaction



both of which serve to suppress the concentration of  $\text{ClO}$ . Differences between the average and diurnal models may be attributed largely to an overestimate of  $\text{ClNO}_3$  by the average model, as discussed above.

Figures 30–32 show the changes in the concentration of  $\text{O}_3$  as a function of altitude which result from perturbations of  $\text{Cl}_x$  and  $\text{N}_2\text{O}$ . Addition of  $\text{NO}_x$  leads to a larger decrease in  $\text{O}_3$  below 24 km in the standard model as compared with the average insolation model (see figure 31). This difference may be attributed to overestimation of  $\text{ClNO}_3$  by the average-insolation model.

Figure 32 shows the influence of enhanced concentrations of tropospheric  $\text{CO}$  and  $\text{CH}_4$ . Tropospheric ozone increases significantly in response to large enhancements of  $\text{CO}$ , as a



consequence of process (35). Increases in ozone also occur in the stratosphere, owing to more efficient termination of the Cl catalytic cycle by the reaction



This effect is more marked for large chlorine abundances.

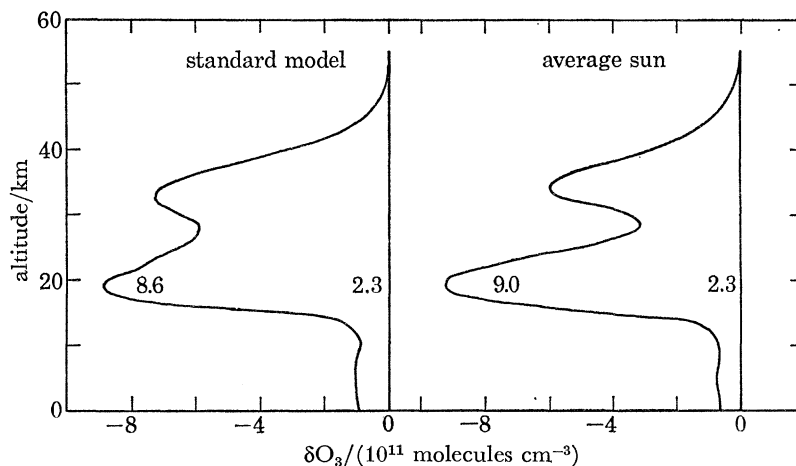


FIGURE 30. Change in the concentration of ozone as a function of altitude for added  $\text{Cl}_x$  at a fixed  $\text{NO}_x$  mixing ratio ( $\text{N}_2\text{O}$  at 0 km =  $300/10^9$ ). The labels on the curves indicate the value of  $\text{Cl}_x$  at 40 km. The left hand panel was calculated with the full diurnal model and the right hand panel with diurnally averaged insolation. The reference profile ( $\delta\text{O}_3 = 0$ ) is the calculated ozone for present-day conditions.

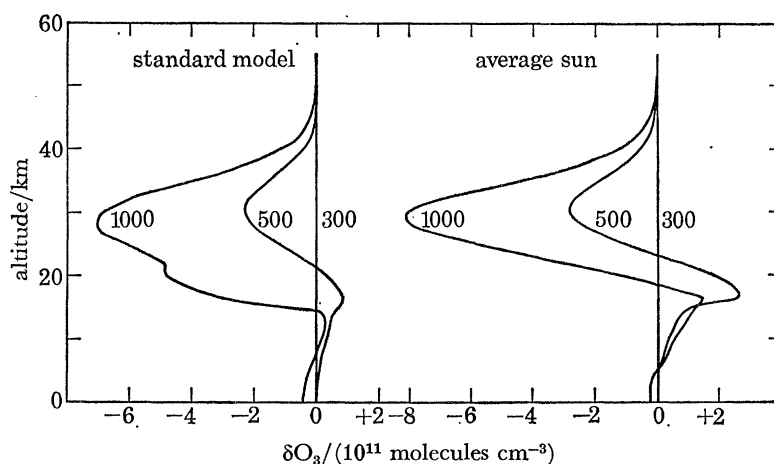


FIGURE 31. Change in the concentration of ozone as a function of altitude for added  $\text{NO}_x$  at a fixed  $\text{Cl}_x$  mixing ratio ( $\text{Cl}_x$  at 40 km =  $2.3/10^9$ ). The labels on the curves show the mixing ratio of  $\text{N}_2\text{O}$  at 0 km. The left hand panel was calculated with the full diurnal model and the right hand panel with diurnally averaged insolation.

We should caution that the computed magnitude of the perturbation to  $\text{O}_3$  may be quite sensitive to uncertainties which currently exist in the chemical model. The point is illustrated in figure 33, which may be compared with figures 28*b* and 29*b*. The models are identical in all respects except that: (i) The rate constant for (3) was set equal to  $2 \times 10^{-11} \text{ cm}^3 \text{ s}^{-1}$ ; (ii) The rate constant for (21) was increased by a factor of 3; and (iii) The rate constant for reaction (41) was increased slightly, with the new rate expression taken as  $7.5 \times 10^{-11} \exp(-737/T)$ .

Both models provide satisfactory descriptions of the natural atmosphere. The rate adjustments are consistent with experimental uncertainty, yet the character of the response to the perturbations is quite different. We may note for example that results in figure 33 would suggest that the column density of  $O_3$  might increase with increasing  $N_2O$ , at current levels of stratospheric  $Cl_x$ .

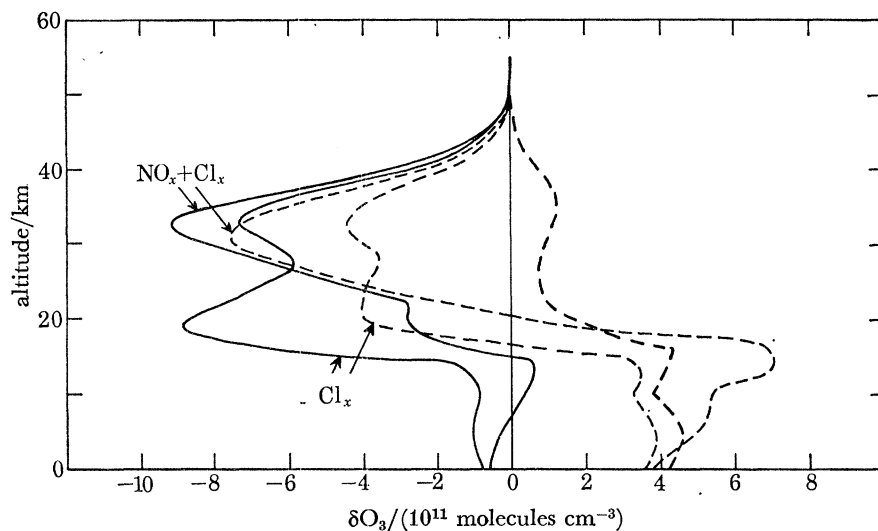


FIGURE 32. Change in ozone number density as a function of altitude for added  $NO_x$ ,  $Cl_x$ ,  $CO$  and  $CH_4$ . The solid curves represent calculations with present-day values for  $CH_4$  and  $CO$ , whereas the dashed curves show the influence of increased tropospheric  $CO$  and  $CH_4$ , by factors of 7 and 2.5 respectively. The curves labelled  $Cl_x$  show the ozone changes which result from increasing  $Cl_x$  to  $8.6/10^9$  at 40 km. The curves labelled  $NO_x$  and  $Cl_x$  show the additional effect of increasing tropospheric  $N_2O$  to  $1000/10^9$ . The reference profile assumes  $N_2O$  at 0 km =  $300/10^9$ ,  $Cl_x$  at 40 km =  $2.3/10^9$ , approximating present-day conditions.

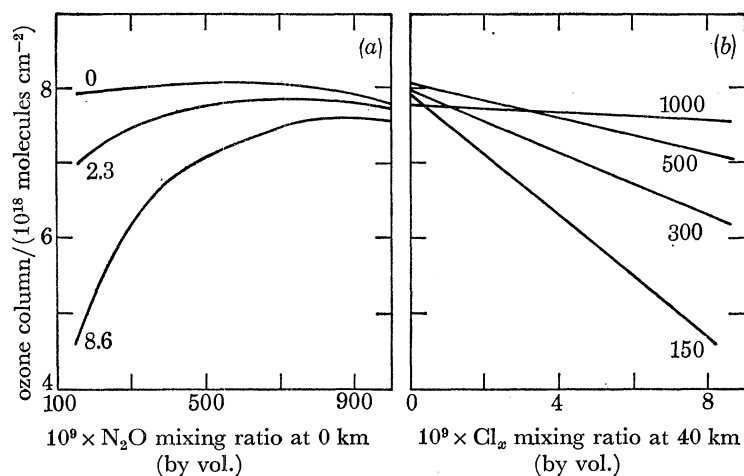


FIGURE 33. Global average ozone column densities as a function of  $N_2O$  and  $Cl_x$ . The curves are labelled as in figures 28 and 29. These results were calculated with diurnally averaged insolation as in figure 28*b*. The modified rates for reactions 3, 21 and 41 described in the text were used.

Inherent limitations of the one-dimensional diffusion model were discussed earlier. The model should provide a satisfactory description of  $O_3$  above about 28 km, but cannot account for the distribution of  $O_3$  at lower levels, where dynamical effects are predominant and inadequately described by one dimensional diffusion. One-dimensional diffusion models have

been applied to the assessment of  $O_3$  perturbations, despite these limitations, with the hope that the models should satisfactorily simulate fractional changes to total  $O_3$ . As an alternate approach one might assume that the transition from chemical to dynamical control of  $O_3$  should occur over a narrow altitude range. Models might be used therefore to estimate the fractional change in the concentration of  $O_3$  at the transition boundary and observed concentrations of  $O_3$  at lower levels might be scaled appropriately to reflect the influence of perturbations. This procedure is useful to the extent that  $O_3$  may be regarded as a passive tracer in the dynamical region, and to the extent that we can identify a well defined boundary separating zones of chemistry and dynamics (see McElroy *et al.* 1974).

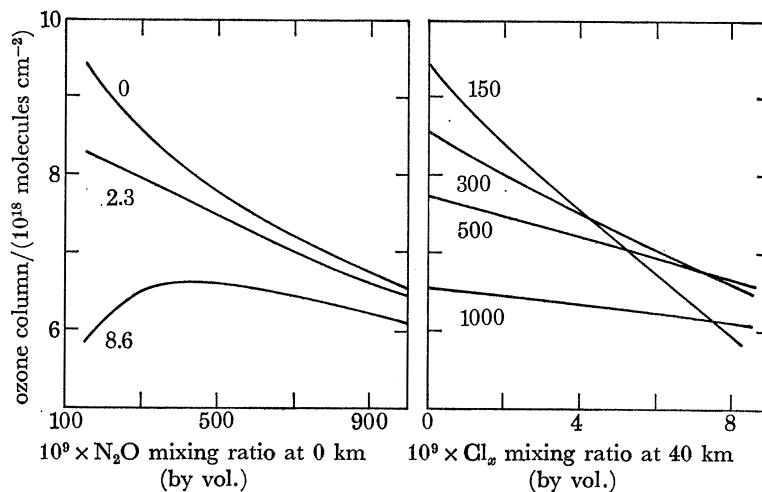


FIGURE 34. Global average ozone column densities as a function of  $N_2O$  and  $Cl_x$ . The curves are labelled as in figures 28 and 29. The full diurnal model was employed above 28 km, and the scaling procedure applied below that level (see text).

The relative influences of chemistry and dynamics may be evaluated by comparison of relevant time constants. The chemical time constant may be defined as the time required for photolytic production of a given concentration of  $O_3$ ,

$$\tau = [O_3]/2J_{O_2}[O_2], \quad (45)$$

where  $J_{O_2}$  is the rate (unit:  $s^{-1}$ ) for photodissociation of  $O_2$ . Chemical time constants for the unperturbed system are shown for several latitudes in figure 35. Consideration of the observational data for  $O_3$  indicates that dynamical time constants cannot exceed about 3 months, and are most probably smaller than this by at least a factor of 3 (Oort & Rasmussen 1971). Implications for  $O_3$  perturbations are summarized in figure 34.

A comparison of figure 34 with figures 28 and 29 suggests that differences between models are most pronounced in their response to low concentrations of  $NO_x$ . The variance between results obtained with the diffusion and scaling approaches provide some subjective estimate of the inherent uncertainty. The diffusion model allows for enhancement of the source for perturbed  $O_3$  at low altitudes, a contribution omitted in the scaling model. On the other hand, the scaling model should account to some extent for the complex influence of global dynamics, and has the additional benefit that results should be reliable in the limit of small perturbations.

We turn our attention now to specific human influences on the atmosphere, emphasizing

possible effects on  $O_3$ . We shall make use of the one-dimensional diffusion model, while presenting sufficient information to allow the reader to gauge modifications which would arise with a scaling approach. We consider a variety of models as summarized in table 3. Models describing perturbations associated with combustion are labelled A. Models incorporating effects of chlorocarbons and  $N_2O$  from recombination of fixed N are designated by symbols B and C, respectively. Numerals are used to distinguish specific models employed to describe possible human influences in each of these broad categories.

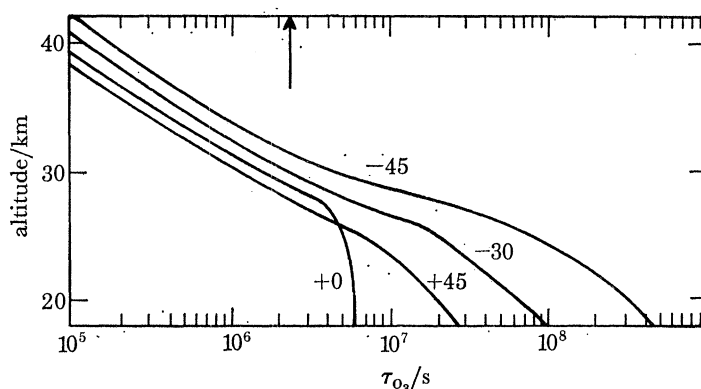


FIGURE 35. The chemical lifetime of ozone (equation (45)) is shown as a function of altitude, for  $20^\circ$  solar declination, and the latitudes marked on the curves. The arrow indicates a lifetime of one month.

TABLE 3. DESCRIPTION OF MODELS

	combustion
A1	CO, $H_2$ from curves A, figure 24
A2	CO, $H_2$ from curves A, figure 24, $N_2O$ from curve E, figure 26 <i>a</i>
A3	CO, $H_2$ from curves B, figure 24
A4	CO, $H_2$ from curves B, figure 24, $N_2O$ from curve E, figure 26 <i>a</i>
	halocarbons
B1	$CFCl_3$ , $CF_2Cl_2$ from curves A, figure 27
B2	$CFCl_3$ , $CF_2Cl_2$ , $CCl_4$ , $CH_3CCl_3$ from curves A, figure 27
B3	$CFCl_3$ , $CF_2Cl_2$ from curves B, figure 27
B4	$CFCl_3$ , $CF_2Cl_2$ , $CCl_4$ , $CH_3CCl_3$ from curves B, figure 27
	nitrogen
C1	$N_2O$ from curves A, C, E, figure 26 <i>a</i>
C2	$N_2O$ from curves A, C, E, figure 26 <i>b</i>
C3	$N_2O$ from curves B, D, E, figure 26 <i>a</i>

Possible effects of combustion are summarized in figure 36. Models A1 and A2 indicate the influence of direct releases of CO and  $H_2$ . Models A3 and A4 show incremental effects associated with combustion-related releases of  $N_2O$ . The increase of total ozone arises principally from enhanced concentrations of the gas in the troposphere, as shown in figures 32 and 37. In the stratosphere, the mixing ratio of  $Cl_x$  increases in response to reduced concentrations of tropospheric OH. This process compensates for the reduced efficiency of the  $Cl_x$  catalytic cycle, due to enhanced levels of  $CH_4$  as discussed above. Anticipated changes in atmospheric  $N_2O$ ,  $CH_4$ , CO,  $CH_3Cl$  and stratospheric  $Cl_x$  are given in figure 36*b*.

Figure 38 summarizes possible effects of chlorocarbons, for both high (upper panel) and low (lower panel) emission rates. Release of  $CFCl_3$  and  $CF_2Cl_2$  at constant rates of  $341\,000\ t\ a^{-1}$

and 410 000 t a<sup>-1</sup> might be expected to lead to reductions in column O<sub>3</sub> by as much as 5% by the year 2000, growing to 15% by 2100. The results shown here were obtained with a model which assumed that stratospheric photolysis was the only removal process for CFCl<sub>3</sub> and CF<sub>2</sub>Cl<sub>2</sub>. The perturbation to ozone would be smaller if there were additional important sinks (cf. Ausloos *et al.* 1977). Inclusion of CO and H<sub>2</sub> emissions diminishes the perturbations to total

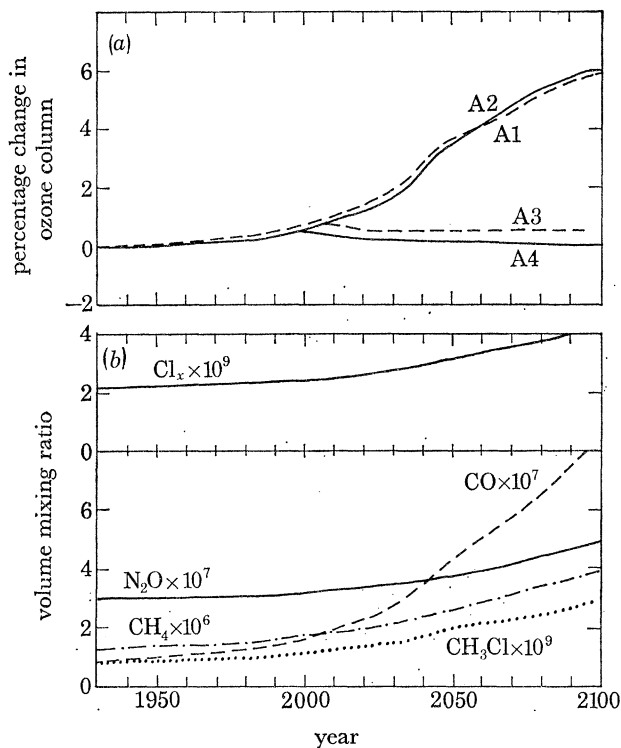


FIGURE 36.

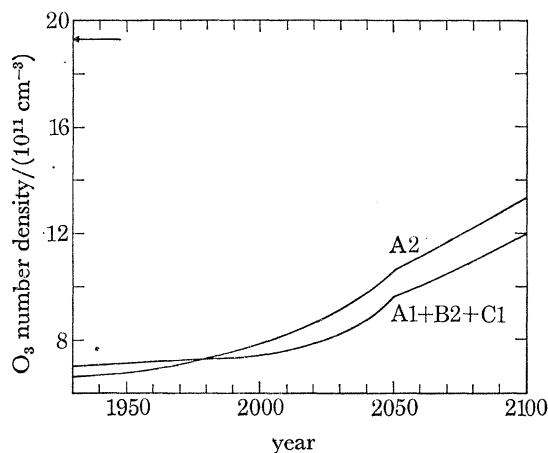


FIGURE 37.

FIGURE 36. (a) Changes in the global average ozone column associated with combustion. A1–A4 include emissions of CO and H<sub>2</sub>, while A2 and A4 include also the combustion related source of N<sub>2</sub>O. The labels on the curves are described in detail in table 3. (b) Time history for the mixing ratios of N<sub>2</sub>O, CO, CH<sub>4</sub> and CH<sub>3</sub>Cl at 0 km and Cl<sub>x</sub> at 40 km for model A2.

FIGURE 37. Changes in the ozone number density at 0 km, arising from combustion related emissions (A2) and multiple perturbations (A1 + B2 + C1). The labels on the curves are described in table 3. The arrow indicates the present E.P.A. National Ambient Air Quality Standard for ground level ozone of 80 parts/10<sup>9</sup> (by vol.).

ozone, as discussed above. The validity of these models is particularly suspect for large perturbations, in that we do not allow for feedback on atmospheric structure and dynamics due to large changes in O<sub>3</sub>. Mixing ratios for CH<sub>4</sub>, CFCl<sub>3</sub>, CF<sub>2</sub>Cl<sub>2</sub>, CH<sub>3</sub>CCl<sub>3</sub> and Cl<sub>x</sub> are given in figure 39 for models B2 and B4.

The possible impact of agricultural and combustion related sources of N<sub>2</sub>O is summarized in figure 40. We may note that results for model C1 are similar to those for C2. The O<sub>3</sub> perturbation is relatively insensitive to the choice of lifetime for atmospheric N<sub>2</sub>O, owing to time delays built into our model of the nitrogen cycle. We have assumed that recombination of fixed N is the major natural source of atmospheric N<sub>2</sub>O and that the yield for production of anthropogenic N<sub>2</sub>O is similar to that for the natural system. On the other hand, waters polluted by human nitrogen are often biologically active and have been observed to provide significant prompt sources of atmospheric N<sub>2</sub>O (Kaplan *et al.* 1978). Assessment of human influence on



$N_2O$  is difficult given the gaps in our understanding of processes which affect the cycle of this gas. The impact on  $O_3$  could be larger, or smaller, than suggested in figure 40. An upper limit to the effect might be estimated if we assume a small natural source for  $N_2O$ , with immediate conversion of anthropogenic nitrogen to this gas. A limit based on this consideration is included in figure 40. This model would imply an increase of  $N_2O$  from 160 parts in  $10^9$  in 1940 to  $300/10^9$  today.

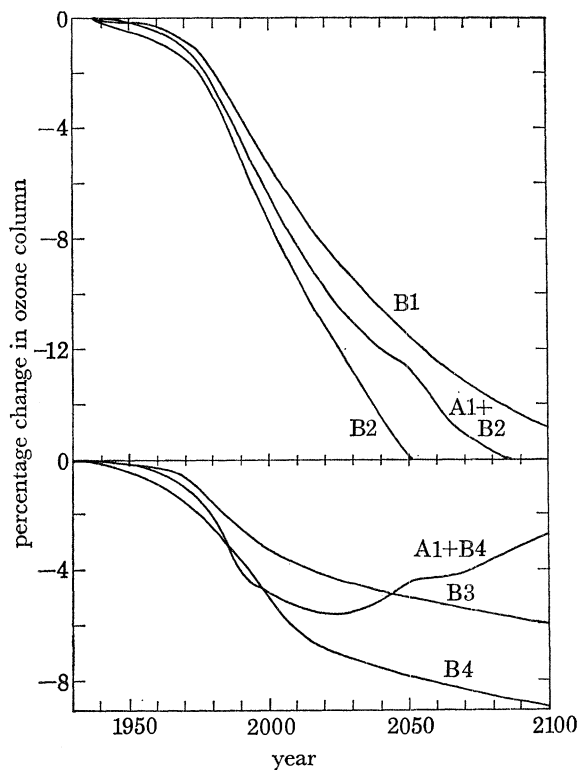


FIGURE 38.

FIGURE 38. Changes in the global average ozone column associated with chlorocarbon use (B1–B4) and combustion (A1). The upper panel employs the high emission rates for chlorocarbons given in figure 27 while the lower panel assumes some regulation of chlorocarbon emissions. The labels on the curves are described in table 3.

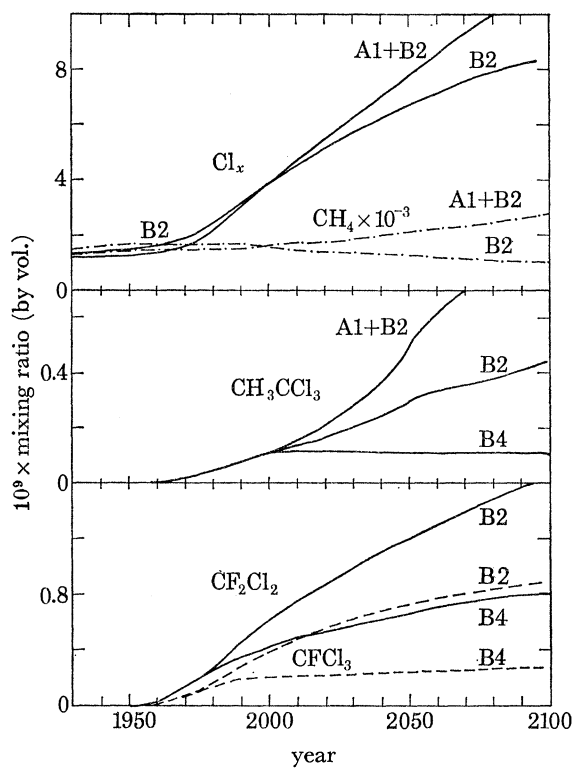


FIGURE 39.

FIGURE 39. Mixing ratios for  $Cl_x$  (at 40 km) and  $CH_4$ ,  $CH_3CCl_3$ ,  $CF_2Cl_2$  and  $CFCl_3$  (at 0 km) for the models in figure 38. The upper panel illustrates the consequences of adding combustion emissions (A1) to the chlorocarbon emissions (B2); the lower panel compares the results of the high and low emission rates in figure 27 (B2 and B4) on the abundances of  $CFCl_3$  and  $CF_2Cl_2$ , while the middle panel shows both effects for  $CH_3CCl_3$ .

The behaviour of  $O_3$  in response to multiple coupled perturbations is illustrated in figure 41. We adopt, as a baseline, an atmosphere subject to what may be regarded as the least discretionary of human influences, combustion and agriculture (curve A1 + C1). The figure summarizes then the additional effects which might arise due to various chlorocarbon release patterns. It is clear that the influence of a combination of human practices is intrinsically non-linear as regards the effect on  $O_3$ . As seen earlier, a constant release of  $CFCl_3$  and  $CF_2Cl_2$  at rates prevalent in 1974 might be expected to cause a reduction of column  $O_3$  by about 15% in the year 2100. Indeed the net perturbation in the fully coupled system is less than that which we derive for the chlorine perturbation alone, 8% as compared to 15%. The 'baseline'



calculation shows the ozone column abundance increasing with time. The additional ozone is present in the troposphere, rather than the stratosphere (see figures 32 and 37). The impact of such a perturbation to tropospheric ozone clearly requires careful study.

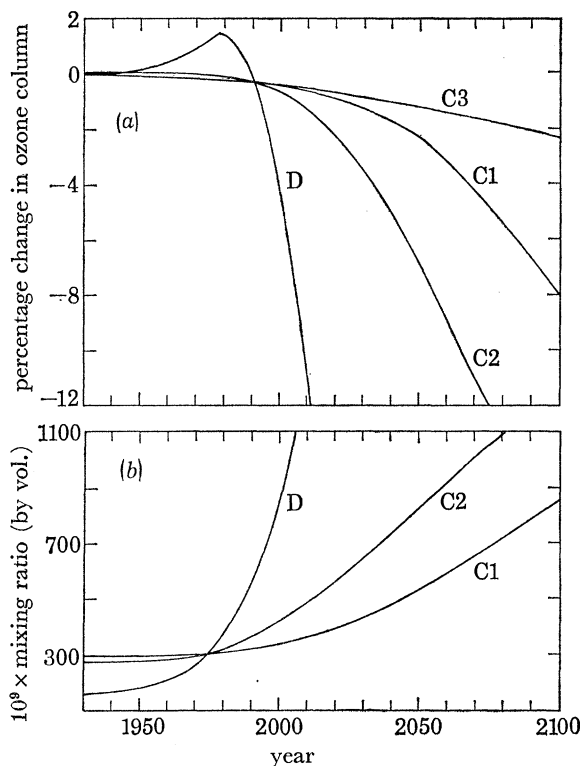


FIGURE 40.

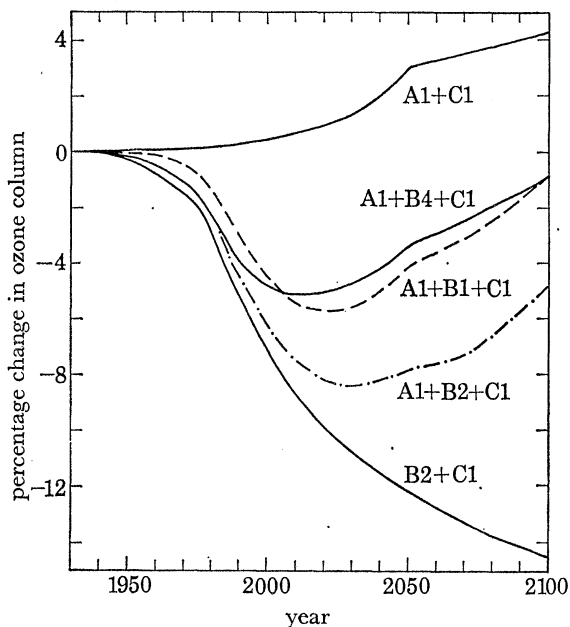


FIGURE 41.

FIGURE 40. (a) Changes in the global average ozone column associated with agricultural and combustion related sources of  $N_2O$ . The labels are described in table 3. C1, C3 and D employ a 140 a lifetime for  $N_2O$ , and curve C2 a 20 a lifetime. Curve D is the result of an upper limit calculation which allows for immediate conversion of anthropogenically fixed nitrogen to  $N_2O$  in 100% yield. (b) Associated changes in  $N_2O$  at 0 km for selected models in (a).

FIGURE 41. Changes in the global average ozone column associated with multiple perturbations (due to combustion (A), chlorocarbon use (B) and fertilizer use (C)). The labels are described in table 3.

## 6. CONCLUDING REMARKS

Human activities associated with combustion, food production, and chlorocarbon industries may be expected to significantly perturb the chemistry of the atmosphere on a global scale. Increases in the mean concentrations of  $CO$ ,  $CO_2$ ,  $CFCl_3$ ,  $CF_2Cl_2$  and  $CH_3CCl_3$  are already apparent, and detectable changes should be evident for  $N_2O$ ,  $CH_4$ ,  $CH_3Cl$  and  $O_3$  within the next fifty years. The average column abundance of  $O_3$  could decrease by more than 10% by the year 2100 if present trends should continue, and tropospheric ozone may be significantly enhanced.

Assessment of Man's impact on the atmosphere requires a comprehensive model which must simulate, not only essential aspects of atmospheric chemistry and dynamics, but also the manner in which the atmosphere interacts with land, hydrosphere and biosphere. Our understanding of these systems is fragmentary. Human influences are strongly interactive, with

feedbacks which are both positive and negative. Chlorocarbon emissions will enhance the supply of chlorine to the stratosphere. The associated reduction in  $O_3$  may be offset however to some extent by an increase in the stratospheric burdens of  $NO_x$  and  $CH_4$  induced by other anthropogenic activity.

Our treatment of human effects on the atmosphere is necessarily incomplete. We ignore for example direct and indirect consequences associated with human exploitation of land, fresh waters, estuaries and oceans and it is clear that these activities could have a predominant influence on the coupled biosphere-atmosphere system.

Our discussion here has sought to describe the atmosphere as an isolated compartment, investigating the consequence for  $O_3$  of various gas exchanges across the lower boundary. Even this limited problem poses major difficulties.

Our model does not account for the present global distribution of  $O_3$ . The deficiencies may be attributed in part to uncertainties in our understanding of atmospheric chemistry, in part to the inadequacy of our model for atmospheric dynamics. Lifetimes for  $N_2O$ ,  $O_3$  and halocarbons may be affected by heterogeneous processes in the troposphere. The abundance and distribution of tropospheric OH is poorly determined and of central importance, in that reactions with OH regulate the stratospheric concentrations of  $CH_4$ ,  $CH_3Cl$  and  $CH_3CCl_3$ . Factors which influence the concentration of stratospheric  $H_2O$  are not defined. The observed variability of stratospheric ClO is puzzling, and raises the possibility of a major gap in our description of the chlorine cycle. Our models do not allow for coupling of dynamics and chemistry, which might influence the residence time of gases in the perturbed stratosphere.

Finally we should emphasize that our understanding of  $N_2O$  and the global nitrogen cycle is seriously incomplete. This problem merits special attention in that the concentration of  $N_2O$  may be affected by non-discretionary human activity and in that  $N_2O$  plays a key rôle in many important areas of atmospheric chemistry.

This work was supported by the National Science Foundation and the National Aeronautic and Space Administration under contracts NASA-NSG-2031 and NSF-ATM-22723 respectively. One of us (J.A.L.) acknowledges support from the Rockefeller Foundation's Fellowship Program in Environmental Affairs. We are indebted to the Ames Research Center of the National Aeronautic and Space Administration for computational facilities. Computer time was also provided by the National Center for Atmospheric Research, which is supported by the National Science Foundation.

#### REFERENCES

- Ackerman, M., Frimont, D., Girard, A., Gottignies, M. & Muller, C. 1976 Stratospheric HCl from infrared spectra. *Geophys. Res. Lett.* **3**, 81.
- Anastasi, C. & Smith, I. W. M. 1976 Rate measurements of reactions of OH by resonance absorption 5: Rate constants for  $OH + NO_2 (+M) \rightarrow HNO_3$  over a wide range of temperature and pressure. *J. chem. Soc. Faraday Trans. II* **72**, 1459.
- Anderson, J. G. 1971 Rocket-borne ultraviolet spectrometer measurement of OH resonance fluorescence with diffusive transport model for mesospheric photochemistry. *J. Geophys. Res.* **76**, 4634.
- Anderson, J. G. 1975 The measurement of atomic oxygen and hydroxyl in the stratosphere. *Proceedings of the Fourth Conference on the Climatic Impact Assessment Program*, 4-7 February 1975, pp. 458-464. U.S. Dept. of Transportation Report no. DOT-TSC-OST-75-38.
- Anderson, J. G. 1976 The absolute concentration of OH ( $X^2\Pi$ ) in the earth's stratosphere. *Geophys. Res. Lett.* **3**, 165.

- Anderson, J. G. & Kaufman, F. 1973 Kinetics of the reaction  $\text{OH}(v = 0) + \text{O}_3 \rightarrow \text{HO}_2 + \text{O}_2$ . *Chem. Phys. Lett.* **19**, 483.
- Anderson, J. G., Margitan, J. J. & Stedman, D. H. 1977 Atomic chlorine and the chlorine monoxide radical in the stratosphere: Three in situ observations. *Science, N.Y.* **198**, 501.
- Atkinson, R., Hansen, D. A. & Pitts, J. N. 1975 Rate constants for the reaction of the OH radical with  $\text{H}_2$  and NO ( $M = \text{Ar}, \text{N}_2$ ). *J. chem. Phys.* **62**, 3284.
- Atkinson, R., Perry, R. A. & Pitts, J. N. 1977 Absolute rate constants for the reaction of OH radicals with allene, 1,3-butadiene and 3-methyl-1-butene over the temperature range 299–424 °K. *J. chem. Phys.* **67**, 3170.
- Ausloos, P., Rebert, R. E. & Glasgow, L. 1977 Photodecomposition of chloromethanes absorbed on silica surfaces. *Natn. Bur. Stds J. Res.* **82**, 1.
- Bates, D. R. & Hays, P. B. 1967 Atmospheric nitrous oxide. *Planet. Space Sci.* **15**, 189.
- Bates, D. R. & Witherspoon, A. 1952 The photochemistry of some minor constituents of the earth's atmosphere. *Mon. Not. R. Astr. Soc.* **112**, 101.
- Baulch, D. L., Drysdale, D. D., Horne, D. G. & Lloyd, A. C. 1972 *Evaluated kinetic data for high temperature reactions*, vol. 1: Homogeneous gas phase reactions of the  $\text{H}_2$ - $\text{O}_2$  system. London: Butterworths.
- Baulch, D. L., Drysdale, D. D. & Horne, D. G. 1973 *Evaluated kinetic data for high temperature reactions*, vol. 2: Homogeneous gas phase reactions of the  $\text{H}_2$ - $\text{N}_2$ - $\text{O}_2$  system. London: Butterworths.
- Becker, K. H., Groth, W. & Thran, D. 1973 Mechanism of the air afterglow  $\text{NO} + \text{O} \rightarrow \text{NO}_2 + h\nu$ . *14th Combustion Symposium*, p. 353. Combustion Institute, Pittsburgh, Pa.
- Bemand, P. P. & Clyne, M. A. A. 1977 Atomic resonance fluorescence for rate constants of rapid bimolecular reactions. Part 6. Hydrogenation reactions:  $\text{H} + \text{Cl}_2$  from 300–700 °K and  $\text{H} + \text{NO}_2$  at 298 °K. *J. chem. Soc. Faraday Trans. II* **73**, 394.
- Bolin, B. 1977 Changes of land biota and their importance for the carbon cycle. *Science, N.Y.* **196**, 613.
- Brice, K. A., Eggleton, A. E. J. & Penkett, S. A. 1977 An important ground surface sink for atmospheric nitrous oxide. *Nature, Lond.* **268**, 127.
- Brown, R. D. H. & Smith, I. W. M. 1975 Absolute rate constants for the reactions of  $\text{O}(^3\text{P})$  atoms with HCl and HBr. *Int. J. Chem. Kin.* **7**, 301.
- Burkert, P., Rabus, D. & Bolle, H. J. 1974 Stratospheric water vapor and methane profiles. *Proceedings of the International Conference on Structure, Composition and General Circulation of the Upper and Lower Atmospheres and Possible Anthropogenic Perturbations*, Melbourne, Australia, pp. 267–274.
- Burnett, C. R. 1976 Terrestrial OH abundance measurement by spectroscopic observation of resonance absorption of sunlight. *Geophys. Res. Lett.* **3**, 319.
- Burnett, C. R. 1977 Spectroscopic measurement of atmospheric OH. Paper presented at American Physical Society Meeting, 25–29 April 1977.
- Burns, R. C. & Hardy, R. W. F. 1975 *Nitrogen fixation in bacteria and higher plants*. New York: Springer-Verlag.
- Burrows, J. P., Harris, G. W. & Thrush, B. A. 1977 Rates of reaction of  $\text{HO}_2$  with OH and O studied by laser magnetic resonance. *Nature, Lond.* **267**, 233.
- Calvert, J. G., Kerr, J. A., Demerjian, K. L. & McQuigg, R. D. 1972 Photolysis of formaldehyde as a hydrogen atom source in the lower atmosphere. *Sciences, N.Y.* **175**, 751.
- Campbell, I. M. & Gray, C. N. 1973 Rate constants for  $\text{O}(^3\text{P})$  recombination and association with  $\text{N}(^4\text{S})$ . *Chem. Phys. Lett.* **18**, 607.
- Campbell, I. M. & Hardy, B. J. 1977 Relative rates of reaction of hydroxyl radicals with  $\text{O}(^3\text{P})$  atoms and CO molecules. *Chem. Phys. Lett.* **47**, 475.
- Campbell, I. M. & Thrush, B. A. 1968 Reactivity of hydrogen to atomic nitrogen and atomic oxygen. *Trans. Faraday Soc.* **64**, 1265.
- Cavender, J. H., Kircher, D. S. & Hoffman, A. J. 1973 *Nationwide air pollutant emission trends 1940–1970*. Washington D.C.: Environmental Protection Agency.
- Chaloner, C. P., Drummond, J. R., Houghton, J. T., Jarnot, R. F. & Rococ, H. K. 1975 Stratospheric measurements of  $\text{H}_2\text{O}$  and the diurnal change of NO and  $\text{NO}_2$ . *Nature, Lond.* **258**, 696.
- Chameides, W. & Walker, J. C. G. 1973 A photochemical theory of tropospheric ozone. *J. Geophys. Res.* **78**, 8751.
- Chan, W. H., Uselman, W. M., Calvert, J. G. & Shaw, J. H. 1977 The pressure dependence of the rate constant for the reaction:  $\text{HO} + \text{CO} \rightarrow \text{H} + \text{CO}_2$ . *Chem. Phys. Lett.* **45**, 240.
- Chapman, C. J. & Wayne, R. P. 1974 The reaction of atomic oxygen and hydrogen with nitric acid. *Int. J. Chem. Kin* **6**, 617.
- Chou, C. C., Smith, W. S., Vera Ruiz, H., Moe, K., Crescentini, G., Molina, M. J. & Rowland, F. S. 1977 The temperature dependence of the ultraviolet absorption cross-sections of  $\text{CCl}_2\text{F}_2$  and  $\text{CCl}_3\text{F}$  and their stratospheric significance. *J. phys. Chem.* **81**, 286.
- C.I.A.P. 1974 *Climatic Impact Assessment Program Report of Findings*. The effects of stratospheric pollution by aircraft. Report DOT-TST-75-50. Washington D.C.: U.S. Department of Transportation.
- Clyne, M. A. A. & Coxon, J. A. 1968 Kinetic studies of oxyhalogen radical systems. *Proc. R. Soc. Lond. A* **303**, 207.
- Clyne, M. A. A. & Down, S. 1974 Kinetic behavior of  $\text{OH } X^2\Pi$  and  $A^2\Sigma^+$  using molecular resonance fluorescence spectrometry. *J. chem. Soc. Faraday Trans. II* **70**, 253.

- Clyne, M. A. A. & McDermid, I. S. 1975 Mass spectrometric determinations of the rates of elementary reactions of NO and NO<sub>2</sub> with ground state N<sup>4</sup>S atoms. *J. chem. Soc. Faraday Trans. I* **71**, 2189.
- Clyne, M. A. A. & Monkhouse, P. B. 1977 Atomic resonance fluorescence for rate constants of rapid bimolecular reactions. Part 5. Hydrogen atom reactions; H+NO<sub>2</sub> and H+O<sub>3</sub>. *J. chem. Soc. Faraday Trans. II* **73**, 298.
- Clyne, M. A. A. & Nip, W. S. 1976 Study of elementary reactions by atomic resonance absorption with a non-reversed source. *J. chem. Soc. Faraday Trans. I* **72**, 838.
- Clyne, M. A. A. & Watson, R. T. 1974 Kinetic studies of diatomic free radicals using mass spectrometry. Part 2. Rapid bimolecular reactions involving the ClOX<sup>2</sup>Π radical. *J. chem. Soc. Faraday Trans. I* **70**, 2250.
- C.A.S.T. 1976 *Council for Agricultural Science and Technology Report*. Effect of increased nitrogen fixation on stratospheric ozone. Department of Agronomy, Iowa State University, Ames, Iowa.
- Cox, R. A. & Derwent, R. G. 1975 Kinetics of the reaction of HO<sub>2</sub> with nitric oxide and nitrogen dioxide. *J. Photochem.* **4**, 139.
- Cox, R. A. & Derwent, R. G. 1976 The ultraviolet absorption spectrum of gaseous nitrous acid. *J. Photochem.* **6**, 23.
- Cox, R. A., Derwent, R. G. & Holt, P. M. 1976 Relative rate constants for the reactions of OH radicals with H<sub>2</sub>, CH<sub>4</sub>, CO, NO, and HONO at atmospheric pressure and 296 °K. *J. chem. Soc. Faraday Trans. I* **72**, 2031.
- Crutzen, P. J. 1970 The influence of nitrogen oxides on the atmospheric ozone content. *Q. J. R. met. Soc.* **96**, 320.
- Crutzen, P. J. 1971 Ozone production rates in an oxygen-hydrogen-nitrogen atmosphere. *J. Geophys. Res.* **76**, 7311.
- Davidson, J. A., Schiff, H., Streit, G. E., McAfee, J. R., Schmeltekopf, A. L. & Howard, C. J. 1977 Temperature dependence of O(<sup>1</sup>D) rate constants for reactions with N<sub>2</sub>O, H<sub>2</sub>, CH<sub>4</sub>, HCl and NH<sub>3</sub>. *J. chem. Phys.* **67**, 5021.
- Davis, D. D., Fischer, S. & Schiff, R. 1974a Flash photolysis resonance fluorescence kinetics study: temperature dependence of the reactions OH+CO → CO<sub>2</sub>+H and OH+CH<sub>4</sub> → H<sub>2</sub>O+CH<sub>3</sub>. *J. chem. Phys.* **61**, 2213.
- Davis, D. D., Herron, J. T. & Huie, R. E. 1973a Absolute rate constants for the reaction O(<sup>3</sup>P)+NO<sub>2</sub> → NO+O<sub>2</sub> over the temperature range 230–339 °K. *J. chem. Phys.* **58**, 530.
- Davis, D. D., Payne, W. A. & Stief, L. J. 1973b The hydroperoxyl radical in atmospheric chemical dynamics: reaction with carbon monoxide. *Science, N.Y.* **179**, 280.
- Davis, D. D., Wong, W. & Lephardt, J. 1973c A laser flash photolysis-resonance fluorescence kinetic study: reaction of O(<sup>3</sup>P) with O<sub>3</sub>. *Chem. Phys. Lett.* **22**, 273.
- Davis, D. D., Wong, W. & Schiff, R. 1974b A dye laser flash photolysis kinetics study of the reaction of ground-state atomic oxygen with hydrogen peroxide. *J. phys. Chem.* **78**, 463.
- Delwiche, C. C. & Likens, G. E. 1977 Biological response to fossil fuel combustion products. *Global chemical cycles and their alterations by man* (ed. W. Stumm), p. 73. Dahlem Konferenzen, Berlin.
- Demerjian, K. L., Kerr, J. A. & Calvert, J. G. 1974 The mechanism of photochemical smog formation. *Adv. Environ. Sci. Tech.* **4**, 1.
- DeMore, W. B. 1977 Chlorofluoromethanes and the stratosphere. *NASA Reference Publication* 1010 (ed. R. D. Hudson), p. 36.
- Ditchburn, R. W. & Young, P. A. 1962 The absorption of molecular oxygen between 1850 and 2500 Å. *J. atmos. terr. Phys.* **24**, 127.
- Ehhalt, D. H. 1974 The atmospheric cycle of methane. *Tellus* **26**, 58.
- Ehhalt, D. H., Heidt, L. E., Lueb, R. H. & Martell, G. A. 1975a Concentrations of CH<sub>4</sub>, CO, CO<sub>2</sub>, H<sub>2</sub>, H<sub>2</sub>O and N<sub>2</sub>O in the upper stratosphere. *J. atmos. Sci.* **32**, 163.
- Ehhalt, D. H., Heidt, L. E., Lueb, R. H. & Pollock, W. 1975b The vertical distribution of trace gases in the stratosphere. *Pure appl. Geophys.* **113**, 389.
- Evans, W. F. J., Hunten, D. M., Llewellyn, E. J. & Jones, A. V. 1968 Altitude profile of the infrared atmospheric system of oxygen in the dayglow. *J. Geophys. Res.* **73**, 2885.
- Eyre, J. R. & Roscoe, H. K. 1977 Radiometric measurement of stratospheric HCl. *Nature, Lond.* **266**, 243.
- Fabian, P., Schmidt, U., Volz, A., Ehhalt, D. H., Seiler, W., Deser, X., Weiler, K. H. & Borchers, R. 1977 Simultaneously measured vertical profiles of H<sub>2</sub>, CH<sub>4</sub>, CO, CO<sub>2</sub>, N<sub>2</sub>O, F-11, F-12, NO and O<sub>3</sub> in the mid-latitude stratosphere. Paper presented at the IAGA/IAMAP meeting, Seattle, 1977. (To be published in *Pure appl. Geophys.*)
- Fang, T.-M., Wofsy, S. C. & Dalgarno, A. 1974 Opacity distribution functions and absorption in Schumann-Runge bands of molecular oxygen. *Planet. Space Sci.* **22**, 413.
- Farmer, C. B., Raper, O. F. & Norton, R. H. 1976 Spectroscopic detection and vertical distribution of HCl in the troposphere and stratosphere. *Geophys. Res. Lett.* **3**, 13.
- Galbali, I. E. 1976 Man-made CCl<sub>4</sub> in the atmosphere. *Science, N.Y.* **193**, 573.
- Gebhart, R., Bojkov, R. & London, J. 1970 Stratospheric ozone: a comparison of observed and computed models. *Beitr. Phys. Atmos.* **43**, 209.
- Gibson, G. E. & Bayliss, N. S. 1933 Variation with temperature of the continuous absorption spectrum of diatomic molecules. Part I. Experimental, the absorption spectrum of chlorine. *Phys. Rev.* **44**, 188.
- Goldan, P. D. 1977 Private communication.
- Goldan, P. D., Bush, Y. A., Fehsenfeld, F. C., Albritton, D. L., Crutzen, P. J., Schmeltekopf, A. L. & Ferguson, E. E. 1978 Tropospheric N<sub>2</sub>O mixing ratio measurements. *J. Geophys. Res.* **83**, 935.



- Goody, R. 1969 Time variations in atmospheric  $N_2O$  in eastern Massachusetts. *Planet. Space Sci.* **17**, 1319.
- Goody, R. & Walshaw, C. D. 1953 The origin of atmospheric nitrous oxide. *Q. J. R. met. Soc.* **74**, 496.
- Graham, R. A. & Johnston, H. S. 1978 The photochemistry of  $NO_3$  and the kinetics of the  $N_2O_5-O_3$  system. *J. phys. Chem.* **82**, 254.
- Graham, R. A. & Johnston, H. S. 1974 Kinetics of the gas-phase reaction between ozone and nitrogen dioxide. *J. chem. Phys.* **60**, 4628.
- Graham, R. A., Winer, A. M. & Pitts, J. N. 1977 Temperature dependence of the unimolecular decomposition of pernitric acid and its atmospheric implications. *Chem. Phys. Lett.* **51**, 215.
- Greiner, N. R. 1969 Hydroxyl radical kinetics spectroscopy. V. Reactions with  $H_2$  and CO in the range 300–500 °K. *J. chem. Phys.* **51**, 5049.
- Griffing, G. W. 1977 Ozone and oxides of nitrogen production during thunderstorms. *J. Geophys. Res.* **82**, 943.
- Griggs, M. 1968 Absorption coefficients of ozone in the ultraviolet and visible regions. *J. chem. Phys.* **49**, 857.
- Grimsrud, E. P. & Rasmussen, R. A. 1975a The analysis of chlorofluorocarbons in the troposphere by gas chromatography mass spectrometry. *Atmos. Environ.* **9**, 1010.
- Grimsrud, E. P. & Rasmussen, R. A. 1975b Survey and analysis of halocarbons in the atmosphere by gas chromatography mass spectrometry. *Atmos. Environ.* **9**, 1014.
- Hack, W., Hoyerman, K. & Wagner, H. G. 1975 The reaction  $NO + HO_2 \rightarrow NO_2 + OH$  with  $OH + H_2O_2 \rightarrow HO_2 + H_2O$  as an  $HO_2$  source. *Int. J. Chem. Kin. Symp.* **1**, 329.
- Hahn, J. & Junge, C. 1977 Atmospheric nitrous oxide: a critical review. *Z. Naturf.* **32a**, 190.
- Hall, T. C. & Blacet, F. E. 1952 Separation of the absorption spectra of  $NO_2$  and  $N_2O_4$  in the range of 2400–5000 Å. *J. chem. Phys.* **20**, 1745.
- Hamilton, E. J., Jr 1975 Water vapor dependence of the kinetics of the self reaction of  $HO_2$  in the gas phase. *J. chem. Phys.* **63**, 3682.
- Hamilton, R. E. 1977 Present and predicted levels of consumption of fossil fuels. *Global chemical cycles and their alterations by man* (ed. W. Stumm), p. 155. Dahlem Konferenzen, Berlin.
- Hampson, R. F. 1973 Survey of photochemical and rate data for 28 reactions of interest in atmospheric chemistry. *J. Phys. Chem. Ref. Data* **2**, 267.
- Hampson, R. F. & Garvin, D. 1975 Chemical kinetic and photochemical data for modelling atmospheric chemistry. *NBS Technical Note* 866, Washington, D.C.
- Harker, A. & Johnston, H. S. 1973 Photolysis of nitrogen dioxide to produce transient O,  $NO_3$  and  $N_2O_5$ . *J. phys. Chem.* **77**, 1153.
- Harries, J. E. 1976 The distribution of water vapor in the stratosphere. *Rev. Geophys. Space Phys.* **14**, 565.
- Heidt, L. E., Lueb, R., Pollock, W. & Ehhalt, D. H. 1975 Stratospheric profiles for  $CCl_3F$  and  $CCl_2F_2$ . *Geophys. Res. Lett.* **2**, 445.
- Heidt, L. E., Pollock, W. H. & Lueb, R. A. 1976 Stratospheric measurements of  $CF_2Cl_2$ ,  $CFCl_3$  and  $N_2O$ . *Proceedings, Joint Symposium on Atmospheric Ozone*. (IAOC/ICACCP) Dresden, G.D.R.
- Hering, W. S. & Borden, T. R. 1967 Ozonesonde observations over North America. *Environmental Research Paper* no. 279. Air Force Cambridge Research Labs., AFCRL-64-30 (IV).
- Hering, W. S. 1975 Unpublished data.
- Hilsenrath, E. 1971 Ozone measurements in the mesosphere and stratosphere during two significant geophysical events. *J. atmos. Sci.* **28**, 295.
- Hilsenrath, E., Serdon, L. & Goodman, P. 1969 An ozone measurement in the mesosphere and stratosphere by means of a rocket sonde. *J. Geophys. Res.* **74**, 6873.
- Hochanadel, C. J., Ghormley, J. A., Boyle, J. W. & Ogren, P. J. 1977 Absorption spectrum and rates of formation and decay of the  $CH_3O_2$  radical. *J. phys. Chem.* **81**, 3.
- Hochanadel, C. J., Ghormley, J. A. & Ogren, P. J. 1972 Absorption spectrum and reaction kinetics of the  $HO_2$  radical in the gas phase. *J. chem. Phys.* **56**, 4426.
- Howard, C. J. 1977 Kinetics of the reaction of  $HO_2$  with  $NO_2$ . *J. chem. Phys.* **67**, 5258.
- Howard, C. J. & Evenson, K. M. 1977 Kinetics of the reactions of  $HO_2$  with NO. *Geophys. Res. Lett.* **4**, 437.
- Hudson, R. D. & Mahle, J. H. 1972 Photodissociation rates of molecular oxygen in the mesosphere and lower thermosphere. *J. Geophys. Res.* **77**, 2902.
- Huie, R. E., Herron, J. T. & Davis, D. D. 1972 Absolute rate constants for the reaction  $O + O_2 + M \rightarrow O_3 + M$  over the temperature range 200–346 °K. *J. phys. Chem.* **76**, 2653.
- Hunten, D. M. 1975 Vertical transport in atmospheres. *Atmospheres of Earth and the planets* (ed. B. M. McCormac), p. 59. Dordrecht, Holland: D. Reidel Pub. Co.
- Inn, E. C. Y. 1975 Absorption coefficient of HCl in the region 1400–2000 Å. *Atmos. Sci.* **32**, 2375.
- Inn, E. C. Y., Vedder, J. F., Tyson, B. J., Brewer, R. B. & Boitnott, C. A. 1977a Stratospheric halocarbon experiment. NASA Ames Research Center, Moffett Field, CA 94035.
- Inn, E. C. Y., Tyson, B. M. & Arvesen, J. C. 1977b Atmospheric halocarbon experiment. NASA Ames Research Center, Moffett Field, CA 94035.
- Jaffe, L. S. 1973 Carbon monoxide in the biosphere: sources, distribution and concentrations. *J. Geophys. Res.* **78**, 5293.

- Johnston, H. S. 1971 Reduction of stratospheric ozone by nitrogen oxide catalysts from SST exhaust. *Science, N.Y.* **173**, 517.
- Johnston, H. S. 1976 Use of excess carbon-14 data to calibrate models of stratospheric ozone depletion by supersonic transports. *J. Geophys. Res.* **81**, 368.
- Johnston, H. S. & Graham, R. 1974 Photochemistry of  $\text{NO}_x$  and  $\text{HNO}_x$  compounds. *Can. J. Chem.* **52**, 1415.
- Johnston, H. S., Morris, E. D. & Van de Bogaerde, J. 1969 Molecular modulation kinetic spectrometry.  $\text{ClO}$  and  $\text{ClO}_2$  radicals in the photolysis of chlorine in oxygen. *J. Am. chem. Soc.* **91**, 7712.
- Kaplan, W. A., Elkins, J. W., Kolb, C. E., McElroy, M. B., Wofsy, S. C. & Duran, A. P. 1978 Nitrous oxide in fresh water systems: an estimate for the yield of atmospheric  $\text{N}_2\text{O}$  associated with the disposal of human waste. *Pure Appl. Geophys.* **116**, 423.
- Keeling, C. D. 1973 Industrial production of carbon dioxide from fossil fuels and limestone. *Tellus* **25**, 174.
- Klemm, R. B., Payne, W. A. & Stief, L. J. 1975 Absolute rate parameters for the reaction of atomic hydrogen with  $\text{H}_2\text{O}_2$ . *Int. J. Chem. Kin. Symp.* **1**, 61.
- Krey, P. W., Lagomarsino, R. J. & Toonkel, L. E. 1977 Gaseous halogens in the atmosphere in 1975. *J. Geophys. Res.* **82**, 1753.
- Krueger, A. J. 1969 Rocket measurements of ozone over Hawaii. *Annls Geophys.* **25**, 307.
- Krueger, A. J., Heath, D. F. & Mateer, C. L. 1973 Variations in the stratospheric ozone field inferred from Nimbus satellite observations. *Pure Appl. Geophys.* **106-108**, 1254.
- Kurzeja, R. 1977 Effects of diurnal variations and scattering on ozone in the stratosphere for present day and predicted future chlorine concentrations. *J. atmos. Sci.* **34**, 1120.
- Lazrus, A. L., Gandrud, B. W. & Woodard, R. N. 1976 Direct measurements of stratospheric chlorine and bromine. *J. Geophys. Res.* **81**, 1067.
- Leu, M.-T. & DeMore, W. B. 1976 Rate constants at 295 °K for the reactions of atomic chlorine with  $\text{H}_2\text{O}_2$ ,  $\text{HO}_2$ ,  $\text{O}_3$ ,  $\text{CH}_4$ , and  $\text{HNO}_3$ . *Chem. Phys. Lett.* **41**, 121.
- Levy, H. 1971 Normal atmosphere: Large radical and formaldehyde concentrations predicted. *Science, N.Y.*, **173**, 141.
- List, R. J. & Telegadas, K. 1969. Using radioactive tracers to develop a model of the circulation of the atmosphere. *J. atmos. Sci.* **26**, 112.
- Lovelock, J. E. 1974 Atmospheric halocarbons and stratospheric ozone. *Nature, Lond.* **252**, 192.
- Lovelock, J. E. 1975 Natural halocarbons in the air and in the sea. *Nature, Lond.* **256**, 193.
- Lovelock, J. E. 1977 Methyl chloroform in the troposphere as an indicator of OH radical abundance. *Nature, Lond.* **267**, 32.
- Lovelock, J. E., Maggs, R. J. & Wade, R. J. 1973 Halogenated hydrocarbons in and over the Atlantic. *Nature, Lond.* **241**, 194.
- McCarthy, R. L., Bower, F. A. & Jesson, J. P. 1977 The fluorocarbon-ozone Theory I: Production and release. World production and release of  $\text{CCl}_3\text{F}$  and  $\text{CCl}_2\text{F}_2$  (fluorocarbons 11 and 12) through 1975. *Atmos. Environ.* **11**, 491.
- McConnell, J. C. & McElroy, M. B. 1973 Odd nitrogen in the atmosphere. *J. atmos. Sci.* **30**, 1465.
- McElroy M. B. 1976 Chemical processes in the solar system: A kinetic perspective. *M.T.P. International Review of Science*, ser. 2, vol. 9, ed. D. Herschbach. London: Butterworths.
- McElroy, M. B., Elkins, J. W., Wofsy, S. C. & Yung, Y. L. 1976 Sources and sinks for atmospheric  $\text{N}_2\text{O}$ . *Rev. Geophys. Space Phys.* **14**, 143.
- McElroy, M. B. & McConnell, J. C. 1971 Nitrous oxide: A natural source of stratospheric NO. *J. atmos. Sci.* **28**, 1095.
- McElroy, M. B., Wofsy, S. C., Penner, J. E. & McConnell, J. C. 1974 Atmospheric ozone: Possible impact of stratospheric aviation. *J. atmos. Sci.* **31**, 287.
- McElroy, M. B., Wofsy, S. C. & Yung, Y. L. 1977 The nitrogen cycle: Perturbations due to man and their impact on atmospheric  $\text{N}_2\text{O}$  and  $\text{O}_3$ . *Phil. Trans. R. Soc. Lond.* **B 277**, 159.
- Margitan, J. J., Kaufman, F. & Anderson, J. G. 1975 Kinetics of the reaction  $\text{OH} + \text{HNO}_3 \rightarrow \text{H}_2\text{O} + \text{NO}_3$ . *Int. J. Chem. Kin. Symp.* **1**, 281.
- Mastenbrook, H. J. 1971 The variability of water vapor in the stratosphere. *J. atmos. Sci.* **28**, 1495.
- Miller, D. E. & Ryder, P. 1973 Measurements of the ozone concentration from 55 to 95 km at sunset. *Planet. Spacc Sci.* **21**, 963.
- Miller, D. E. & Stewart, K. H. 1965 Observations of atmospheric ozone from an artificial Earth satellite. *Proc. R. Soc. Lond. A* **288**, 540.
- Molina, L. T. & Molina, M. J. 1977 Ultraviolet absorption spectrum of chlorine nitrite,  $\text{ClONO}$ . *Geophys. Res. Lett.* **4**, 83.
- Molina, L. T., Spencer, J. E. & Molina, M. J. 1977 The rate constant for the reaction of  $\text{O}(^3\text{P})$  atoms with  $\text{ClONO}_2$ . *Chem. Phys. Lett.* **45**, 158.
- Morris, E. D. & Niki, H. 1971 Mass spectrometric study of the reaction of hydroxyl radicals with formaldehyde. *J. chem. Phys.* **55**, 1991.
- Murcray, D. G., Barker, D. B., Brooks, J. N., Goldman, A. & Williams, W. J. 1975 Seasonal and latitudinal variation of the stratospheric concentration of  $\text{HNO}_3$ . *Geophys. Res. Lett.* **2**, 223.



- Murcray, D. G., Goldman, A., Williams, W. J., Murcray, F. H., Bonomo, F. S., Bradford, C. M., Cook, G. R., Hanst, P. L. & Molina, M. J. 1977 Upper limit for stratospheric ClONO<sub>2</sub> from balloon-borne infrared measurements. *Geophys. Res. Lett.* **4**, 227.
- Murcray, D. G., Goldman, A., Williams, W. J., Murcray, F. H., Brooks, J. N., Stocker, R. N. & Snider, D. E. 1974 Stratospheric mixing ratio profiles of several trace gases as determined from balloon borne infrared spectrometers. *Proceedings of the International Conference on structure, composition and general circulation of the upper and lower atmosphere and possible anthropogenic perturbations*. Melbourne, Australia, p. 292.
- National Academy of Sciences 1976 *Halocarbons: Effects on stratospheric ozone*. Washington, D.C.: N.A.S.
- Neely, W. B. & Plonka, J. H. 1978 An estimate of the time averaged hydroxyl radical concentration in the troposphere. *Env. Sci. & Tech.* **12**, 317.
- Nicolet, M. 1965 Nitrogen oxides in the chemosphere. *J. Geophys. Res.* **70**, 679.
- Nicolet, M. 1975 Stratospheric ozone: An introduction to its study. *Rev. Geophys. Space Phys.* **13**, 593.
- Nicolet, M. & Vergison, A. 1971 L'oxyde azoteux dans la stratosphere. *Aeron. Acta*, **90**, 1.
- Niki, H., Maker, P. D., Savage, C. M. & Breitenbach, L. P. 1977 Fourier transform IR spectroscopic observation of pernitric acid formed via HOO + NO<sub>2</sub> → HOONO<sub>2</sub>. *Chem. Phys. Lett.* **45**, 564.
- Niki, H., Maker, P. D., Savage, C. M. & Breitenbach, L. P. 1978 Mechanism for hydroxyl radical initiated oxidation of olefin-nitric oxide mixtures in parts per million concentrations. *J. phys. Chem.* **82**, 135.
- Noxon, J. F. 1975 NO<sub>2</sub> in the stratosphere and troposphere measured by ground based absorption spectroscopy. *Science, N.Y.* **189**, 147.
- Noxon, J. F., Whipple, E. C. & Hyde, R. S. 1977 Stratospheric NO<sub>2</sub>. Manuscript in preparation.
- Oort, A. H. & Rasmussen, E. M. 1971 Atmospheric circulation statistics. *N.O.A.A. professional paper* 5.
- Organization for Economic Cooperation and Development 1976 *O.E.C.D. Economic Outlook* 19. Special supplement: A growth scenario to 1980.
- Overend, R. & Paraskevopoulos, G. 1977 The question of a pressure effect in the reaction OH + CO at room temperature. *Chem. Phys. Lett.* **49**, 109.
- Paukert, T. T. & Johnston, H. S. 1972 Spectra and kinetics of the hydroperoxyl free radical in the gas phase. *J. chem. Phys.* **56**, 2824.
- Penfield, H., Litvak, M. M., Gottlieb, C. A. & Lilley, A. E. 1976 Mesospheric ozone measured from ground-based millimeter wave observations. *J. Geophys. Res.* **81**, 6115.
- Penner, J. E., McElroy, M. B. & Wofsy, S. C. 1977 Sources and sinks for atmospheric H<sub>2</sub>: A current analysis with projections for the influence of anthropogenic activity. *Planet. Space Sci.* **25**, 521.
- Perry, R. A., Atkinson, R. & Pitts, J. N. 1977 Kinetics of the reaction of OH radicals with C<sub>2</sub>H<sub>2</sub> and CO. *J. chem. Phys.* **67**, 5577.
- Philen, D. L., Watson, R. T. & Davis, D. D. 1977 A quantum yield determination of O(<sup>1</sup>D) production from ozone via laser flash photolysis. *J. chem. Phys.* **67**, 3316.
- Phillips, L. F. & Schiff, H. I. 1962 Mass-spectrometric studies of atom reactions. I. Reactions in the atomic nitrogen-ozone system. *J. chem. Phys.* **36**, 1509.
- Pierotti, D. & Rasmussen, R. A. 1976 Combustion as a source of nitrous oxide in the atmosphere. *Geophys. Res. Lett.* **3**, 265.
- Preston, K. F. & Cvetanovic, R. J. 1966 Collisional deactivation of excited oxygen atoms in the photolysis of NO<sub>2</sub> at 2288 Å. *J. chem. Phys.* **45**, 2888.
- Raper, O. F., Farmer, C. B., Toth, R. A. & Robbins, B. D. 1977 The vertical distribution of HCl in the 20–40 km region of the stratosphere. *Geophys. Res. Lett.* **4**, 531.
- Rasmussen, R. A. 1970. Isoprene: Identified as a forest-type emission to the atmosphere. *Environ. Sci. Tech.* **4**, 667.
- Rasmussen, R. A. & Jones, C. A. 1973 Emission of isoprene from leaf discs of Hamamelis. *Phytochem.* **12**, 15.
- Rasmussen, R. A., Pierotti, D., Krasnec, J. & Halter, B. 1976 Trip report on the cruise of the Alpha Helix Research Vessel from San Diego, Cal. to San Martin, Peru, 5–20 March.
- Richtmeyer, R. D. 1957 *Difference methods for initial value problems*, p. 101. New York: Interscience Pub. Co.
- Ridley, B. A., Bruin, J. T., Schiff, H. I. & McConnell, J. C. 1976 Altitude profile and sunset decay measurements of stratospheric nitric oxide. *Atmosphere* **14**, 180.
- Riegler, G. R., Atreya, S. K., Donahue, T. M., Liu, S. C. & Wasser, B. 1977 U.V. stellar occultation measurements of nighttime equatorial ozone. *Geophys. Res. Lett.* **4**, 145.
- Robbins, D. E. 1976 Photodissociation of CH<sub>3</sub>Cl and CH<sub>3</sub>Br in the atmosphere. *Geophys. Res. Lett.* **3**, 213. Errata, *Geophys. Res. Lett.* **3**, 757.
- Rogers, J. W., Stair, A. T., Degges, T. C., Wyatt, C. L. & Baker, D. J. 1977 Rocketborne measurement of mesospheric H<sub>2</sub>O in the auroral zone. *Geophys. Res. Lett.* **4**, 366.
- Romand, J. & Mayence, J. 1949 Spectre d'absorption de l'oxyde azoteux gazeux dans la region de Schumann. *C. r. hebdomadaire Séanc. Acad. Sci., Paris* **228**, 998.
- Rowland, F. S. & Molina, M. J. 1975 Chlorofluoromethanes in the environment. *Rev. Geophys. Space Phys.* **13**, 1.
- Rowland, F. S., Spencer, J. E. & Molina, M. J. 1976a Estimated relative abundance of chlorine nitrate among stratospheric chlorine compounds. *J. phys. Chem.* **80**, 2713.
- Rowland, F. S., Spencer, J. E. & Molina, M. J. 1976b Stratospheric formation and photolysis of chlorine nitrate. *J. phys. Chem.* **80**, 2711.

- Sanadze, G. A. 1963 On the condition of evolution of the diene  $C_6H_8$  (isoprene) from leaves. *Fiziol. Rast.* **11**, 49 (Russian); **11**, 42 (English).
- Schmeltekopf, A. L., Goldan, P. D., Henderson, W. R., Harrop, W. J., Thompson, T. L., Fehsenfeld, F. C., Schiff, H. I., Crutzen, P. J., Isaksen, I. S. A. & Ferguson, E. E. 1975 Measurements of stratospheric  $CF_2Cl_2$ ,  $CF_2Cl_2$  and  $N_2O$ . *Geophys. Res. Lett.* **2**, 393.
- Schmeltekopf, A. L., Albritton, D. L., Crutzen, P. J., Goldan, P. D., Harrop, W. J., Henderson, W. R., McAfee, J. R., McFarland, M., Schiff, H. I., Thompson, T. L., Hoffmann, D. J. & Kjome, N. T. 1977 Stratospheric nitrous oxide profiles at various latitudes. *J. Atmos. Sci.* **34**, 729.
- Schmidt, U. 1974 Molecular hydrogen in the atmosphere. *Tellus* **26**, 78. Errata, *Tellus* **27**, 93.
- Schott, G. & Davidson, N. 1958 Shock waves in chemical kinetics: The decomposition of  $N_2O_5$  at high temperatures. *J. Am. Chem. Soc.* **80**, 1841.
- Schumb, W. C., Sallerfield, C. N. & Wentworth, R. L. 1955 *Hydrogen peroxide*. New York: Reinhold Pub. Co. ACS Monograph Series.
- Seery, D. J. & Britton, D. 1964 The continuous absorption spectra of chlorine, bromine, bromine chloride, iodine chloride and iodine bromide. *J. Phys. Chem.* **68**, 2263.
- Seiler, W. 1974 The cycle of atmospheric CO. *Tellus* **26**, 118.
- Seiler, W. & Schmidt, U. 1974 New aspects of CO and  $H_2$  cycles in the atmosphere. *Proceedings of the International Conference on the structure, composition and general circulation of the upper and lower atmospheres and possible anthropogenic perturbations*, Melbourne, Australia, p. 192.
- Selwyn, G., Podolske, J. & Johnston, H. S. 1977 Nitrous oxide ultraviolet absorption spectrum at stratospheric temperatures. *Geophys. Res. Lett.* **4**, 427.
- Shemansky, D. E. 1972  $CO_2$  extinction coefficient 1700–3000 Å. *J. Chem. Phys.* **56**, 1582.
- Shortridge, R. G. & Lin, M. C. 1975 CO vibrational population distributions in the reactions of COS with  $O(^3P_2)$  and  $O(^1D_2)$  atoms. *Chem. Phys. Lett.* **35**, 146.
- Sie, K. T., Simonaitis, R. & Heicklen, J. 1976 The reaction of OH with CO. *Int. J. Chem. Kin.* **8**, 85.
- Simonaitis, R. & Heicklen, J. 1973 Reaction of  $HO_2$  with  $O_3$ . *J. Phys. Chem.* **77**, 1932.
- Simonaitis, R. & Heicklen, J. 1976 Reactions of  $HO_2$  with NO and  $NO_2$  and of OH with NO. *J. Phys. Chem.* **80**, 1.
- Singh, H. B., Salas, L. J. & Cavanagh, L. A. 1977a Distribution, sources and sinks for atmospheric halogenated compounds. *J. Air Pollution Control. Assoc.* **27**, 332.
- Singh, H. B., Salas, L., Shiegeshi, H. & Crawford, A. 1977b Urban-non urban relationships of halocarbons,  $SF_6$ ,  $N_2O$  and other atmospheric trace constituents. *Atmos. Environ.* **11**, 819.
- Slanger, T. G., Wood, B. J. & Black, G. 1972 Kinetics of  $O(^3P) + CO + M$  recombination. *J. Chem. Phys.* **57**, 233.
- Smith, I. W. M. & Zellner, R. 1974 Rate measurements of reactions of OH by resonance absorption. Part 3. Reactions of OH with  $H_2$ ,  $D_2$  and hydrogen and deuterium halides. *J. Chem. Soc. Faraday Trans. II* **70**, 1045.
- Smith, W. S., Chou, C. C. & Rowland, F. S. 1977 The mechanism for ultra-violet photolysis of gaseous chlorine nitrate at 302.5  $\mu m$ . *Geophys. Res. Lett.* **4**, 517.
- Soderland, R. & Svensson, B. H. 1976 The global nitrogen cycle. In *Nitrogen, phosphorus and sulphur global cycles* (eds B. H. Svensson & R. Soderland), p. 22. Scope Report 7, Ecological Bulletin no. 22, Stockholm.
- Streit, G. E., Howard, C. J., Schmeltekopf, A. L., Davidson, J. A. & Schiff, H. I. 1976 Temperature dependence of  $O(^1D)$  rate constants for reactions with  $O_2$ ,  $N_2$ ,  $CO_2$ ,  $O_3$ , and  $N_2O$ . *J. Chem. Phys.* **65**, 4761.
- Stuhl, F. & Niki, H. 1971 Measurements of rate constants for termolecular reactions of  $O(^3P)$  with  $NO$ ,  $O_2$ ,  $CO$ ,  $N_2$  and  $CO_2$  using a pulsed vacuum-u.v. photolysis chemiluminescent method. *J. Chem. Phys.* **55**, 3943.
- Sun, H. & Weissler, G. L. 1954 Absorption cross-sections of methane and ammonia in the vacuum ultraviolet. *J. Chem. Phys.* **1160**.
- Sweeney, R. E., Lui, K. K. & Kaplan, I. R. 1977 Oceanic nitrogen isotopes and their uses in determining the source of sedimentary nitrogen. *Proceedings of International Symposium on Stable Isotope Geochemistry*, New Zealand.
- Sze, N. D. 1977 Anthropogenic CO emissions: Implications for atmospheric CO–OH– $CH_4$  cycle. *Science, N.Y.* **195**, 673.
- The National Energy Plan 1977 Executive Office of the President, Washington, D. C., 29 April.
- Thompson, B. A., Harreck, P. & Reeves, R. R. 1963 Ultraviolet absorption coefficients of  $CO_2$ , CO,  $O_2$ ,  $H_2O_2$ ,  $N_2O$ ,  $NH_3$ , NO,  $SO_2$  and  $CH_4$  between 1850 and 4000 Å. *J. Geophys. Res.* **68**, 6431.
- Volz, A., Ehhalt, D. H., Heidt, L. E. & Pollock, W. 1976 Vertical profiles of  $CH_4$ , CO and  $CO_2$  in the stratosphere. *Proceedings Joint Symposium on Atmospheric Ozone*. (IAOC/ICACCP) Dresden, G.D.R.
- Watanabe, T. & Tohmatsu, T. 1976 An observational evidence for the seasonal variation of ozone concentration in the upper stratosphere and the mesosphere. *Rep. Ionosph. Space Res. Japan* **30**, 47.
- Watanabe, T. & Zelikoff, M. 1953 Absorption coefficients of water vapor in the vacuum ultraviolet. *J. Opt. Soc. Am.* **43**, 753.
- Watanabe, K., Zelikoff, M. & Inn, E. C. Y. 1953 Absorption coefficients of several atmospheric gases. *Air Force Cambridge Research Center Technical Report* no. 53–23.
- Waters, J. W., Gustincic, J. J., Kaker, R. K., Kerr, A. R., Roscoe, H. K. & Swanson, P. N. 1977 The microwave limb sounder experiment: observations of stratospheric and mesospheric  $H_2O$ . Contribution to the NASA Report on the 1976 Convair-990 latitude survey expedition.

- Watson, R. T. 1977 Rate constants of  $\text{ClO}_x$  of atmospheric interest. *J. Phys. Chem. Ref. Data* **6**, 871.
- Watson, R. T., Machado, G., Conaway, B., Wagner, S. & Davis, D. D. 1977 A temperature dependent kinetics study of the reaction of OH with  $\text{CH}_2\text{Cl}_2\text{F}$ ,  $\text{CHCl}_2\text{F}$ ,  $\text{CHClF}_2$ ,  $\text{CH}_3\text{CCl}_3$ ,  $\text{CH}_3\text{CF}_2\text{Cl}$  and  $\text{CF}_2\text{ClCFCl}_2$ . *J. phys. Chem.* **81**, 256.
- Weiss, R. F., Dowd, W. & Craig, H. 1976 Nitrous oxide: Atmospheric concentrations 1964–1976, Industrial sources and air-sea exchange. Paper presented at the International Conference on the Stratosphere and Related Problems, Logan, Utah, September 1976.
- Weiss, R. F. & Craig, H. 1976 Production of atmospheric nitrous oxide by combustion. *Geophys. Res. Lett.* **3**, 751.
- Westenberg, A. A. & deHaas, N. 1969 Reinvestigation of the rate coefficients for  $\text{O} + \text{H}_2$  and  $\text{O} + \text{CH}_4$ . *J. chem. Phys.* **50**, 2512.
- Westenberg, A. A., deHaas, N. & Roscoe, J. M. 1970 Radical reactions in an electron spin resonance cavity homogeneous reactor. *J. phys. Chem.* **74**, 3431.
- Widman, R. P. & DeGraff, B. A. 1973 On the gas-phase recombination of chlorine atoms. *J. phys. Chem.* **77**, 1325.
- Williams, W. J., Kusters, J. J., Goldman, A. & Murcray, D. G. 1976 Measurement of the stratospheric mixing ratio of HCl using infrared absorption techniques. *Geophys. Res. Lett.* **3**, 383.
- Wofsy, S. C. 1976 Interactions of  $\text{CH}_4$  and CO in the Earth's atmosphere. *A. Rev. Earth Planet. Sci.* **4**, 441.
- Wofsy, S. C. 1978 Temporal and latitudinal variations of stratospheric trace gases: A critical comparison between theory and experiment. *J. Geophys. Res.* **83**, 364.
- Wofsy, S. C., McConnell, J. C. & McElroy, M. B. 1972 Atmospheric  $\text{CH}_4$ , CO and  $\text{CO}_2$ . *J. Geophys. Res.* **77**, 4477.
- Wofsy, S. C. & McElroy, M. B. 1973 On vertical mixing in the upper stratosphere and lower mesosphere. *J. Geophys. Res.* **78**, 2619.
- Wofsy, S. C., McElroy, M. B. & Sze, N. D. 1975a Freon consumption: Implications for atmospheric ozone. *Science, N.Y.* **187**, 535.
- Wofsy, S. C., McElroy, M. B. & Yung, Y. L. 1975b The chemistry of atmospheric bromine. *Geophys. Res. Lett.* **2**, 215.
- Wong, W. & Davis, D. D. 1974 A flash photolysis resonance fluorescence study of the reaction of atomic hydrogen with molecular oxygen,  $\text{H} + \text{O}_2 + \text{M} \rightarrow \text{HO}_2 + \text{M}$ . *Int. J. Chem. Kin.* **6**, 401.
- Yung, Y. L. 1976 A numerical method for calculating the mean intensity in an inhomogeneous Rayleigh scattering atmosphere. *J. Quant. Spectrosc. Radiat. Trans.* **16**, 755.
- Zahniser, M. S., Chang, J. S. & Kaufman, F. 1977 Chlorine nitrate: Kinetics of formation by  $\text{ClO} + \text{NO}_2 + \text{M}$  and of reaction with OH. *J. chem. Phys.* **67**, 997.
- Zahniser, M. S., Kaufman, F. & Anderson, J. G. 1974 Kinetics of the reaction of OH with HCl. *Chem. Phys. Lett.* **27**, 507.
- Zahniser, M. S., Berquist, B. M. & Kaufman, F. 1978 Kinetics of the reaction  $\text{Cl} + \text{CH}_4 \rightarrow \text{CH}_3 + \text{HCl}$  from 200° to 500 °K. *Int. J. Chem. Kin.* **10**, 15.
- Zelikoff, M., Watanabe, K. & Inn, E. C. Y. 1953 Absorption coefficients of gases in the vacuum ultraviolet. Part 2. Nitrous oxide. *J. chem. Phys.* **21**, 1643.
- Zipf, E. C. & Dubin, M. 1976 Laboratory studies on the formation of  $\text{NO}_x$  compounds and ozone by lightning. Paper presented at the A.G.U. meeting, San Francisco, December 1976. (*EOS Transactions* **57**, 965.)